

MODIFIED HYDRODYNAMICS IN FRAGMENTED CANOPIES EXPOSED TO OSCILLATORY FLOWS

Nazha El Allaoui

Per citar o enllaçar aquest document:
Para citar o enlazar este documento:
Use this url to cite or link to this publication:
<http://hdl.handle.net/10803/403066>



<http://creativecommons.org/licenses/by-nc/4.0/deed.ca>

Aquesta obra està subjecta a una llicència Creative Commons Reconeixement-NoComercial

Esta obra está bajo una licencia Creative Commons Reconocimiento-NoComercial

This work is licensed under a Creative Commons Attribution-NonCommercial licence



DOCTORAL THESIS

**Modified hydrodynamics in
fragmented canopies exposed to
oscillatory flows**

Nazha El Allaoui

2016



DOCTORAL THESIS

**Modified hydrodynamics in
fragmented canopies exposed to
oscillatory flows**

Nazha El Allaoui

2016

Doctoral Programme in Water Science and Technology

Supervisors:

Teresa Serra Putellas

Marianna Soler Ortega

Thesis submitted for the degree of Doctor of Philosophy by the University of Girona

La Dra. Teresa Serra Putellas, professora Titular del Departament de Física de la Universitat de Girona, i la Dra. Marianna Soler Ortega, professora Agregada Interina del Departament de Física de la Universitat de Girona,

CERTIFIQUEN:

Que aquest treball, titulat "Modified hydrodynamics in fragmented canopies exposed to oscillatory flows", que presenta l'estudiant de doctorat Nazha El Allaoui per a l'obtenció del títol de doctora, ha estat realitzat sota la seva direcció.

I, perquè així consti i tingui els efectes oportuns, signen aquest document.

Dra. Teresa Serra Putellas

Dra. Marianna Soler Ortega

Girona, 15 d'abril del 2016

Acknowledgments

First and the most important I would like to thank my supervisors Dr. Teresa Serra Putellas and Dr. Marianna Soler for giving me the opportunity to begin my research career with them, which has led to this doctoral Thesis, and for their guidance and support during these years.

My sincere acknowledgments to the members of the projects: Dr. Jordi Colomer Feliu , especially because without his support regarding statistical analysis the thesis would have remained incomplete, and Dr. Xavier Casamitjana.

I would like to express my gratitude to Dr. Carolyn Oldham, for the valuable suggestions and for their high value contributions and comments to our manuscripts.

I also want to thank all my colleagues, Doctors and Professors, of the Department of Physics in the University of Girona, and specially my fellow Ph.D. students, for the friendship and good times: Dr. Dolors Pujol, Dr. Montserrat Costa Surós, Dr. Conxi Pau, Àlex Ros, Dr. Fatiha Kail and Dr. Maha El Bana. Without forgetting the Service and Administration Personal (PAS) of the Department of Physics: Anna Espígol, Xevi Baca, Xicu Gómez, Marc Rodríguez, and Quico Pazo.

Finally, I want to thank my family, Mohammed Maaroufi and my friends throughout the given support.

This thesis has also been possible thanks to Ministry of Science and Innovation of the Spanish Government, for their support through grant CGL2010-17289

Contents

Contents.....	iv
Publications and communications related to the thesis	vi
List of abbreviations.....	viii
List of Figure Legends.....	xi
List of Tables	xvii
Abstract.....	xviii
Resum	xx
Resumen	xxii
Chapter 1. Introduction	1
1.1 Seagrasses and saltmarshes.....	1
1.2 The fragmentation of seagrasses and saltmarshes.....	4
1.3 The objectives of study and the organization of the thesis.....	7
Chapter 2. Materials and methods.....	11
2.1 The flume	11
2.2 Acoustic Doppler Velocimeter (16 Mhz- ADV, Sontek Inc.).....	13
2.3 The model canopy.....	14
2.3.1 The rigid model canopy.....	14
2.3.2 The flexible model canopy	15
2.4 The methods	16
2.4.1 Solid Plant Fraction, SPF.....	16
2.4.2 Description the calculation of U_c , $U_{w,rms}$, TKE, α_w and β_w	17
Chapter 3. Hydrodynamics in canopies with longitudinal gaps exposed to oscillatory flows.....	21
3.1 Experimental set up for a canopy with a longitudinal gap	22
3.2 Results.....	28
3.2.1 Mean wave induced currents - submerged rigid vegetation.....	28
3.2.2 Mean wave induced currents - emergent rigid vegetation	30

3.2.3 Wave velocities – submerged rigid vegetation	32
3.2.4. Wave velocities – emergent rigid vegetation	35
3.2.5 Submerged flexible vegetation	38
3.3 Discussion.....	40
3.3.1 Interaction between plant density and flows through gaps.....	40
3.3.2 Vertical flow structure within a rigid canopy.....	41
3.3.3 Differences between rigid and flexible vegetation	42
3.3.4 Sedimentary significance	43
Chapter 4. Hydrodynamics in boundary of vegetation to oscillatory flows	45
4.1. Experimental set up for the study of the boundary of a canopy.....	47
4.2 Results.....	48
4.2.1 The mean current distribution.....	48
4.2.2 The wave velocity field.....	51
4.2.3 The turbulent kinetic energy (TKE)	52
4.3 Discussion.....	54
Chapter 5. Hydrodynamics canopies with transversal gaps exposed to oscillatory flows.....	62
5.1 Experimental set up for the study of canopies with transversal gaps.....	62
5.2 Results.....	65
5.3. Discussion.....	71
Chapter 6. General Discussion	79
6.1. The effect of the gap orientation.....	80
6.2. The effect of the plant flexibility.....	81
6.3. Ecological implications.....	81
Chapter 7. Conclusions	85
Chapter 8. References.....	89
Annex	99

Publications and communications related to the thesis

Peer-reviewed papers (published/accepted):

Modified hydrodynamics in canopies with longitudinal gaps exposed to oscillatory flows. Authors: **Nazha El Allaoui**, Teresa Serra, Marianna Soler, Jordi Colomer, Dolors Pujol and Carolyn Oldham. 2015. Journal of Hydrology. 531: 840-849. (Impact factor 3.053, journal 4 of 125, 1st Quartile of the Civil Engineering category)

Peer-reviewed paper (minor revisions):

Title: Modified hydrodynamics in fragmented canopies exposed to oscillatory flows. Authors: **Nazha El Allaoui**, Teresa Serra, Marianna Soler, Jordi Colomer, Xavier Casamitjana and Carolyn Oldham. PLOS ONE.

Communication Posters:

Title: Modified hydrodynamics of coastal canopies by longitudinal gaps exposed to oscillatory flows. Conference: Integrating New Advances in Mediterranean Oceanography and Marine Biology Barcelona . Authors: **Nazha El-Allaoui** , Teresa Serra, Marianna Soler, Jordi Colomer, Dolors Pujol and Xavier Casamitjana. Year: 2013.

Title: Modified hydrodynamics of coastal canopies by longitudinal gaps. Conference: SIL XXXII in Budapest (Hungary). Authors: **Nazha El-Allaoui** , Teresa Serra, Marianna Soler, Jordi Colome and Carolyn Oldham. Year: 2013.

Title: Wave induced velocities inside a riparian seagrass bed. Conference: European Geosciences Union. General Assembly (EGU2012) in Vienna. Authors: **Nazha El-Allaoui** , Teresa Serra, Marianna Soler and Jordi Colomer. Year: 2012.

Chapter in book:

Chapter title: Us d'una població de *Dafnia* per millorar aigües residuals depurades.

Author: Nazha el Allaoui, Book title: "Recerques en Medi Ambient, Màster Universitari en Medi Ambient 2006/2010". Coord.: Pintó, J. Ed.: Documenta Universitaria. Year: 2011. ISBN: 978-84-8458-362-2.

List of abbreviations

a: amplitude of the wave

a_f : frontal area per volume

α_w : attenuation of the wave velocity

A_{total} : total area

A_f : frontal area of the blade

A_{∞}^{rms} : root-mean-square wave orbital excursion length of the free-stream

A_{stem} : stem area

β_w : wave velocity ratio

C_d : drag coefficient

C_f : friction coefficient

C_m : inertial force coefficient

C_1, C_2, C_3 : constant parameters

d: diameter of the plant

d_p : penetration depth

E: modulus of elasticity

ERV: emergent rigid vegetation

f: oscillating frequency

F_d : drag force

F_B : buoyancy force

F_r : rigidity restoring force

g: gravity constant

GW : gap width

φ : phase

h: mean water height

h_v : height of the vegetation

H: height of the wave

k: wavenumber

k_m : added mass

I: second moment of area

λ : wavelength

λ_1 and λ_2 : geometrical and dynamical dimensional parameters

λ_f and λ_p : canopy parameters

δ_c : Boundary layer thickness based on the mean current transect

$\delta_{c_{in}}$: Boundary layer thickness based on the mean current transect for in the canopy

$\delta_{c_{out}}$: Boundary layer thickness based on the mean current transect for outside the canopy

δ_w : Boundary layer thickness based on the wave velocity transect

$\delta_{w_{in}}$: Boundary layer thickness based on the wave velocity transect for in the canopy

$\delta_{w_{out}}$: Boundary layer thickness based on the wave velocity transect for outside the canopy

n_{stems} : stem density

ρ_w : density of the water

ρ_s : density of the flexible blades

R: rigid canopy model

R^2 : correlation coefficient

S: plant-to-plant distance

SAV: submerged aquatic vegetation

SPF: solid plant fraction (%)

SR: semi-rigid canopy model

SRV: submerged rigid vegetation

SFV: submerged flexible vegetation

t: time

t_b : thickness of the flexible blade

t_f : theoretical breaking time

TKE: turbulent kinetic energy

TKE₅: turbulent kinetic energy at $z= 5\text{cm}$

TKE₇: turbulent kinetic energy at $z= 7\text{cm}$

TKE₁₀: turbulent kinetic energy at $z= 10\text{cm}$

u : instantaneous velocity

U_c : mean velocity

u' : turbulent velocity

u_0 : root-mean-square of turbulent velocity

U_w : wave velocity

$U_{w,\text{no-veg}}$: wave velocity of without plants

$U_{w,\text{no gap}}$: wave velocity of full vegetation

$U_{w,\text{rms}}$: root-mean-square of the wave velocity

$U_{\infty,w}^{\text{rms}}$: wave velocity root-mean-square unaffected by the canopy roughness

ν : kinematic viscosity

ω : radian frequency

w_b : width of the blade

wp: without plants

X: longitudinal axis

Y: transversal axis

Z: vertical axis

List of Figure Legends

Figure	Page
Figure 2.1 Photographs of the laboratory experimental flume. a) Lateral view of the flume. b) Lateral view with a distribution of flexible vegetation. c) Paddle wavemaker situated at the beginning of the flume. d) Variable speed motor. e) Plywood beach of slope 1:3 situated at the end of the flume.....	12
Figure 2.2 Photograph of Acoustic Doppler Velocimeter (16 Mhz- ADV, Sontek Inc.).....	13
Figure 2.3 Photographs of vegetation studied. a) Submerged rigid vegetation mode, b) Emerged rigid vegetation model	14
Figure 2.4 Photograph of submerged flexible vegetation model.....	16
Figure 2.5 The distribution of SPFs. a) SPF=2.5%, b) SPF=5%, c) SPF=7.5%, d) SPF=10%	16
Figure 3.1 a) Schematic diagram of the experimental flume. Vertical grey lines represent the vegetation model. The ADV is the Doppler sensor for the velocity measurement. The wave maker is schematized at the beginning of the flume. b) Transversal section with the gap and the vegetation zones. Vertical dashed lines represent the y-positions where vertical velocity profiles were measured. Vertical grey bars represent the distribution of the vegetation, submerged (middle panels) and emergent (bottom panels)	24
Figure 3.2 Photographs of canopy with a longitudinal gap	25
Figure 3.3 Wave velocity transects along the y-axis at z=5 cm for submerged vegetation for a 0.25 gap (a), for a 0.375 (b) and for emergent vegetation for a 0.25 gap (c) and for a 0.375 gap	

(d). Vertical dashed lines show the y -positions where vertical velocity profiles were measured. Grey boxes represent the zone covered by the vegetation..... 27

Figure 3.4 Mean current (U_c) for the submerged rigid vegetation experiments. a) for 0.25 gap and 5% SPF; b) 0.375 gap and 5% SPF; c) 0.25 gap and 10% SPF; d) 0.375 gap and 10% SPF. Horizontal dashed lines show the limits of the above-canopy region (> 14 cm above the bottom), the canopy-top region (7 - 14 cm) and the canopy-base region (< 7 cm). Horizontal error bars represent the standard deviation of the mean over different replicas 28

Figure 3.5 Mean current (U_c) for the emergent rigid vegetation experiments. a) for 0.25 gap and 5% SPF; b) 0.375 gap and 5% SPF; c) 0.25 gap and 10% SPF; d) 0.375 gap and 10% SPF. The dashed horizontal line represents the limit of the in-canopy region (< 17 cm above the bottom) and the surface boundary layer (> 17 cm). Horizontal error bars represent the standard deviation of the mean over different replicas 31

Figure 3.6 Wave velocity (U_w) profiles for all the experiments carried out with submerged vegetation at 10% SPF and for the 0.25 gap. The horizontal scale has been reduced to be able to see the details in U_w at both the canopy-top and the canopy-base regions 33

Figure 3.7 Wave velocity attenuation (α_w) for the submerged rigid vegetation experiments for a) 0.25 gap, SPF= 5%; b) 0.375 gap, SPF= 5%; c) 0.25 gap, SPF= 10%; d) 0.375 gap, SPF=10%. Horizontal dashed lines show the limits of the above-canopy region (> 14 cm), the canopy-top region (7 - 14 cm) and the canopy-base region (< 7 cm). Horizontal error bars represent the standard deviation of the mean over different replicas 34

Figure 3.8 Wave velocity attenuation (α_w) for the emergent rigid vegetation experiments for a) 0.25 gap, SPF=5%; b) 0.375 gap, SPF=5%; c) 0.25 gap, SPF= 10%; d) 0.375 gap, SPF=10%. The

dashed horizontal line represents limits of the in-canopy region (< 17 cm above the bottom) and the surface boundary layer (> 17 cm). Horizontal error bars represent the standard deviation of the mean over different replicas. 36

Figure 3.9 $\langle\alpha_w\rangle$ in the gap (a) and in the lateral vegetation (b) and $\langle\beta_w\rangle$ in the gap (c) and in the lateral vegetation (d) plotted against GW/hv . Different vegetation density (SPF) treatments are plotted and regression equations were $y=0.15x+0.78$ (SPF=5%, $R^2=0.813$) and $y=0.25x+0.62$ (SPF=10%, $R^2=0.922$) for (a), $y=0.13x+0.78$ (SPF=5%, $R^2=0.805$) and $y=0.13x+0.61$ (SPF=10%, $R^2=0.851$) for (b), $y=0.10x+1.02$ (SPF=5%, $R^2=0.788$) and $y=0.22x+1.13$ (SPF=10%, $R^2=0.823$) for (c) and $y=0.08x+1.03$ (SPF=5%, $R^2=0.752$) and $y=0.13x+1.027$ (SPF=10%, $R^2=0.730$), all 95% probability level. Crossed symbols in figures (a) and (b) correspond to no gap experiments considering as the ‘gap width’ the plant to plant distance. Error bars represent the standard deviation of $\langle\alpha_w\rangle$ and $\langle\beta_w\rangle$ through the canopy base layer 37

Figure 3.10 Mean current (U_c) (a) and wave velocity attenuation (α_w) (b) for experiments with submerged flexible vegetation for a 0.25 gap and 10% SPF. Horizontal dashed lines show the limits of the above-canopy region (> 14 cm above the bottom), the canopy-top region (4 - 14 cm) and the canopy-base region (< 4 cm). Horizontal error bars represent the standard deviation of the mean over different replicas 39

Figure 4.1 Scheme of the experimental set up. a) lateral-view of the flume with the canopy distribution, the wave maker and the beach. b) Top-view of the canopy and boundary 47

Figure 4.2 Mean current velocity transects at $z=5$ cm (bottom panels, c and d), $z=7$ cm (middle panels, b and e) and $z=10$ cm (top panels, a and d) along the y -axis for the different experiments carried out for the flexible (left panels) and rigid (right panels) vegetations. Vertical dashed line

represented the position of boundary. The horizontal dashed line corresponds to the U_c for the without plants experiment. Different plots in each figure represent different SPFs 50

Figure 4.3 Wave velocity transect at $z=5$ cm (bottom panels, c and f), $z=7$ cm (middle panels, b and e) and $z=10$ cm (top panels, a and d) along the y -axis for the different experiments carried out for the flexible (left panels) and rigid (right panels) vegetation. Vertical dashed line represented the position of the canopy boundary. The horizontal dashed lines correspond to the U_w result for the without plants experiment. Different plots in each figure represent different SPFs 51

Figure 4.4 Turbulent kinetic energy transect at $z=5$ cm (bottom panels, c and f), $z=7$ cm (middle panels, b and e) and $z=10$ cm (top panels, a and d) along the y -axis for the different experiments carried out for the flexible (left panels) and rigid (right panels) vegetation. Vertical dashed line represented the position of the edge of the canopy. The horizontal dashed lines correspond to the TKE result for the without plants experiment. Different plots in each figure represent different SPFs 53

Figure. 4.5 Scheme of the direction on the mean current velocity in the region free of plants and in the region covered by the vegetation for the layer $z < 14$ cm above the bottom. The diagram corresponds to a canopy of rigid vegetation (a) and a canopy of flexible vegetation (b) 56

Figure 4.6 Boundary layer thickness based on the mean current transect (δ_c) versus the solid plant fraction (SPF) for the region within the canopy, $\delta_{c_{in}}$ (a) and and for the region outside the canopy, $\delta_{c_{out}}$ (b). c) Diagram of the boundary layers $\delta_{c_{out}}$ and $\delta_{c_{in}}$ 58

Figure 4.7 Boundary layer thickness based on the wave velocity transect (δ_w) versus the solid plant fraction (SPF) for, the region within the canopy, $\delta_{w_{in}}$ (a) and and for the region outside the canopy, $\delta_{w_{out}}$ (b). c) Diagram of the boundary layers $\delta_{w_{out}}$ and $\delta_{w_{in}}$ 60

Figure 5.1 Scheme of the experimental set up. a) Side-view of the flume with the canopy distribution, the wave maker and the beach. b) Top-view of the three different gaps studied63

Figure 5.2 Photographs of canopies with transversal gaps 64

Figure 5.3 Vertical profiles of the wave velocity for the no-canopy, no-gap and the gapped canopy of $GW=2h_v$ for a) 2.5% SPF and b) 10% SPF. The center of the gap was the point selected in x for the wave velocity profile within the gap. Horizontal dashed lines represent the vertical extension of the three layers, the above canopy layer, the canopy top layer and the within canopy layer 66

Figure 5.4 Vertical profiles of the turbulent kinetic energy for the no-canopy, no-gap and the gapped canopy of $GW=2h_v$ for a) 2.5% SPF and b) 10% SPF. The center of the gap was the point selected in x for the wave velocity profile within the gap. Horizontal dashed lines represent the vertical extension of the three layers, the above canopy layer, the canopy top layer and the within canopy layer 67

Figure 5.5 Wave velocity transect at $z=5$ cm along the x -axis for the different experiments carried out for a) 2.5% SPF and b) 10% SPF. Vertical dashed lines represent the positions of the boundary for the three different gap widths considered. Horizontal arrows at the top of the figure represent the lengths of the gap widths considered 69

Figure 5.6 Turbulent kinetic energy transect at $z=5$ cm along the x -axis for the different experiments carried out for a) 2.5% SPF and b) 10% SPF. Vertical dashed lines represent the positions of the boundary for the three different gap widths considered. Horizontal arrows at the top of the figure represent the lengths of the gap widths considered 70

Figure 5.7 Turbulent kinetic energy transect at $z=10$ cm along the x -axis for the different experiments carried out for a) 2.5% SPF and b) 10% SPF. Vertical dashed lines represent the positions of the boundary for the three different gap widths considered. Horizontal arrows at the top of the figure represent the lengths of the gap widths considered 72

Figure 5.8 Relationship between the non-dimensional number $(TKE_5/U_{w,5}^2)5$ and $(x/S)^{-0.20}(Aw/GW)^{-0.16}$ The distance x is the closest distance to the nearest canopy boundary .. 75

Figure 5.9 Relationship between the mean TKE at the top of the canopy ($z=10$ cm, $\langle TKE_{10} \rangle$) and the ratio GW/h_v for the two canopy densities of SPF=2.5% and SPF=10%..... 77

List of Tables

Table 3.1 Summary of different experimental conditions. A is the horizontal area and b is the width of flume 25

Table 4.1 Summary of different experimental conditions. A is the horizontal area and b is the width of flume 48

Table 5.1 Summary of different experimental conditions. A is the horizontal area and b is the width of flume 64

Abstract

Fragmented meadows are defined as discontinuous meadows with the presence of gaps of vegetation. A gap is defined as a zone of bare soil within a meadow. Gaps within canopies are expected to modify hydrodynamics and as a result to have ecological implications. While the ecological significance of gaps has been studied, we know little about their impact on the hydrodynamics within the canopy. With the aim of understanding the effect of gaps within canopies on the hydrodynamics, a series of laboratory experiments have been carried out with different goals.

The first objective in this Thesis was the study of the effect of a longitudinal gaps (i.e. gap aligned with the direction of the wave propagation) on the hydrodynamics within the gap and within the vegetation (Chapter 3). The presence of the gap modified the mean current associated with the waves in both the gap and the lateral vegetation. A gap within a canopy of 5% solid plant fraction did not show differences in the wave attenuation between the gap and the lateral vegetation. In contrast, gaps within canopies of 10% solid plant fraction resulted in large differences between the gap and the lateral vegetation. In all the experiments, the effect of a gap within a canopy reduced the wave attenuation within the lateral vegetation adjacent to the gap when compared with a canopy without a gap. In canopies with rigid plants, the lateral vegetation modified the wave attenuation in the nearby gap. In contrast, the lateral flexible vegetation did not produce any effect on the wave attenuation of the adjacent gap.

The second objective of this Thesis was to give a detailed picture of the hydrodynamics in the region close to the boundary layer vegetation-bare soil for both rigid and flexible plants (Chapter 4). The distribution of the turbulent kinetic energy, the mean flow and the wave velocity have been found to depend not only on the canopy density but on the canopy structure, whether stems were flexible or rigid. Both the submerged rigid and flexible vegetation have been found to attenuate the wave associated mean current in the canopy boundary zone (within the vegetation and outside the

vegetation). Based on the mean flow, the rigid boundary layer can be divided in three regions, the layer within the vegetation, the layer far from the vegetation (i.e. that for the without plants) and the boundary layer nearby the plants with the presence of a shear across the density interface.

The third objective was to study the hydrodynamics within a meadow with the presence of a transversal gap (i.e. a gap oriented perpendicular to the wave direction (Chapter 5)). The wave velocity has been found to increase within the gap for the two canopy densities studied attaining the wave velocity found for the without plants study. The turbulent kinetic energy within the gap has been found to increase within the gap but it has been found to remain below that for the without plants experiments.

All the experiments in this Thesis have been carried out in the laboratory with a canopy distribution and an experimental set up that tried to mimic real field situations. Such situations correspond to canopies situated in the coastal area. The major part of the experiments have been carried out with submerged plants with the aim to model a *Posidonia oceanica* canopy. However, for completeness some experiments have been carried out with rigid plants and just in one case with emergent vegetation, extending such conditions to saltmarsh areas. The flow regime in all the experiments has been the same, a wave flow characteristic of shallow areas like one would expect in coastal zones.

At the end of the Thesis I include a copy of a publication of the results of Chapter 3, in *the Journal of Hydrology*. This journal is included in the category of Civil Engineering and occupies the 4th position out of 125 journals. It occupies the quartile 1 and has an impact factor of 3.053.

Resum

Una praderia fragmentada es defineix com una praderia discontinua amb la presència dels gaps (espais sense plantes) a l'interior de la vegetació, i s'especula que aquests gaps tenen importants implicacions ecològiques i també es suposa que modifiquen la hidrodinàmica en la vegetació aquàtica. S'han fet molts estudis sobre la importància ecològica de la fragmentació de les praderies, però cal aprofundir en l'impacte en la hidrodinàmica de la vegetació aquàtica. Amb l'objectiu d'entendre l'efecte dels gaps sobre la hidrodinàmica dins la vegetació aquàtica, s'han dut a terme una sèrie d'experiments de laboratori amb diferents objectius.

El primer objectiu d'aquesta tesi és l'estudi de l'efecte d'un gap longitudinal (és a dir, espai sense plantes alineat amb la direcció de la propagació de les onades) sobre la hidrodinàmica dins el gap i dins la vegetació (capítol 3). La presència del gap modifica el corrent mitjà associat amb les onades, tant al gap com a la vegetació lateral. Pel que fa a l'atenuació de l'ona quan hi ha un gap en un model de vegetació aquàtica de la $SPF = 5\%$ (fracció vegetal sòlida), els resultats de velocitat de l'ona no presenten diferència entre el gap i la vegetació lateral. Ara bé, quan la SPF és del 10% hi ha gran diferència entre els valors de velocitat de l'ona dins el gap i dins la vegetació lateral. En tots els experiments, l'efecte d'un gap dins d'un model de vegetació aquàtica redueix l'atenuació de l'onada dins de la vegetació lateral adjacent al gap, quan es compara amb un model de vegetació aquàtica sense un gap. En el model de vegetació rígida, la vegetació lateral modifica l'atenuació de l'onada en la zona propera al gap. Per contra, la vegetació lateral flexible no produeix cap efecte sobre l'atenuació de l'onada a la zona adjacent al gap.

El segon objectiu d'aquesta tesi és donar una imatge detallada de la hidrodinàmica de la regió propera a la frontera entre la vegetació i la zona sense vegetació per a dos models: de plantes rígides i flexibles (capítol 4). S'ha trobat que la distribució de l'energia cinètica turbulenta, el flux mitjà i la velocitat de l'onada, no només depenen de la densitat del model de la vegetació aquàtica, sinó també

de l'estructura del model, si les tiges són flexibles o rígides. Ambdós tipus de vegetació submergida rígida i flexible, atenuen l'onada a la frontera dins i fora de la vegetació. Basat en el flux mitjà, la frontera de plantes rígida es pot dividir en tres regions, la zona dins la vegetació, la zona lluny de la vegetació sense plantes i la zona propera de les plantes amb la presència d'una cisallament.

El tercer objectiu és l'estudi de la hidrodinàmica en un model de vegetació aquàtica amb la presència d'un gap transversal, és a dir, un gap orientat perpendicularment a la direcció de l'onada (capítol 5). S'ha trobat que la velocitat de l'onada augmenta dins el gap per a les dues densitats estudiades fins que arriba als valors de la velocitat d'onada del cas sense plantes. Els resultats mostren que l'energia cinètica turbulenta dins el gap augmenta, però es manté inferior a l'energia cinètica turbulenta de l'experiment sense plantes.

Tots els experiments en aquesta tesi s'han dut a terme al laboratori amb una distribució del model de vegetació aquàtica i una configuració experimental per imitar situacions reals del camp. Aquest tipus de situacions es corresponen a la praderia de la zona costanera. La major part dels experiments s'han dut a terme amb plantes submergides per tal de modelar una praderia de *Posidonia oceanica*. No obstant això, alguns experiments s'han dut a terme amb plantes rígides i només es presenta un cas amb vegetació emergent per tal de simular les condicions en zones poc profundes. El règim de flux en tots els experiments ha estat el mateix, és el flux de l'onada que caracteritza les ones en aigües poc profundes.

Al final de la tesi s'inclou una còpia de la publicació dels resultats del capítol 3 a la revista *Journal of Hydrology*. Aquesta revista està inclosa en la categoria Civil Engineering i ocupa la posició 4 de les 125 revistes incloses en la categoria (Font: ISI Web of Knowledge). És una revista de quartil 1 i té un índex d'impacte de 3.053.

Resumen

Una pradera fragmentada se define como una pradera discontinua con la presencia de gaps (espacio sin plantas) en el interior de la vegetación, y se especula que estos gaps tienen importantes implicaciones ecológicas y también se supone que modifican la hidrodinámica en la vegetación acuática. Se han hecho muchos estudios sobre la importancia ecológica de la fragmentación de las praderas, pero se sabe poco sobre su impacto en la hidrodinámica de la vegetación acuática. Con el objetivo de entender el efecto de los gaps sobre la hidrodinámica en la vegetación acuática, se han llevado a cabo una serie de experimentos de laboratorio con diferentes objetivos.

El primer objetivo de estudio en esta tesis es determinar el efecto de un gap longitudinal (es decir, espacio sin plantas alineado con la dirección de la propagación de las olas), sobre la hidrodinámica dentro del gap y dentro de la vegetación (capítulo 3). La presencia del gap modificó la corriente mediana asociado con las olas, tanto en el gap como en la vegetación lateral. Por cuanto a la atenuación de la ola cuando hay un gap en un modelo de vegetación acuática del $SPF = 5\%$ (fracción vegetal sólida) los resultados de velocidad de la ola no presentan diferencia entre el gap y la vegetación lateral. Por el contrario, cuando la SPF es 10% hay una gran diferencia entre los valores de velocidad de la ola en el gap y dentro de la vegetación lateral.

En todos los experimentos, el efecto de un gap dentro de un modelo de la vegetación acuática reduce la atenuación de la ola dentro de la vegetación lateral adyacente al gap cuando se compara con un modelo de la vegetación acuática sin un gap. En el modelo de la vegetación rígida, la vegetación lateral modificó la atenuación de la ola en la zona cercana al gap. En contra, la vegetación flexibles lateral no produjo ningún efecto sobre la atenuación de la ola en la zona adyacente al gap.

El segundo objetivo de esta tesis es dar una imagen detallada de la hidrodinámica de la región cercana a la frontera entre la vegetación y la zona sin vegetación por dos modelos: de plantas rígidas y flexibles (capítulo 4). Se ha encontrado que la distribución de la energía cinética turbulenta, el flujo

medio y la velocidad de la ola no sólo dependen de la densidad del modelo de la vegetación acuática, sino que también de la estructura del modelo, si los tallos son flexibles o rígidos. Los dos tipos de vegetación sumergida rígida y flexible atenúan la ola en la frontera dentro y fuera de la vegetación. Basado en el flujo medio, la frontera de plantas rígida se puede dividir en tres regiones, la zona dentro de la vegetación, la zona lejos de la vegetación sin plantas y la zona cercana de las plantas con la presencia de una cizalla.

El tercer objetivo es el estudio de la hidrodinámica en un modelo de vegetación acuática con la presencia de un gap transversal, es decir, un gap orientado perpendicularmente a la dirección de la ola (capítulo 5). Se ha encontrado que la velocidad de la ola aumenta dentro al gap para las dos densidades estudiadas hasta que llegue a los valores de velocidad de la ola del caso sin plantas. Los resultados muestran que la energía cinética turbulenta dentro del gap aumenta, pero se mantiene inferior a la energía cinética turbulenta del experimento de sin plantas.

Todos los experimentos en esta tesis se han llevado a cabo en el laboratorio con una distribución de vegetación acuática y una configuración experimental para imitar situaciones reales del campo. Este tipo de situaciones se corresponde a la pradera de la zona costera. La mayor parte de los experimentos se han llevado a cabo con plantas sumergidas para modelar una pradera de *Posidonia oceanica*. Sin embargo, algunos experimentos se han llevado a cabo con plantas rígidas y sólo se presenta un caso con vegetación emergente, a fin de simular las condiciones en zonas poco profundas. El régimen de flujo en todos los experimentos ha sido el mismo, es el flujo de la ola que caracteriza las olas en aguas poco profundas.

Al final de la tesis se incluye una copia de la publicación de los resultados del capítulo 3 en la revista *Journal of Hydrology*, esta revista está incluida en la categoría Civil Engineering y ocupa la posición 4 de las 125 revistas en la categoría (Fuente: ISI Web of Knowledge). Es una revista de cuartil 1 y tiene un índice de impacto de 3.053.

Chapter 1. Introduction

1.1 Seagrasses and saltmarshes

Salt marshes, seagrass meadows and mangroves forests are characteristic of shallow coastal and littoral zones and support a large variety of infauna relative to bare sand areas (Feller and McKee, 1999; Fredriksen et al., 2010; Hendriks et al., 2011; Coulombier et al., 2012). These vegetated systems cover less than 0.5% of the sea bed but account for up to 70% of the carbon storage in ocean sediments (Duarte, 2002). Submerged and emergent aquatic plants characteristic of saltmarshes and seagrass meadows influence the spatial distribution of key water quality parameters. Therefore, aquatic plants are recognized as water quality indicators and their restoration and protection is a priority given that their regrowth is slow and variable (Moore et al., 2000, Orth et al., 2009). Seagrass and saltmarsh habitats provide

many benefits to the society that are known as ecosystem services, such as the conservation of the marine biodiversity, the regulation of the quality of coastal waters or the protection of the coast line (EEC, 1992). All of these issues are beneficial to humans and have economic implications. Furthermore, the presence of seagrasses is an indicator of the status of the coastal zones and might bring clues to whether strategies are required to improve the environmental quality of the zone.

Wetlands and coastal zones are governed by external physical forcings that result in the presence of tidal currents, waves, wind and currents among others. This Thesis starts from the hypothesis that the presence of aquatic vegetation modifies the hydrodynamics climate around submerged and emergent vegetation. The modification of the flow will depend on the status of the canopy, whether it is dense or sparse or whether it is continuous or fragmented or formed by flexible or rigid plants. The Thesis aims to study fragmented canopies with different gap structures and orientations, a gap being defined as a region without plants within a meadow. It also aims to study whether canopies produce sheltering in gaps or nearby bare soil areas and if it is the case under which conditions this sheltering results.

Coastal canopies reduce ambient flows and turbulence (Koch et al., 2006, Pujol et al., 2010, Pujol et al., 2013a, Pujol et al., 2013b) and attenuate waves (Granata et al., 2001, Lowe et al., 2005, Luhar et al., 2010, Pujol et al., 2013a), resulting in a reduction in sediment resuspension (Gacia and Duarte, 2001, Bouma et al., 2007, Hendriks et al., 2008, Coulombier et al., 2012, Ros et al 2014). Seagrasses therefore provide shelter to many species that cannot sustain the drag forces exerted by the flow (Hendriks et al., 2011). Emergent vegetation reduces turbulence depending on wind stress and macrophyte mechanical forcing (Coates and Folkard, 2009). Aquatic vegetation ranges in flexibility, from rigid emergent mangroves to highly flexible canopies such as submerged seagrasses. Coral reefs can also be considered to be a rigid structure (Lowe et al., 2005). Pujol et al. (2010 and 2013a) found that flexibility and

canopy density play a major role in the effectiveness of the canopy to attenuate waves and turbulence. Meadows of seagrasses are known to alter benthic coastal zones in the way that they support good quality standards and large variety of fauna compared to nearby bare sand areas (Fredriksen et al., 2010). Seagrasses provide microhabitat for a large number of organisms which could not live in unvegetated areas. The rhizomes and roots provide the substratum for attachment. As a result, the biodiversity of fauna living in these ecosystems is considerably greater than in adjacent unvegetated areas (Tanner, 2005). Among quality standards we recall the fact that dense and tall canopies show reduction in turbidity and increase in light penetration (Gruber and Kemp, 2010). The increased quality of water within canopies is associated with complex interactions between the hydrodynamics and the canopies at both canopy and plant scales.

All of these above mentioned effects of seagrasses on the modification of hydrodynamics make seagrasses a recognized and valuable habitat for coastal zone development. As such, *Posidonia oceanica* is one of the seagrass meadows listed as priority habitats in the EC Directive 92/43/EEC on the Conservation of Natural Habitats and of Wild Flora and Fauna (EEC1992). Therefore, submerged aquatic plants are recognized as water quality indicators and their restoration and protection is a priority considering that their regrowth is slow and variable (Orth et al., 2009).

The global extent of seagrasses is believed to be about 0.6×10^6 km² (Charpy-Rouband and Sournia, 1990). Some seagrass species have been able to form long-lasting meadows >4000 years old (Duarte, 2002). *Posidonia oceanica* meadows are experiencing a great decline in many areas of the Mediterranean Sea due to both natural and anthropogenic disturbances (Marbà et al., 1996; Boudouresque et al., 2009; Lasagna et al., 2011). Human activities, such as trawling or anchoring are known to alter marine ecosystems directly, whereas others such as jetty constructions also alter marine ecosystems indirectly, through the effects driven by the

management (Lasagna et al., 2011) or indirectly through a change in the hydrodynamics. The construction of new ports is associated with changes in sediment transport patterns, involving both increased erosion and sediment accumulation along the adjacent coast. These changes can exert significant damage on seagrass ecosystems kilometers away, which can be impacted by both erosion and burial with the changing sedimentary patterns. Furthermore, the construction of new ports entails other problems such as an increase in contamination due to the increase in ship traffic and also other damaging activities such as dredging and ship anchoring. The response of the meadows to such natural and man-induced disturbances is complex and not fully understood. However, while some meadows still persist, some others have already been lost (Duarte, 2002). Some authors report the response of the meadows to both a decline in biomass and canopy density (Terrados and Medina-Pons, 2010) or to a partially modification of the spatial structure, in terms of spatial variations in within –bed architectural characteristics (Borg et al., 2005).

1.2 The fragmentation of seagrasses and saltmarshes

Seagrasses along European coasts are often described as degraded when they have low shoot densities, high mortality rates and high fragmentation (Airoldi and Beck, 2007). In their review, Airoldi and Beck (2007) state that fragmentation occurs when previous continuous habitats become patchier. Meadow–scale morphodynamics modifications result in fragmented seagrass communities defined by the discontinuous presence of patches of plants and gaps. Gaps within seagrasses decrease the connectivity between patches of vegetation, especially when such gaps are large. Seagrass discontinuities affect hydraulics and consequently macroscale suspended particulate matter budgets (Fonseca and Fisher, 1986; Folkard, 2005). This effect is generally quantified through drag coefficients, which may be functions of plant size, morphology, density and flow depth. Seagrasses require an underwater irradiance generally above 11% the incident at the water surface for growth. This requirement generally

sets their water lower depth limit (Duarte, 1991). The upper depth where a seagrass can be found is imposed by their requirement for sufficient immersion in seawater, the depth where waves interact with the bottom (Vacchi et al., 2012) and by ice at high latitudes (Hemminga and Duarte, 2000). Therefore, the lower depth of *Posidonia oceanica* might change in future climate change scenarios, increasing the vulnerability of these seagrasses. Once a gap is formed within a meadow it changes the local environmental conditions. Ewel et al. (1998) found that water temperature, salinity and light in mangrove forest gaps were all greater than those within the canopy. Gaps of vegetation produced within a canopy leave the bottom exposed either to waves and currents, and the underlying mate is no longer protected against erosion (Pergent et al., 2014). Gaps within a canopy may have different patterns or structures depending on the evolution of the gapping agent. Seagrass meadows may be interrupted by erosive intermats, sagittal channels and structural intermats. Storms may erode mattes, both directly by tearing whole sections away, and indirectly, by scouring their sediments, thus 'gapping' the meadow. Sagittal channels in meadows run perpendicular to the coast and are formed by return currents transporting wind- and/or wave-mixed surface waters to depth. Erosive intermats appear like oval potholes in seagrass mattes and are probably formed by whirling currents carrying rocks and stones to depth, locally destroying the mats (Bianchi and Buia, 2008). Small gaps (with size $1.5 h_v$, where h_v is the plant height) in mangrove forests result from insect attacks (Feller and McKee, 1999).

The formation of gaps within meadows may also be triggered by human activities such as anchoring, trawling, fish farming, laying cables and pipes (Boudouresque et al., 2012). Seagrasses reproduce mainly by vegetative growth (clonal seagrasses) and eventually by seed dispersal (non-clonal species). Clonal species have been found to better persist in large patches than in small patches (Robinson et al., 1992), i.e. in fragmented canopies. However, soil mineralization and plant succession were not affected by seagrass fragmentation (Robinson et al., 1992). The shape and orientation of seagrass is known to determine seagrass epifauna in

such a way that patches oriented perpendicular to the flow will intercept more colonists than patches oriented parallel with the current (Tanner, 2003). Habitat fragmentation is expected to increase the edge area versus the interior seagrass area. Species adapted to live within seagrasses might experience a decline when compared to species adapted to seagrass edges that would experience an increase with habitat fragmentation (Tanner, 2005). Tanner (2005) found an increase in seagrass abundance from the region outside a seagrass meadow towards the canopy reaching a maximum within the canopy. Therefore, an increase in fragmentation would result in a heterogeneous distribution of plants along the canopy that needs to be addressed in the future to understand its impact on the overall ecosystem. Fragmented canopies have been found to present smaller nitrate and detritus concentrations than continuous canopies (Ricart et al., 2015). However, Ricart et al. (2015) did not find different deposit patterns for allochthonous sediments in fragmented canopies compared to continuous canopies. Probably, an increase in sediment resuspension and currents in fragmented canopies could explain the decrease of nitrates and detritus in such canopies.

Although there are many studies that state the regression of seagrasses (Pergent et al., 2014), only few studies address the effect of the gaps on the modification of the hydrodynamics in the system. Folkard (2011) found different flow regimes in unidirectional flows through transversal gaps of submerged vegetation and showed that Reynolds number (based on canopy overflow speed and the gap depth) and the gap aspect ratio were the most important parameters in determining the modification of bed shear stress. Koch and Gust (1999) found that plants play different roles depending on the environmental hydrodynamics, thus waves are able to penetrate more within the canopy due to the back and forth movement of the blades compared to the case of unidimensional flow. The more the penetration the greater the mixing between the water in the canopy layer and the water above the canopy layer will be.

Alterations of hydrology due to the constructions of levees, culverts and floodgates have had devastating effects on saltmarshes and their faunal communities (Saintilian, 2009). These effects range from habitat destruction to modification of the ecology. When estuaries are closed or tidally blocked, water levels rise as a default of localized freshwater run off, partially or totally inundating the saltmarsh for extended periods of time. The partial inundation leads to the fragmentation or disconnection of saltmarsh fragments (or patches) of vegetation. Many saltmarsh plants such as *Sarcocornia spp* can only withstand short periods of time inundated before plants quickly root and decompose (Adams and Bate, 1994). At big spatial scales, saltmarshes have been broken up within urban areas or bisected by roads or other hard surfaces. The fragmentation in other habitats such as forests has been shown to cause a decrease in the biodiversity (Tscharncke et al., 2002). Species that are specialized will be the most susceptible in front of fragmentation. Instead, trophic generalists are expected to be more resilient to the external impacts associated with fragmentation (Hopkins et al., 2002).

1.3 The objectives of study and the organization of the thesis

Consequently, the general objective of this doctoral thesis has been to contribute to understand the modification of hydrodynamics in fragmented canopies, i.e. canopies with the presence of gaps. The effect of different parameters will be studied along the experiments such as the canopy density, the plant height and plant flexibility, the architecture of the gap and the gap width. Within the frame of this general goal, several specific objectives are also addressed:

- 1) The first objective has been to study the effect of a longitudinal gap within a canopy on the hydrodynamics within the canopy and the gap. As a longitudinal gap we understand a gap with its main axis in the same direction as the wave propagation. Attention is paid to the modification of ambient hydrodynamics as a

function of the ratio of gap width to plant height. Laboratory experiments were conducted on a longitudinal gap using a model canopy exposed to waves, mimicking structural disturbances of canopies in benthic salt marshes and seagrasses that are dominated by waves in shallow conditions. The results of this experiment are presented in **Chapter 3**.

2) The second objective was to study the hydrodynamics in a boundary of vegetation aligned to the direction of the wave propagation. Detailed measurements of the hydrodynamics within and outside the canopy are expected to provide information of the effect of the effect of the canopy on the nearby bare soil and vice-versa, the effect of the bare soil on the nearby canopy. The results of this experiment are presented in **Chapter 4**.

3) The third objective investigated the effect of transversal gaps within a canopy on the hydrodynamics within the canopy and within the gap. A transversal gap was understood as a gap with the main axis of the gap in the direction perpendicular to the direction of the wave propagation. Furthermore, it was interesting to check whether and in what conditions the nearby vegetation sheltered the gap. Attention was paid to the modification of ambient hydrodynamics as a function of the gap width and the canopy density. The specific objectives of our study were firstly, to quantify the wave field and turbulence found in the interior of simulated transversal gaps, and secondly, to determine how these gaps affected the hydrodynamic environment within the adjacent vegetation. Special attention was paid to the effects of both the gap width and the canopy density on the hydrodynamics within the gaps. The results of these experiments are presented in **Chapter 5**.

The General discussion of this Doctoral thesis are presented in **Chapter 6**.

The Conclusions of this Doctoral thesis are presented in **Chapter 7**.

The References of this Thesis are presented in **Chapter 8**.

Chapter 9 presents the list of publications obtained from the research of this doctoral Thesis.

Chapter 2. Materials and methods

2.1 The flume

The research was carried out in a 6 m-long, 0.5 m-wide and 0.5 m-deep flume, where the mean water height was $h=0.3$ m. The flume was equipped with a vertical paddle-type wave maker that was placed at the beginning of the flume. The vertical paddle was driven by a variable-speed motor that operated in all the experiments carried out at a frequency of 1.2 Hz. This frequency was chosen in accordance to the frequencies used by other authors (Bradley and Houser, 2009; Hansen and Reidenbach, 2012; Pujol et al., 2013a and 2013b). Furthermore, with this frequency, waves had a wavelength of 1.03 m, which corresponds to transitional water waves, typical for regions dominated by the presence of aquatic vegetation. A plywood beach of slope 1:3 was situated at the end of the flume. It was covered in foam to better

attenuate incoming waves. The longitudinal direction is defined as x , and $x = 0$ is situated at the first boundary of the gap performed within the vegetation; y is the lateral direction and $y = 0$ at the centreline of the tank, and z is the vertical direction, with $z = 0$ at the flume bed.

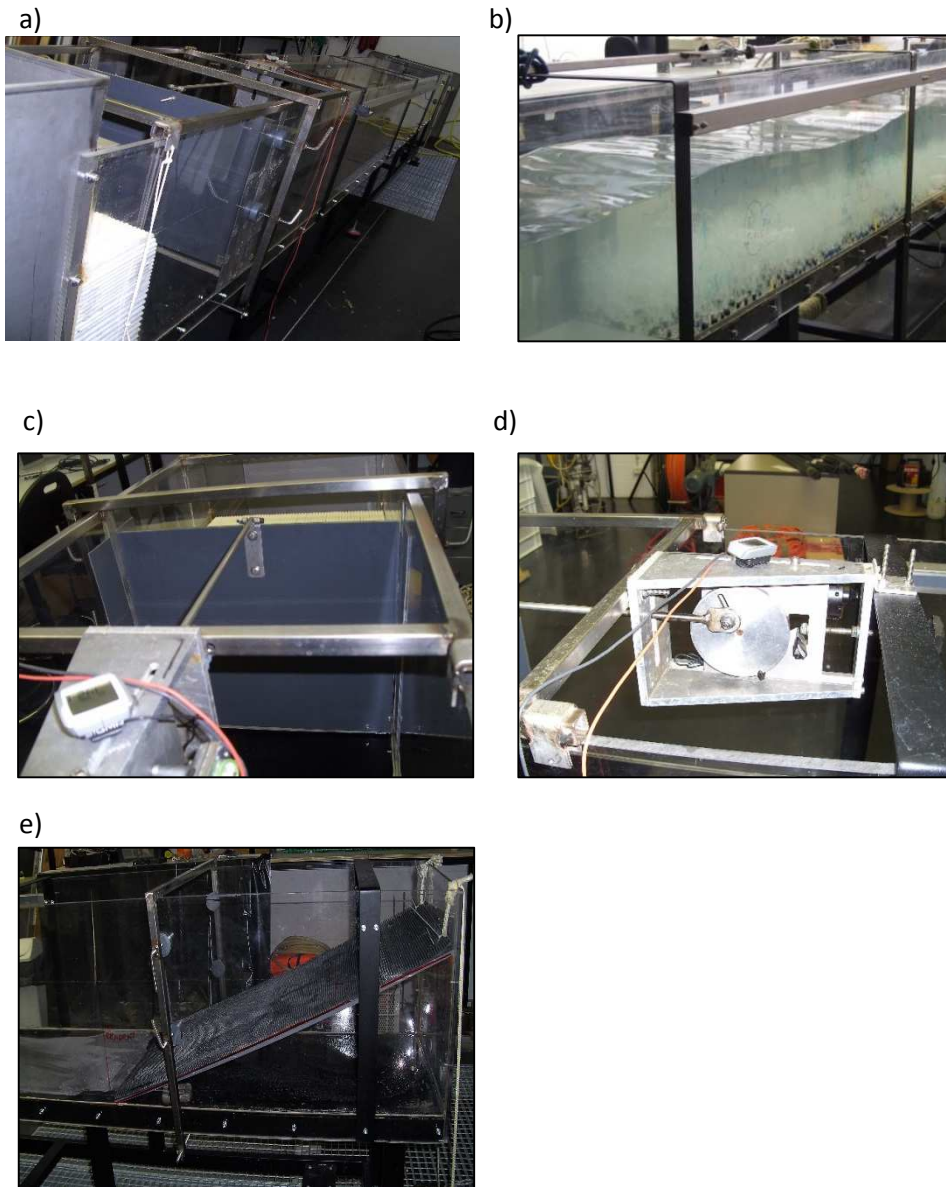


Figure 2.1 Photographs of the laboratory experimental flume. a) Lateral view of the flume. b) Lateral view with a distribution of flexible vegetation. c) Paddle wavemaker situated at the beginning of the flume. d) Variable speed motor. e) Plywood beach of slope 1:3 situated at the end of the flume.

2.2 Acoustic Doppler Velocimeter (16 Mhz- ADV, Sontek Inc.)

Measurements were made with an Acoustic Doppler Velocimeter (16 Mhz- ADV, Sontek Inc., Figure 2.2). This instrument is designed to record the three instantaneous velocity components at a single-point situated 5 cm far from the tip of the probe with a high frequency (50 Hz). The ADV was placed in the flume in a down looking configuration and connected to a PC with data acquisition software. The ADV instrument was configured to transmit 50 signals per second with a sampling time interval of 10 minutes (30000 recording per sample).



Figure 2.2 Photograph of acoustic doppler velocimeter (16 Mhz- ADV, Sontek Inc.).

To avoid spikes in the data record, beam correlations lower than 80 % were removed. Low correlation was obtained at two vertical positions ($z = 8$ cm and $z = 20$ cm above the bottom). These depths are known as “weak spots”. These “weak spots” occur when the first pulse emitted from the ADV is reflected at the bottom of the flume and meets in time and space the second pulse at the sampling volume (Pujol et al., 2013a). As the time lag between pulses depends on the velocity range, the ADV operational range was changed for these points (Sontek YSI, Acoustic Doppler Velocimeter Technical Instrumentation). To determine the effect of the ADV operational range on wave velocity, measurements were done 10 cm above the bed of the flume in two ranges: up to 30 cm s^{-1} and up to 100 cm s^{-1} ; wave velocities only differed by 0.7%.

In order to obtain valid data acquisition within the canopy, a few stems were removed to ensure the ADV beam was not blocked and the acoustic receivers and transmitter performed properly (Neumeier and Ciavola, 2004, Neumeier and Amos, 2006). To test the effect of the ‘hole’ on the ambient hydrodynamics, velocities were measured half a centimetre above the top of the canopy, both with and without the hole. A 3% difference in velocities between “hole” and “no hole” canopies was observed at the highest SPF; only 1% difference was observed at the lowest SPF. We therefore concluded that the ‘hole’ made minimal modification to the ambient hydrodynamics.

2.3 The model canopy

2.3.1 The rigid model canopy

The model canopies were 2.5 m long along the main axis of the flume and occupied all the width. Canopies were made of PVC cylinders of 1 cm width. A rigid canopy model was considered, with two heights, submerged (plant height $h_v = 14$ cm) and emergent (plant height $h_v = 29$ cm), where emergent canopies were defined as vegetation whose height was emergent for nearly half of the wave cycle. The canopy was constructed using cylinders that were inserted in a plate situated on the base of the flume that was 1 cm thickness.

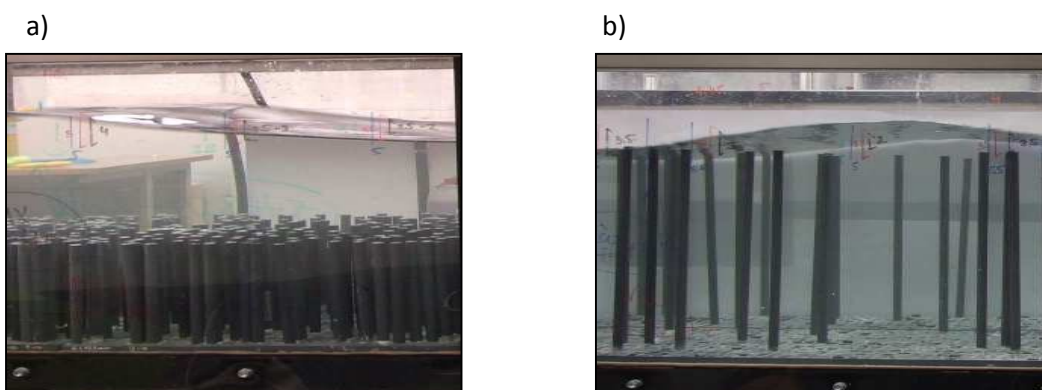


Figure 2.3 Photographs of vegetation studied. a) Submerged rigid vegetation mode, b) Emergent rigid vegetation model.

2.3.2 The flexible model canopy

The flexible canopy model was constructed following Pujol et al. (2013a), i.e., six individuals of high-density polyethylene blades of 0.14 m of length and 0.004 m of width were attached with a plastic band to a PVC dowel (2-cm long x 1-cm diameter). The thickness of the plastic blades was of ~ 0.075 mm. The model plants were dynamically and geometrically similar to typical seagrasses. Dynamic similarity is based on two independent ratios, λ_1 (which is the ratio between the buoyancy force and the rigidity restoring force of the blade) and λ_2 (which is the ratio between the restoring force due to the blade rigidity and the drag force). The drag force is defined as $F_d = \rho_w A_f C_d U_c$, the buoyancy force as $F_B = (\rho_w - \rho_s) g h_v w_b t_b$, and the rigidity restoring force of the blade as $F_r = E I / h_v$ (Luhar et al., 2010); where ρ_w is the density of the water (1000 kg m^{-3}); A_f is the frontal area of the blade; C_d is the blade drag coefficient (of order 1); U_c is the mean in-canopy velocity; ρ_s is the density of the blades (956.5 kg m^{-3}); g is the gravitational constant (9.8 m s^{-2}); h_v is the height of the vegetation (0.14 m); w_b is the width of the blade; t_b is the thickness of the blade ($0.075 \cdot 10^{-3} \text{ m}$); $I = w_b t_b^3 / 12$ is the second moment of area; and E is the modulus of elasticity ($3 \cdot 10^8 \text{ Pa}$). As noted by Ghisalberti and Nepf (2002), the dependence of λ_2 on U_c makes λ_2 vary tremendously in the field, so λ_1 was chosen as the critical design parameter. For the blade model used in this study, λ_1 is $0.07 \text{ s}^2 \text{ m}^{-1}$. Using the measurements given by Folkard (2005) for a model of *Posidonia oceanica* (ρ_s is $910 \pm 110 \text{ kg m}^{-3}$; h_v is 0.25 m; E is $4.7 \pm 0.6 \cdot 10^8 \text{ Pa}$; and t_b is $0.2 \cdot 10^{-3} \text{ m}$) that was found to mimic the real *Posidonia oceanica*, we obtained $\lambda_1 = 0.075 \text{ s}^2 \text{ m}^{-1}$, close to that used by the Folkard (2005) model, which shows that our prototype of vegetation could dynamically mimic the properties of coastal seagrasses.

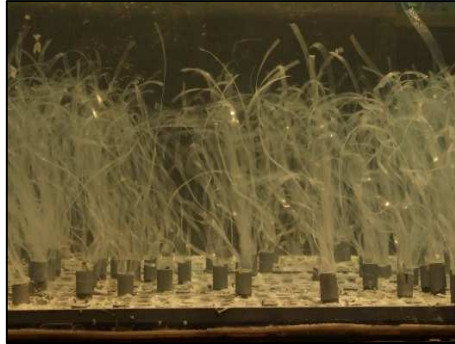


Figure 2.4 Photograph of submerged flexible vegetation model.

2.4 The methods

2.4.1 Solid Plant Fraction, SPF

Four canopy densities were used (Solid Plant Fraction, SPF) of 2.5, 5, 7.5 and 10%, which corresponded to 320, 640, 960 and 1280 shoots/m², respectively. The distribution of each SPF was made by means of a computer randomisation function with the distributions shown in figure 2.5.

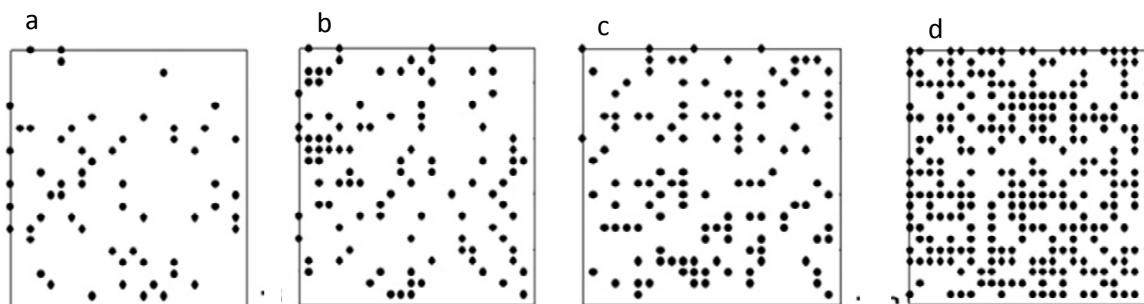


Figure 2.5 The distribution of SPFs. a) SPF=2.5%, b) SPF=5%, c) SPF=7.5%, d) SPF=10%.

The SPF can be defined as the fractional plant area at the bottom occupied by stems $SPF(\%) = n_{\text{stems}}A_{\text{stem}}/A_{\text{total}} \times 100$, where n_{stems} is the number of stems, A_{stem} is the horizontal area of each stem ($A_{\text{stem}} = \pi d^2/4$), where d is the plant diameter and A_{total} is the total horizontal area occupied by plants.

Typical vegetation densities in salt marshes are from 296 stems m^{-2} to 505 stems m^{-2} (Capehart et al., 1989). Paul and Amos (2011) found that a seagrass population of *Zostera noltii* had strong seasonal variability, from 4600 shoots m^{-2} in summer to 600 shoots m^{-2} in winter. Fonseca and Cahalan (1992) found densities of 1900-2870 shoots m^{-2} for *Halodule wrightii*, 230-1350 shoots m^{-2} for *Syringodium filiforme*, 850-1500 shoots m^{-2} for *Thalassia testudinum* and 750-1000 shoots m^{-2} for *Zostera marina*. Neumeier and Amos (2006) reported densities of 1140 and 1450 shoots m^{-2} for a salt marsh canopy of *Spartina anglica*.

2.4.2 Description the calculation of U_c , $U_{w,rms}$, TKE, α_w and β_w

In oscillatory flows the instantaneous velocity u can be decomposed into mean wave induced current (U_c), orbital velocity (U_w) and turbulent velocity (u') components as

$$u = U_c + U_w + u'. \quad (2.1)$$

The above decomposition was made by using a phase-averaging technique (Luhar et al., 2010, Pujol et al., 2013a). The Hilbert transform was used to average oscillatory flow velocities with a common phase (φ). The velocity readings were binned into different phases following the procedure described by Pujol et al. (2013a). The instantaneous velocity measurements for each phase bin $u(\varphi)$ were then time-averaged for the entire record to yield the phase-averaged velocity values, U_c .

$$U_c = \frac{1}{2\pi} \int_0^{2\pi} u(\varphi) d\varphi \quad (2.2)$$

The root mean square of $u(\varphi)$ was then defined as the orbital velocity U_w^{rms} as:

$$U_w^{rms} = \sqrt{\frac{1}{2\pi} \int_0^{2\pi} (u(\varphi) - U_c)^2 d\varphi}. \quad (2.3)$$

U_w^{rms} will be named hereafter as U_w .

To calculate the TKE profile for stationary velocity records, the instantaneous velocities (u, v, w) at each point were decomposed into the sum of time-averaged velocities (U_c, V_c, W_c) and the turbulent components (u', v', w'), which means that the TKE can be calculated from the following equation:

$$TKE = 1/2(\overline{u'^2} + \overline{v'^2} + \overline{w'^2}) \quad (2.4)$$

The turbulent Reynolds stress, $u'w'$, was calculated multiplying the turbulent horizontal and vertical components and averaging over time.

The wave velocity ratio $\alpha_w = U_w / U_{w,wp}$ (called hereafter wave attenuation) was calculated with the aim to quantify the difference in the wave velocity for cases with the presence of plants with cases without plants. Since this above mentioned ratio can vary with height within the canopy, a vertically averaged ratio, $\langle \alpha_w \rangle$, over the canopy layer was considered as representative for the local wave attenuation induced by the canopy. Also, the wave velocity ratio $\beta_w = U_w / U_{w,no-gap}$ was calculated to quantify the difference in the wave velocity in canopies with gaps compared with canopies without gaps. Also, a vertically averaged value of β_w within the canopy will be calculated and denoted as $\langle \beta_w \rangle$.

The specific geometry of the canopy stems is known to determine the flow structure within a canopy. Several studies (Britter and Hanna, 2003, Lowe et al., 2005 and Luhar et al. 2010) use the lambda parameters λ_p and λ_r to determine the flow structure within the canopy, where

$$\lambda_f = \frac{h_p d}{(S+d)^2} \quad \text{and} \quad \lambda_p = \frac{\pi d^2}{4(S+d)^2} \quad (2.5)$$

where d is the stem diameter and S is the plant-to-plant distance.

Lowe et al (2005) defined different canopy flow regimes depending on the ratio A_∞^{rms}/S , where $A_\infty^{\text{rms}} = U_{\infty,w}^{\text{rms}}/\omega$ ($\omega = 2\pi f$ and $U_{\infty,w}^{\text{rms}}$ is the wave velocity above the canopy layer). A_∞^{rms} is the rms wave orbital excursion length of the free-stream potential flow. Lowe et al. (2005) classified the flow into three possible regimes: the canopy independent flow, the inertia flow dominated regime and the unidirectional limit. The experiments considered in this study corresponded to the inertia dominated regime. From Lowe et al. (2005), in the inertia flow dominated regime, the wave attenuation can be calculated from the lambda parameters as,

$$\alpha_w = \frac{1-\lambda_p}{1+(C_M-1)\lambda_p}. \quad (2.6)$$

Here, C_M was considered equal to 2 for potential flow around circular cylinders (Dean and Dalrymple, 2002).

Chapter 3. Hydrodynamics in canopies with longitudinal gaps exposed to oscillatory flows

Salt marshes, seagrasses and mangroves are vulnerable to environmental changes. Small gaps (with size $1.5 h_v$, where h_v is the plant height) in mangrove forests result from insect attacks (Feller and McKee, 1999). Gaps may have different patterns or structures depending on the evolution of the gapping agent. Lightning strikes usually create small circular gaps while seagrass meadows may be interrupted by erosive intermats, sagittal channels and structural intermats. All these gaps have both natural and human origins (Boudouresque et al., 2009, Lasagna et al., 2011). Storms may also erode mattes, both directly by tearing whole sections away, and indirectly, by scouring their sediments, thus 'gapping' the meadow. Sagittal channels in meadows run perpendicular to the coast and are formed by return currents transporting wind- and/or wave-mixed surface waters to depth. Erosive intermats appear like

oval potholes in seagrass mattes and are probably formed by whirling currents carrying rocks and stones to depth, locally destroying the mats (Bianchi and Buia, 2008). The formation of gaps within meadows may also be triggered by human activities such as anchoring, trawling, fish farming, laying cables and pipes (Boudouresque et al., 2012). Once formed the gap changes the local environmental conditions and Ewel et al. (1998) found that water temperature, salinity and light in mangrove forest gaps were all higher than those within the canopy.

Despite their variety, little has been investigated to elucidate the effects of gaps on adjacent vegetation, especially in wave-dominated domains. Therefore this study investigates the effect of a longitudinal gap (with the main axis of the gap in the same direction as the wave propagation) within a canopy on the hydrodynamics within the canopy and the gap. Attention is paid to the modification of ambient hydrodynamics as a function of the ratio of gap width to plant height. Laboratory experiments were conducted on a longitudinal gap using a model canopy exposed to waves, mimicking structural disturbances of canopies in benthic salt marshes and seagrasses that are dominated by waves in shallow conditions. The specific objectives of our study were firstly, to identify and quantify the patterns of mean flow and turbulence found in the interior of simulated longitudinal gaps, and secondly, to determine how these gaps affected the hydrodynamic environment within the adjacent vegetation patches. Special attention was paid to the effects of both the gap width to plant height ratios and the canopy density on the hydrodynamics within the gaps.

3.1 Experimental set up for a canopy with a longitudinal gap

In this sub-chapter I present the detailed methodology corresponding to the experiments for longitudinal gaps within a canopy. In this study, a longitudinal gap is a gap

within a canopy with its main axis aligned to the wave flow propagation. In this case the direction of the wave propagation is aligned to the main axis of the flume.

The model canopies were 2.5 m long and they were situated at the centre of the flume beginning at 1 m from the paddle wave maker. A rigid canopy model was considered, with two heights, submerged (plant height $h_v = 14$ cm) and emergent (plant height $h_v = 29$ cm), where like Pujol et al. (2013b) emergent canopies were defined as vegetation whose height was emergent for nearly half of the wave cycle. A flexible submerged model canopy (with plant height $h_v = 14$ cm) was also considered under study.

A region free of plants (hereafter called the gap) was situated at the center of the flume in the y direction and extended longitudinally along the main axis of the flume all though the full length of the canopy (Figure 3.1). Two different gap widths (GW) were considered with $GW = 0.25b$ and $GW = 0.375b$, where b is the width of the flume (Figure 3.1).

Considering the plant heights used for both submerged ($h_v = 14$ cm) and emergent ($h_v = 29$ cm) vegetation, the ratios GW/h_v were of ~ 0.9 and 1.3 for the submerged canopies and of ~ 0.4 and 0.6 for the emergent vegetation. For the rigid canopy, two canopy densities of 640 and 1280 shoots m^{-2} were considered. For experiments with the submerged flexible vegetation, the canopy density of 1280 shoots m^{-2} and the 0.25 gap width were considered. Experiments with a full coverage of plants (i.e. without a gap) for all the cases and a study without plants were also carried out. A complete list of the experiments carried out is listed in Table 3.1, accounting for a total of 15 experiments.

The ADV was mounted in a frame and velocity profiles measured from 1 - 23 cm from the bottom of the flume, with a vertical resolution of 1 cm. Velocity measurements near the surface were limited by both wave shape and the 5 cm sampling volume of the ADV.

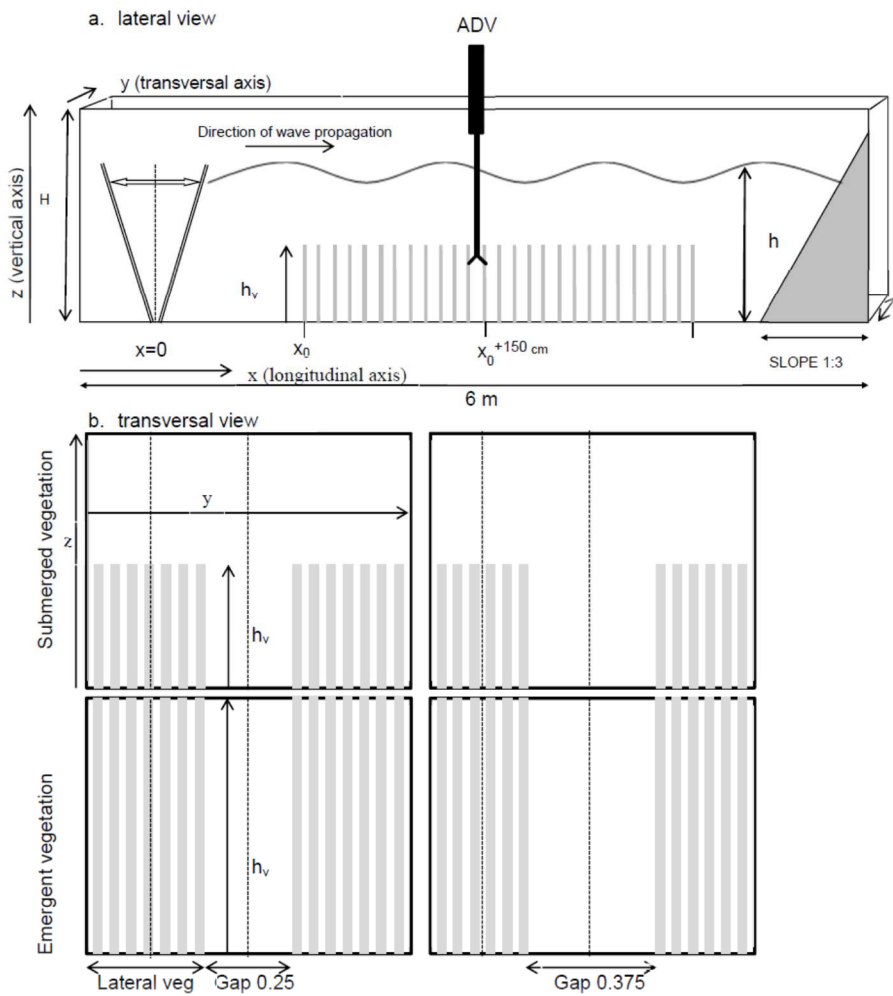


Figure 3.1 a) Schematic diagram of the experimental flume. Vertical grey lines represent the vegetation model. The ADV is the Doppler sensor for the velocity measurement. The wave maker is schematized at the beginning of the flume. b) Transversal section with the gap and the vegetation zones. Vertical dashed lines represent the y -positions where vertical velocity profiles were measured. Vertical grey bars represent the distribution of the vegetation, submerged (middle panels) and emergent (bottom panels).

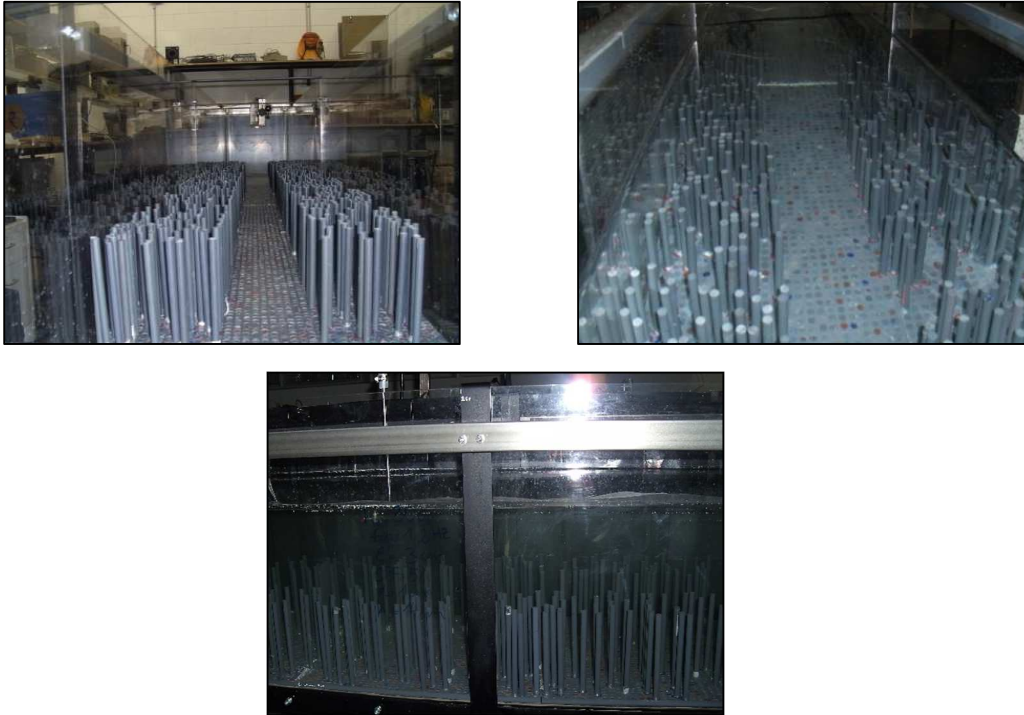


Figure 3.2 Photographs of canopy with a longitudinal gap.

SPF(%)	$n/A(\text{shoots}/\text{m}^2)$	GW/b	$h_v(\text{cm})$	Type
5	640	0.25	14	Rigid
5	640	0.375	14	Rigid
5	640	0	14	Rigid
10	1280	0.25	14	Rigid
10	1280	0.375	14	Rigid
10	1280	0	14	Rigid
5	640	0.25	29	Rigid
5	640	0.375	29	Rigid
5	640	0	29	Rigid
10	1280	0.25	29	Rigid
10	1280	0.375	29	Rigid
10	1280	0	29	Rigid
10	1280	0	14	Flexible
10	1280	0.25	14	Flexible
0	0	-	-	-

Table 3.1. Summary of the different experimental conditions. A is the horizontal area and b is the width of the flume.

Vertical profiles of U_c were measured for experiments using submerged rigid vegetation with two gap widths and two solid plant fractions (SPF). In addition, five control experiments were conducted, one without plants (denoted as “no-veg”) and another with a fully vegetated canopy i.e. without a gap (denoted as “no-gap”), one for each SPF studied for rigid emergent and submerged vegetation and one for the experiment with submerged flexible vegetation. Velocities were measured at the center of the gap and at the middle of the lateral vegetation, and were compared to velocities measured within similar canopies with no gaps and experiments with no vegetation (Figure 3.1).

Preliminary profiles of wave velocities were completed to characterize the different boundary layers, and to ensure measurements were taken at locations outside the flume wall boundary layer and also outside the boundary layers generated by the gap and the vegetation. Transects of U_w along the transversal section of the flume at $z=5$ cm above the bottom were used to characterize the different boundary layers at $SPF=10\%$ for both submerged (Figures 3.3.a and 3.3.b) and emergent (Figures 3.3.c and 3.3.d) plants. For experiments with a 0.25 gap, U_w was almost constant from -13 cm to -19 cm within the lateral vegetation for both the submerged (Figure 3.3.a) and emergent (Figure 3.3.c) plants. Within the lateral vegetation of the 0.375 gap condition, U_w may be partially affected by the gap boundary layer (Figures 3.3.b and 3.3.d). The vegetation boundary layer within the gap may affect those experiments using the 0.25 gap (Figures 3.3.a and 3.3.c). In contrast, U_w within the 0.375 gap was almost constant from -9 cm and 5 cm for the submerged vegetation (Figure 3.3.b) and from -5 cm to 5 cm for the emergent vegetation (Figure 3.3.d) suggesting that the measurements were not affected by the vegetation boundary layer. A wall boundary layer formed in the region from -20 cm to -25 cm for the emergent vegetation (Figures 3.3.c and 3.3.d). From these measurements, values of current velocity U_c and wave velocity U_w were calculated following the calculations presented in the analysis section. For experiments without plants, profiles of U_c in the center

of the flume were not significantly different to profiles closer to the flume side-wall, indicating that the mean current was not biased in the transversal section of the channel.

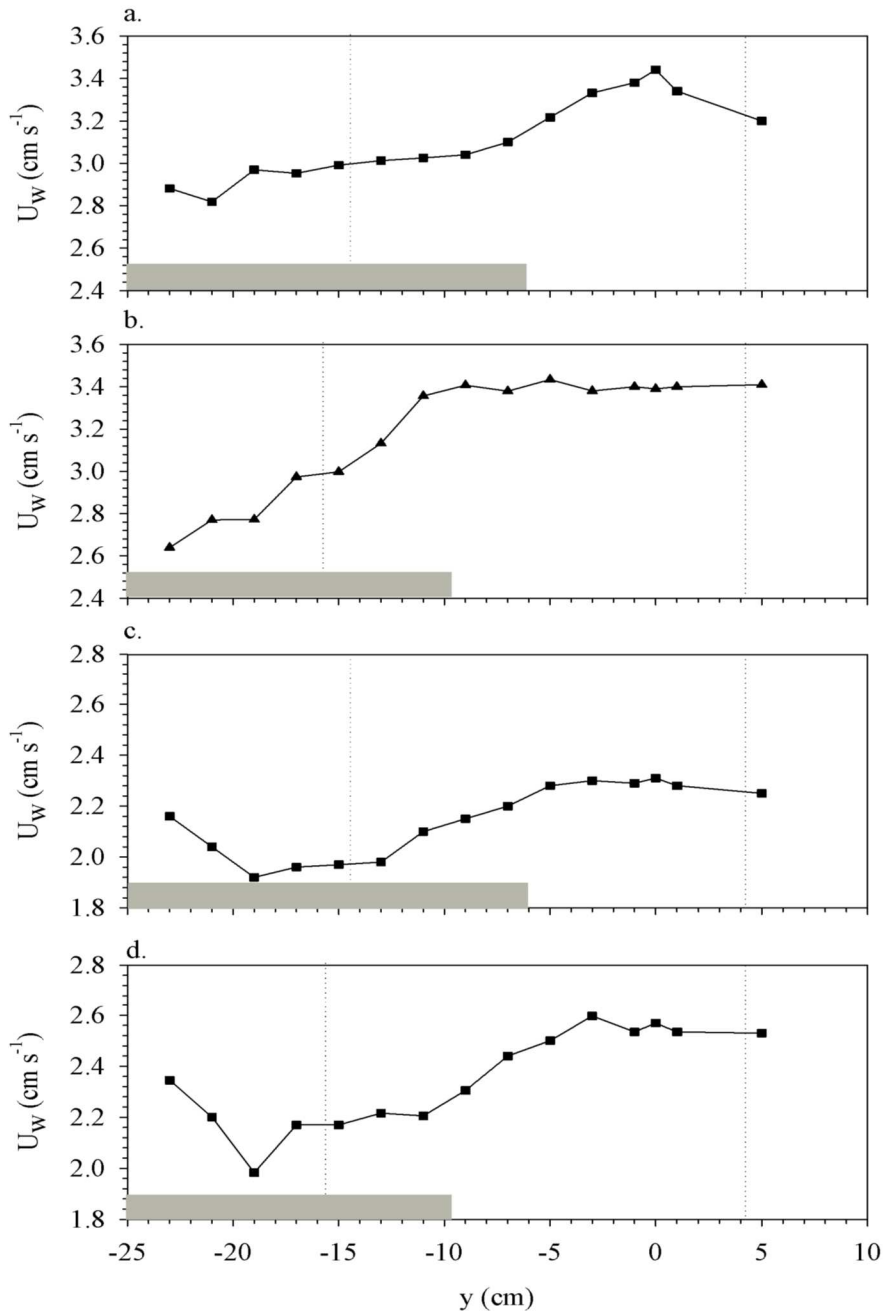


Figure 3.3 Wave velocity transects along the y-axis at $z=5$ cm for submerged vegetation for a 0.25 gap (a), for a 0.375 (b) and for emergent vegetation for a 0.25 gap (c) and for a 0.375 gap (d). Vertical dashed lines show the y-positions where vertical velocity profiles were measured. Grey boxes represent the zone covered by the vegetation.

3.2 Results

3.2.1 Mean wave induced currents - submerged rigid vegetation

From the vertical profiles, three vertical regions were distinguished: the above-canopy region ($z > 15$ cm above the bottom, up to the water surface), the canopy-top region ($z = 7 - 15$ cm), and the canopy-base region ($z = 0 - 7$ cm).

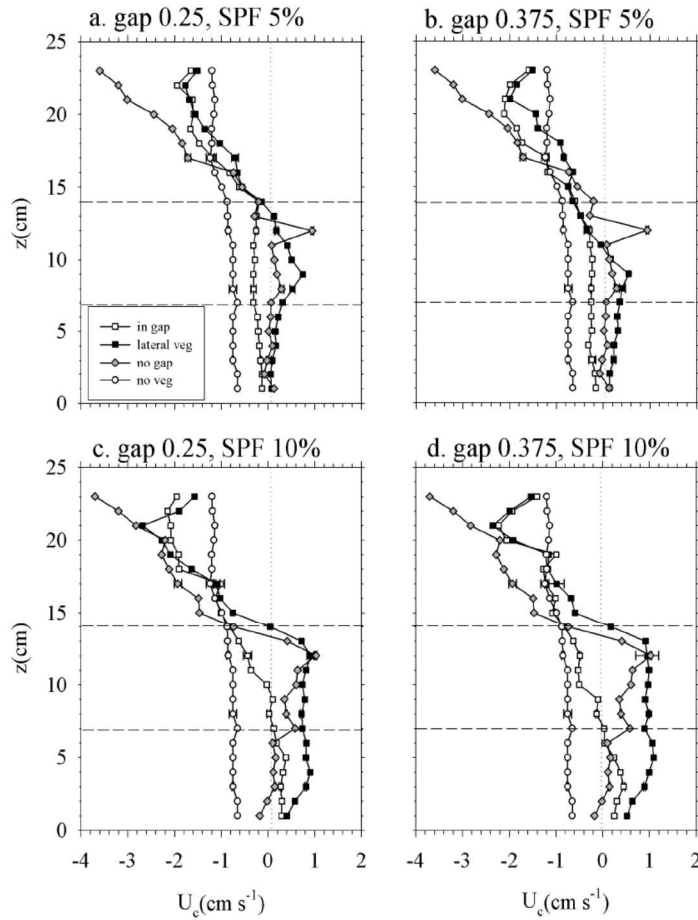


Figure 3.4 Mean current (U_c) for the submerged rigid vegetation experiments. a) for a 0.25 gap and 5% SPF; b) 0.375 gap and 5% SPF; c) 0.25 gap and 10% SPF; d) 0.375 gap and 10% SPF. Horizontal dashed lines show the limits of the above-canopy region (> 14 cm above the bottom), the canopy-top region (7 - 14 cm) and the canopy-base region (< 7 cm). Horizontal error bars represent the standard deviation of the mean over different replicas.

Canopy density, SPF, impacted on U_c in both the above-canopy and canopy-top regions (Figure 3.4). For 5% SPF and 0.25 gap width, $U_c \sim 0 \text{ cm s}^{-1}$ at the canopy-base region within the lateral vegetation, in the gap itself and in the no-gap control experiment (Figure 3.4.a). However, in the no-veg experiment U_c at the canopy-base region was negative. At the canopy-top region, different behaviours could be distinguished. Within the lateral vegetation, U_c increased across the canopy-base region and then decreased to 0 cm s^{-1} at the canopy-top region (Figure 3.4.a). For the no-gap experiments, U_c was slightly positive at the canopy-base region and increased at the canopy-top region. At the canopy-top region within the gap, U_c was nearly constant with slightly negative values (Figure 3.4.a). At the above-canopy region, U_c within the gap was similar to that found at the lateral vegetation. The no-gap control case showed larger negative velocities in the above-canopy region, (Figure 3.4.a). U_c in the no-veg experiments was nearly constant in both the canopy-base and canopy-top regions with increasingly negative values until 23 cm and then showed again a tendency to reverse above 23 cm.

Increasing to 0.375 gap width (at the same 5% SPF) created small differences in U_c (Figure 3.4.b). U_c at the canopy-base region showed some differences between the lateral vegetation, within the gap and for the no-gap experiment. In the lateral vegetation, U_c was small and positive (Figure 3.4.b) then increased slightly from the bottom upwards, whereas U_c in the no-gap control experiment was $\sim 0 \text{ cm/s}$. At the canopy-top region within the lateral vegetation, U_c increased negatively (Figure 3.4.b). This negative velocity was not observed for the 0.25 gap width experiment (Figure 3.4.a). In contrast, U_c in the no-gap experiment presented a peak of U_c at the canopy-top region. At the above-canopy region, U_c within the gap and in the lateral vegetation were similar. U_c for these cases increased to a maximum negative value at 20 cm above the bottom with a tendency to reverse upwards (Figure 3.4.b).

As was found for the case of 0.25 gap widths, U_c in the above-canopy region was larger than measured in the no-veg control experiment but smaller than measured in the no-gap experiment.

Similarly, when using 10% SPF, an increase in the gap width moderated velocities, particularly within the lateral vegetation (Figures 3.4.c and 3.4.d). For 0.25 gap width, U_c in the lateral vegetation was positive at the canopy-base region, increasing slightly upwards above the bottom, and then remaining constant in the canopy-top region. In the above-canopy region, the magnitude of U_c increased negatively (Figure 3.4.c), with a tendency to reverse towards the water surface. Within the gap, U_c at the canopy-base region was slightly positive. In the upper part of the canopy-top region, U_c increased negatively, becoming similar to that found in the lateral vegetation. For the no-gap control experiment, $U_c \sim 0$ cm/s at the canopy-base region. At the above-canopy region U_c increased negatively, with a tendency to reverse closer to the water surface. At the canopy-top region in the no-veg experiments U_c was more negative than in the gap but smaller in the above-canopy region. Increasing to 0.375 gap width showed an increase in U_c within the lateral vegetation (Figure 3.4.d). Within the gap, U_c was slightly positive at the canopy-base region (Figure 3.4.d). U_c in the gap was negative at the canopy-top region, increasing above the canopy. At the above-canopy region U_c within the gap and within the lateral vegetation reached a maximum at 21 cm with a tendency to reverse closer to the water surface.

3.2.2 Mean wave induced currents - emergent rigid vegetation

In the emergent rigid vegetation experiments, the SPF had a large effect on U_c within the lateral vegetation, but SPF did not have an effect on U_c within the gap (in contrast to the submerged vegetation experiments). The most significant differences between the submerged and the emergent vegetation was observed in the top 10 cm of the surface waters. Two distinct regions within the U_c profiles were observed: an in-canopy region ($z < 17$ cm), and a

surface boundary layer region ($z > 17$ cm). For 5% SPF and 0.25 gap width U_c at the in-canopy region within the lateral vegetation was negative (Figure 3.5.a).

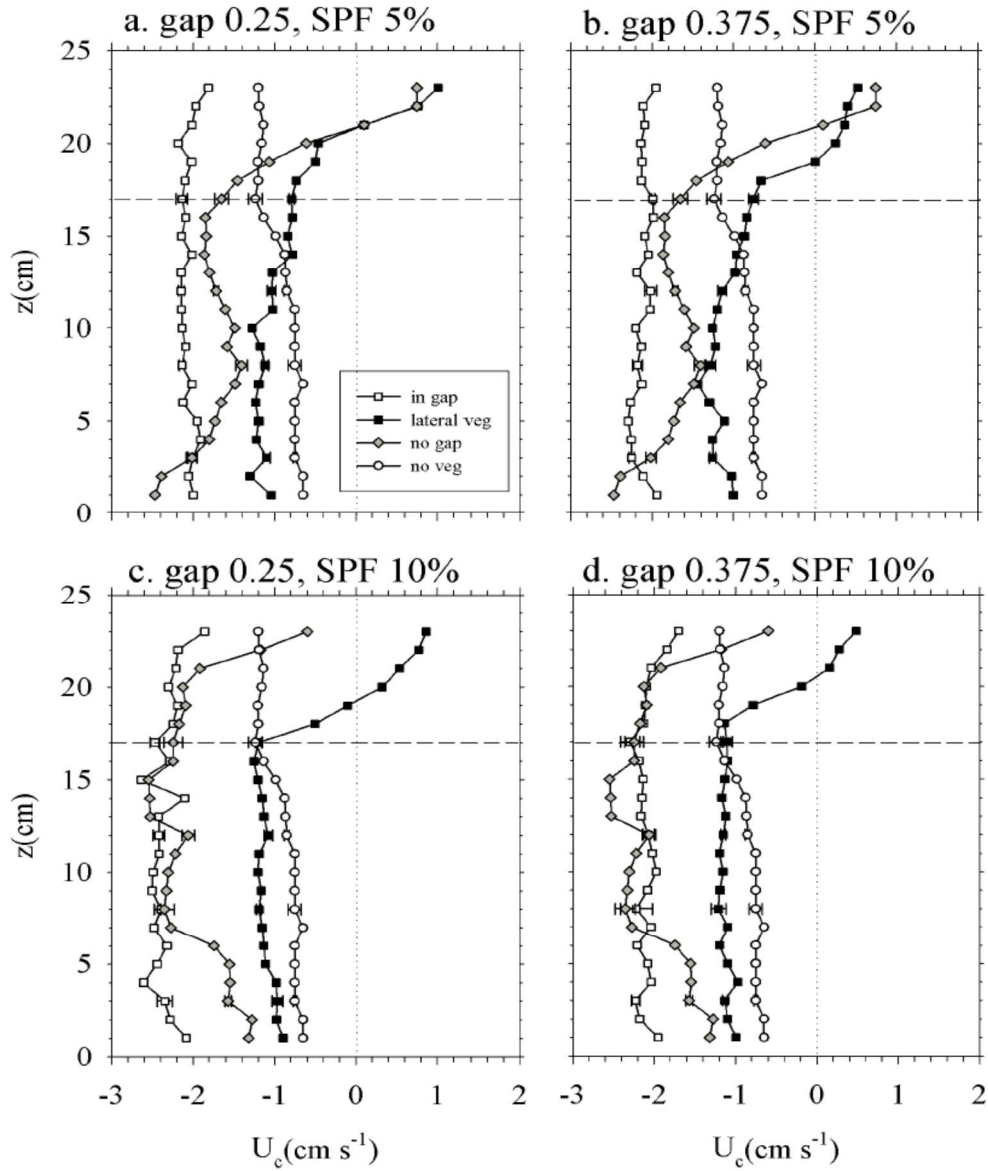


Figure 3.5 Mean current (U_c) for the emergent rigid vegetation experiments. a) for a 0.25 gap and 5% SPF; b) 0.375 gap and 5% SPF; c) 0.25 gap and 10% SPF; d) 0.375 gap and 10% SPF. The dashed horizontal line represents the limit of the in-canopy region (< 17 cm above the bottom) and the surface boundary layer (> 17 cm). Horizontal error bars represent the standard deviation of the mean over different replicas.

The largest U_c was measured within the gap and U_c for the no-gap control experiments was larger than measured within the lateral vegetation. The no-veg control experiments resulted in the smallest mean velocity observed at the in-canopy region. U_c became constant and negative throughout most of the surface boundary layer within the gap and for the no-veg control experiments, however above 20 cm within the gap and in the lateral vegetation U_c had a tendency to reverse, becoming positive at 21 cm above the bottom. The increase to 0.375 gap width did not produce appreciable changes in the U_c profiles (Figure 3.5.b). The increase in the canopy density to 10% SPF with 0.25 gap width increased U_c within the gap, within the lateral vegetation and also for the no-gap experiment (Figure 3.5.c). Within the surface boundary layer, U_c for the no-gap experiment with 10% SPF (Figure 3.5.c) did not reach positive values in contrast to the experiments with 5% SPF (Figure 3.5.a). As was found for the 5%, the increase to 0.375 gap width with 10% SPF did not result in changes in U_c (Figure 3.5.d).

3.2.3 Wave velocities – submerged rigid vegetation

The wave velocity ratio $\alpha_w = U_w / U_{w, \text{no veg}}$ (called hereafter wave attenuation) will be calculated with the aim to quantify the difference in the wave velocity for cases with the presence of plants with cases with no vegetation. Since this above mentioned ratio can vary with height within the canopy, a vertically averaged ratio, $\langle \alpha_w \rangle$, over the canopy layer will be considered as representative for the local wave attenuation induced by the canopy. Also, the wave velocity ratio $\beta_w = U_w / U_{w, \text{no-gap}}$ will be calculated to quantify the difference in the wave velocity in canopies with gaps compared with canopies without gaps. Also, a vertically averaged value of β_w within the canopy will be calculated and denoted as $\langle \beta_w \rangle$.

For all the experiments, U_w was calculated at different depths. U_w profiles for the case of the submerged vegetation of 5% SPF and 0.25 gap is presented in Figure 3.6.

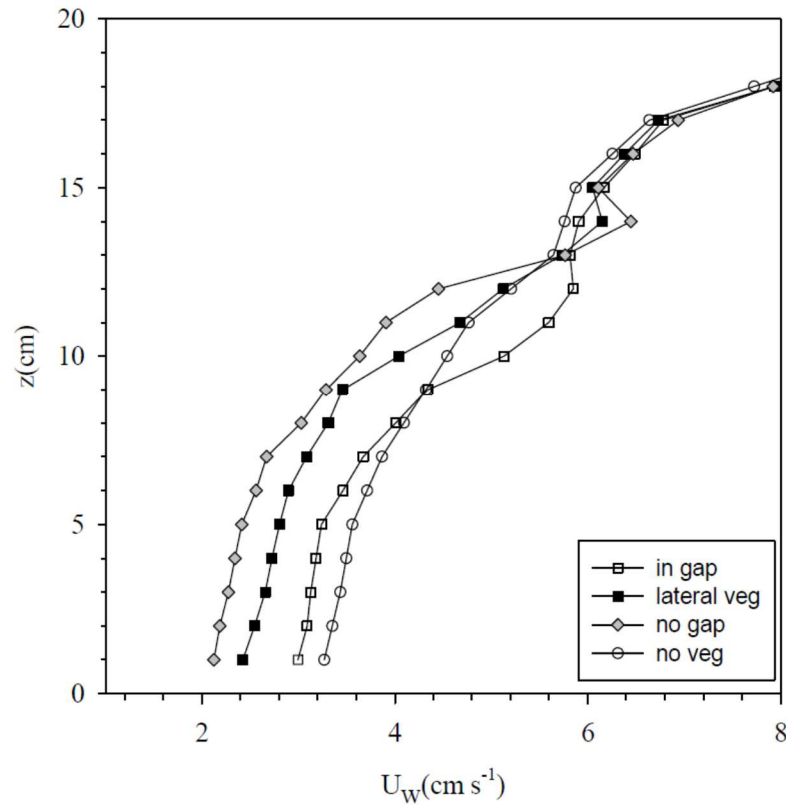


Figure 3.6 Wave velocity (U_w) profiles for all the experiments carried out with submerged vegetation at 10% SPF and for the 0.25 gap. The horizontal scale has been reduced to be able to see the details in U_w at both the canopy-top and the canopy-base regions.

U_w above the canopy in either the lateral vegetation, in the gap or in the canopy without gap was close to the U_w for the without plants experiment. However, in the layer occupied by the canopy U_w was reduced compared with the without plants. The minimum U_w , i.e. the maximum wave reduction compared with the without plants experiment, was for the no-gap canopy experiment.

Vertical profiles of orbital velocity (U_w) were normalized by the $U_{w,no-veg}$ profile in order to obtain the wave attenuation α_w as described in the Methods section for all the experiments carried out at different SPF and gap widths (Figures 3.7.a-d).

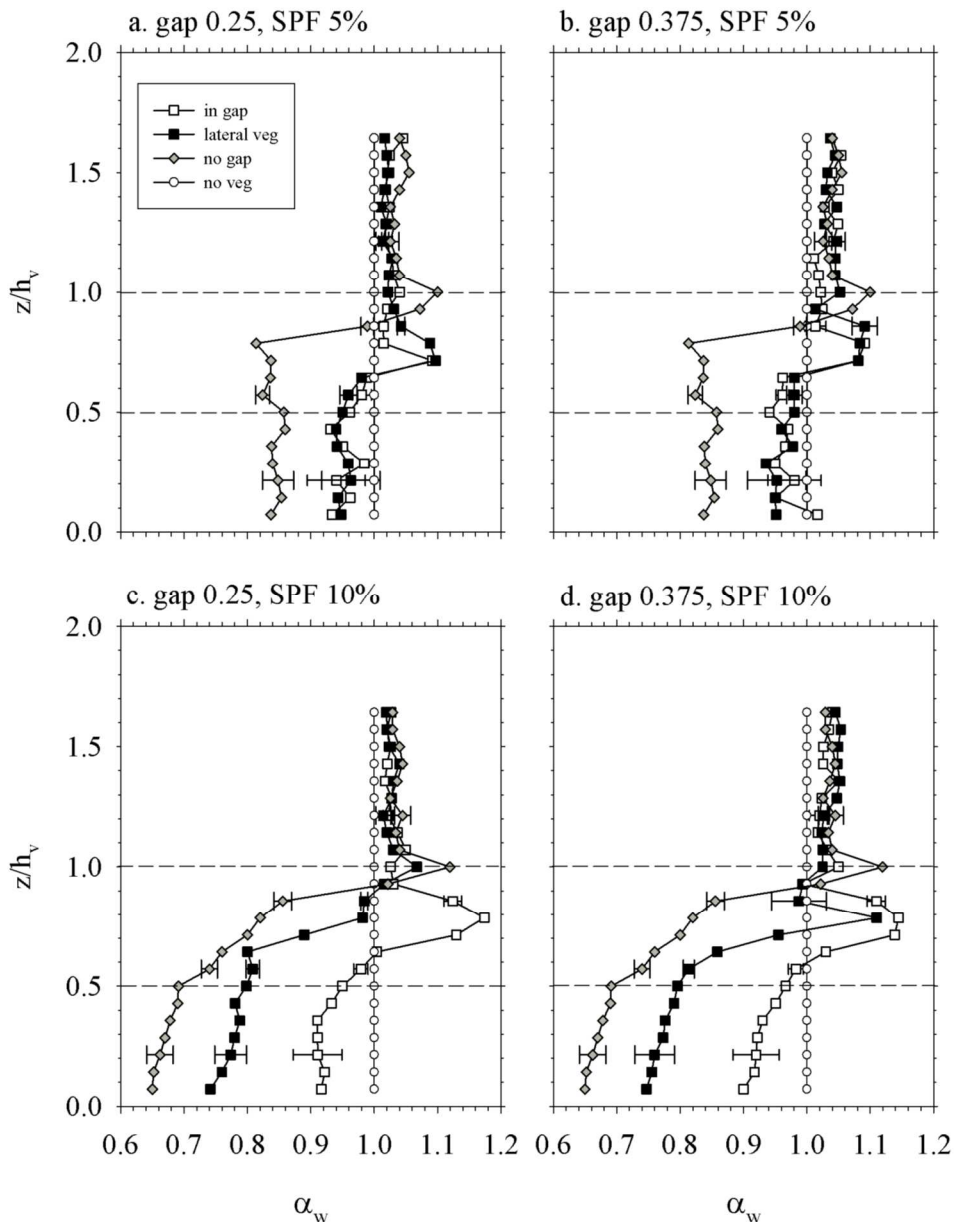


Figure 3.7 Wave velocity attenuation (α_w) for the submerged rigid vegetation experiments for a) 0.25 gap, SPF= 5%; b) 0.375 gap, SPF= 5%; c) 0.25 gap, SPF= 10%; d) 0.375 gap, SPF=10%. Horizontal dashed lines show the limits of the above-canopy region (> 14 cm), the canopy-top region (7 - 14 cm) and the canopy-base region (< 7 cm). Horizontal error bars represent the standard deviation of the mean over different replicas.

The wave velocity was, in general, reduced at the canopy-base region in the gap and lateral vegetation compared to the no vegetation experiment, although it was greater than compared to the no-gap experiment. In all experiments, and above the canopy region, α_w in

the gap and in the lateral vegetation (including the no-gap experiment) was slightly above 1 (Figures 3.7.a-d). In the canopy-top region, for both gaps studied (Figures 3.7.a and 3.7.b), α_w for both within the gap and the lateral vegetation, increased to a maximum at $z/h_v = 0.7$ (mid-depth of the canopy-top region). At the canopy-base region, for 5% SPF, α_w within the gap was close to that measured within the lateral vegetation (Figures 3.7.a and 3.7.b) but still with $\alpha_w < 1$, indicating an equal wave attenuation in both the gap and the lateral vegetation. However, this value was above that for the no-gap control experiment. α_w for the no-gap control experiment peaked in the upper part of the canopy-top region.

In contrast, for the densest canopy of 10%, α_w was smaller in the lateral vegetation than in the gap for both gap widths studied (Figures 3.7.c and 3.7.d).

3.2.4 Wave velocities – emergent rigid vegetation

In the experiments using emergent rigid vegetation, SPF had a significant effect on the wave velocity attenuation, similar to the experiments with submerged vegetation.

In all the cases, vertical profiles of α_w within the lateral vegetation and the gap were greater than measured for the no-gap experiments. For 5% SPF, there were minimal differences between α_w within the lateral vegetation and the gap (Figure 3.8.a), remaining constant with depth but slightly above α_w for the no-gap experiment (Figure 3.8.a). An increase to 0.375 gap width did not change the α_w vertical profile within the gap nor within the lateral vegetation (Figure 3.8.b). However an increase to 10% SPF caused a decrease in α_w within the lateral vegetation (Figures 3.8.c and 3.8.d). For experiments of 10% SPF, an increase in the gap width resulted in an increase in α_w in both the lateral vegetation and the gap (Figure 3.8.d).

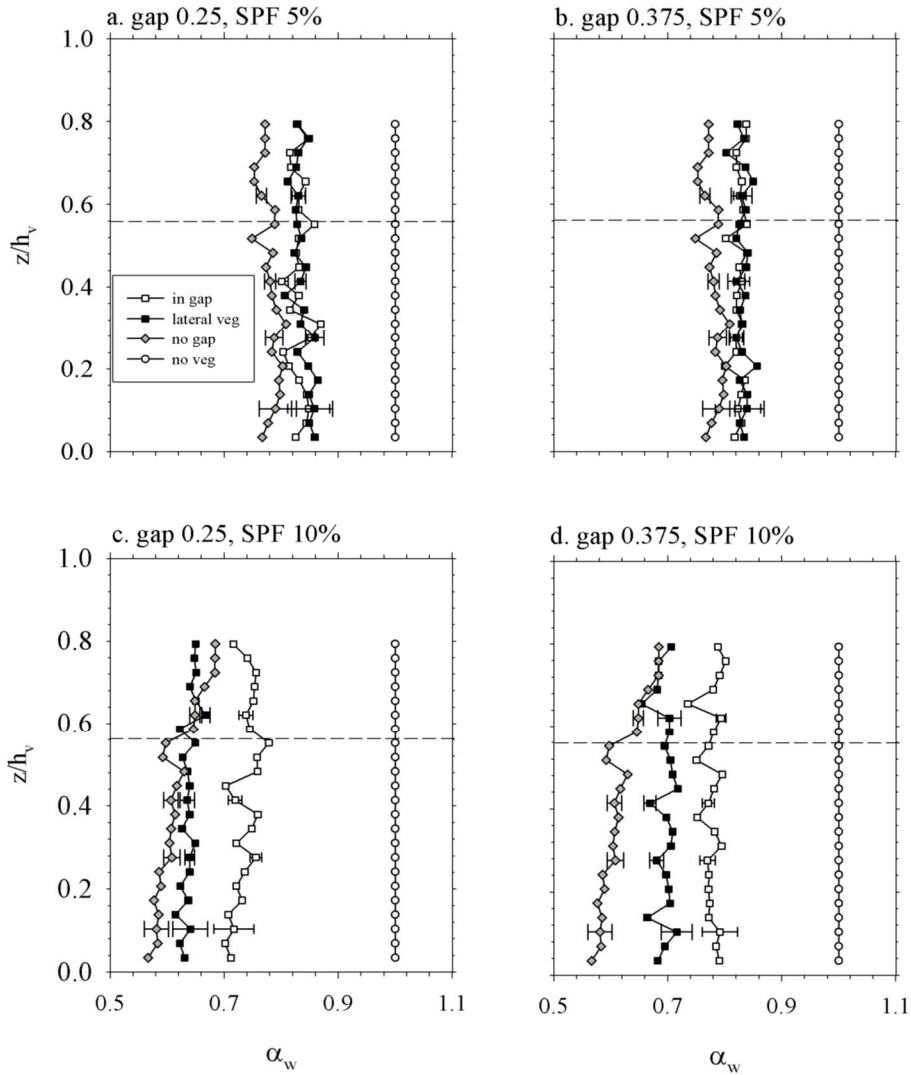


Figure 3.8 Wave velocity attenuation (α_w) for the emergent rigid vegetation experiments for a) 0.25 gap, SPF=5%; b) 0.375 gap, SPF=5%; c) 0.25 gap, SPF= 10%; d) 0.375 gap, SPF=10%. The dashed horizontal line represents limits of the in-canopy region (< 17 cm above the bottom) and the surface boundary layer (> 17 cm). Horizontal error bars represent the standard deviation of the mean over different replicas.

The vertical profile of the orbital velocity (U_w) was normalized by the vertical profile measured in the no-gap control experiment, $U_{w, \text{no gap}}$ in order to obtain β_w as described in the Methods section. The mean vertical value of the orbital velocity ratios ($\langle \alpha_w \rangle$ and $\langle \beta_w \rangle$) in

the canopy-base region were calculated and plotted versus the non-dimensional gap width (GW/h_v , where GW is the gap width and h_v is the plant height).

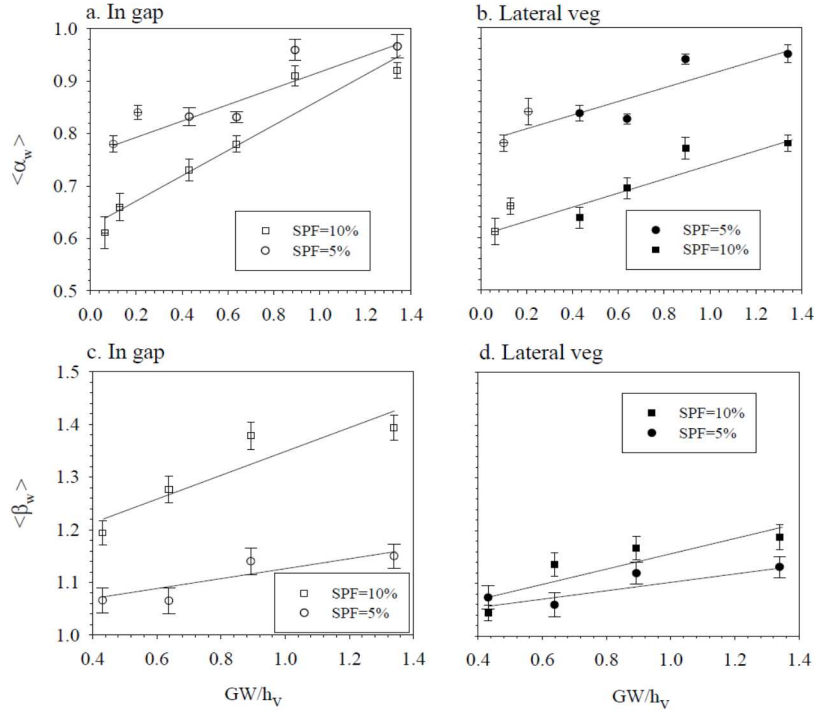


Figure 3.9 $\langle \alpha_w \rangle$ in the gap (a) and in the lateral vegetation (b) and $\langle \beta_w \rangle$ in the gap (c) and in the lateral vegetation (d) plotted against GW/h_v . Different vegetation density (SPF) treatments are plotted and regression equations were $y=0.15x+0.78$ (SPF=5%, $R^2=0.813$) and $y=0.25x+0.62$ (SPF=10%, $R^2=0.922$) for (a), $y=0.13x+0.78$ (SPF=5%, $R^2=0.805$) and $y=0.13x+0.61$ (SPF=10%, $R^2=0.851$) for (b), $y=0.10x+1.02$ (SPF=5%, $R^2=0.788$) and $y=0.22x+1.13$ (SPF=10%, $R^2=0.823$) for (c) and $y=0.08x+1.03$ (SPF=5%, $R^2=0.752$) and $y=0.13x+1.027$ (SPF=10%, $R^2=0.730$), all 95% probability level. Crossed symbols in figures (a) and (b) correspond to no gap experiments considering as the ‘gap width’ the plant to plant distance. Error bars represent the standard deviation of $\langle \alpha_w \rangle$ and $\langle \beta_w \rangle$ through the canopy base layer.

In Figures 3.9.a and 3.9.b, experiments with no gap were also included for completeness. In these experiments, the plant to plant distance (S) was considered as a proxy for the gap width. The ratio between the gap width (GW) and the plant height was found to

have a large effect on the wave attenuation in the canopy layer. The larger the GW/h_v the lower the wave attenuation compared with the no-veg experiment, within both the lateral vegetation and the gap. For these cases, the higher the canopy density the larger the wave attenuation when compared with the no-veg experiment. $\langle \alpha_w \rangle$ increased with the ratio GW/h_v within both the gap (Figures 3.9.a) and the lateral vegetation (Figure 3.9.b) for both 5% and 10% SPF. $\langle \alpha_w \rangle$ was smallest for the largest canopy density. The change in SPF had a larger effect in $\langle \alpha_w \rangle$ at the lateral vegetation (Figure 3.9.b) than at the gap (Figure 3.9.a). $\langle \beta_w \rangle$ also increased with GW/h_v within the gap and the lateral vegetation (Figures 3.9.c and 3.8.d, respectively). $\langle \beta_w \rangle$ within the gap and the lateral vegetation was smaller for the larger SPF. The change in SPF impacted velocities within the gap (Figure 3.9.c) more than within the lateral vegetation (Figure 3.9.d).

3.2.5 Submerged flexible vegetation

For experiments using submerged flexible vegetation with 10% SPF, the flexibility of the plant reduced the thickness of the canopy-base layer, allowing the wave and the mean current to penetrate deeper inside the vegetation. The vertical profiles of U_c measured in the lateral vegetation and in the no-gap control experiment were similar, with positive values at the canopy-base (Figure 3.10.a).

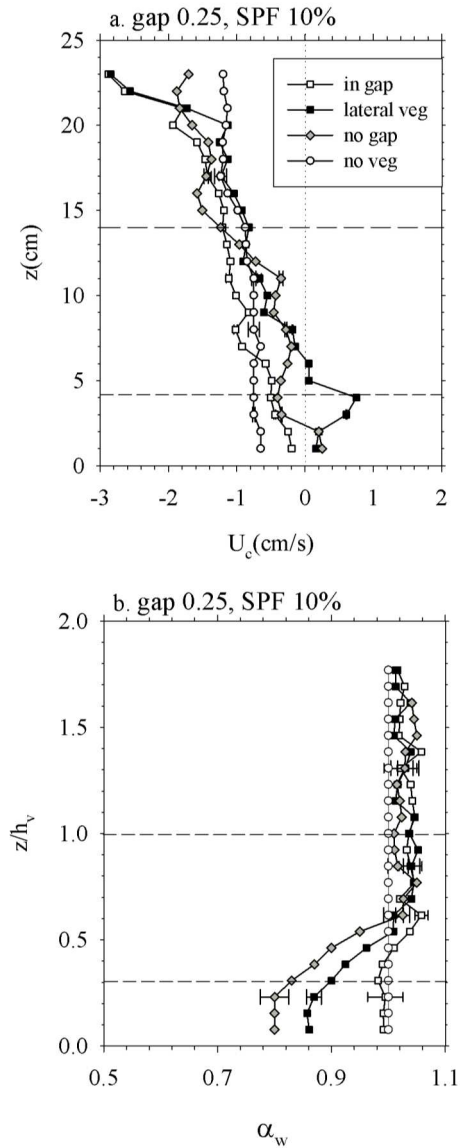


Figure 3.10 Mean current (U_c) (a) and wave velocity attenuation (α_w) (b) for experiments with submerged flexible vegetation for a 0.25 gap and 10% SPF. Horizontal dashed lines show the limits of the above-canopy region (> 14 cm above the bottom), the canopy-top region (4 - 14 cm) and the canopy-base region (< 4 cm). Horizontal error bars represent the standard deviation of the mean over different replicas.

In this case, the canopy-base region was defined as $z = 0 - 4$ cm above the bottom. The canopy-top region was defined as the layer $z = 4 - 14$ cm, and the above-canopy region was defined as $z > 14$ cm. U_c at the canopy-top region increased upwards, within the lateral

vegetation and the no-gap experiment. U_c in the gap was similar to that measured within the lateral vegetation for the canopy top layer, while at the canopy-base it was more similar to that found for the no-veg experiment (Figure 3.10.a).

At the above-canopy region, α_w was slightly above 1 as was measured in the experiments with submerged rigid vegetation. However, in the upper part of the canopy-top region, α_w was slightly above 1 and decreased gradually below 1 in the lower part of the region (Figure 3.10.b). Below 7 cm, α_w remained close to 1 within the gap. However for the lateral vegetation, α_w decreased to 0.85 (Figure 3.10.b), which was greater than measured in the no-gap experiment, with a value of 0.8 at the bottom (Figure 3.10.b).

3.3 Discussion

The presence of a longitudinal gap within a rigid canopy was found to alter the mean wave induced current in the lateral vegetation. This occurred whether the vegetation was submerged or emergent. At the same time, the lateral vegetation determined hydrodynamics within the gap.

3.3.1 Interaction between plant density and flows through gaps

The canopy density was found to be a key parameter in determining not only sheltering within the vegetation but also the hydrodynamics in the nearby gap. The increase in the canopy density to 10% SPF produced considerable differences in the hydrodynamics within the gap and in the lateral vegetation. The reduction in wave velocities inside both intermediate and high density canopies agrees with the results of Manca et al. (2012) and Pujol et al. (2013a), i.e. the higher the canopy density, the larger the reduction in the wave velocity inside the canopy. Furthermore, the wave attenuation inside the canopy with a nearby gap was smaller than for the no-gap experiment. In their study on the hydrodynamics around and within canopy patches under uni-directional flow, Bouma et al. (2007) highlighted the

variability across a canopy. They found a larger erosion rate at the front of a canopy patch than well inside the patch, showing the heterogeneous spatial distribution of energy. Furthermore, they found that denser patches produced larger sedimentation rates when compared with sparser patches. These results are in accordance with the findings in the present study, where there is a larger reduction in the wave velocities within denser canopies.

3.3.2 Vertical flow structure within a rigid canopy

In general, the submerged vegetation induces a positive mean flow (i.e. in the direction of the wave propagation) within the canopy with greater positive values for the densest canopies, and a stronger return current above the canopy relative to the no-vegetation case. This result is in accordance with the results found by Luhar et al. (2010) and Pujol et al. (2013b). For the emergent vegetation, U_c was always negative in the canopy. This result might have important implications for the flushing of solids and nutrients in areas dominated by vegetation. At the canopy-base layer, opening a gap within a submerged canopy also increased the mean flow through the vegetation that was greater for larger gap widths. This mean current at the canopy-base was greater for denser canopies.

In emergent vegetation, the presence of a gap affected wave velocities in the lateral vegetation and in the gap, and facilitated sheltering inside the canopy; this effect was augmented at high canopy densities. This effect has been documented in salt marshes where emergent vegetation attenuates the flow at the edge of the vegetation differently to that within the vegetation patch (Bouma et al., 2007, Coates and Folkard, 2009).

Our results suggested that large values of GW/h_v could be associated with lower sheltering of the adjacent vegetation, and small GW/h_v could be associated to a large sheltering of the adjacent vegetation. Furthermore, increasing canopy density had a larger effect in the lateral vegetation than in the gap, with a greater wave velocity attenuation in the

lateral vegetation than in the gap. Results also show that the wave attenuation in a gap adjacent to nearby vegetation becomes larger for low GW/h_v . Denser canopies provided greater wave attenuations within the gap. Furthermore, in the gap and independently on the canopy density, it can be estimated that for $GW > 1.5h_v$, the wave does not attenuate (Figure 3.9.a). In contrast, the wave velocity in the canopy layer was greater than the wave velocity for the no-gap experiment. This result showed that the greater GW/h_v , i.e. lower sheltering, the larger the wave velocity at both the gap and at the lateral vegetation. Furthermore, the presence of a gap played a greater effect at the gap than at the lateral vegetation, with greater $\langle \beta_w \rangle$ at the gap than in the lateral vegetation. Within the lateral vegetation, for $GW < 0.4h_v$, β_w approached 1, that is, U_w was closer to that for the no-gap canopy.

Considering now only the experiments of rigid submerged vegetation, and for canopies of 5% SPF and 10% SPF without a gap, $\langle \alpha_w \rangle$ was 0.84 and 0.68, respectively. The theoretical value of α_w can be calculated considering that the inertial flow dominated regime holds for the case here studied. The inertial flow dominated regime results when $A_\infty^{rms}/S < 1$. In the present study $A_\infty^{rms} = 0.24$ for 5% SPF and 0.39 for 10% SPF. The lambda parameters in the present study are $\lambda_p = 0.05$ (for 5% SPF) and $\lambda_p = 0.10$ (for 10% SPF), giving $\alpha_w = 0.9$ and 0.82, respectively. The experimental values obtained in this study were below those predicted by the theory. The reason for this discrepancy might be in the fact that the model presented by Lowe et al (2005) holds for cases where the wave velocity varies minimally over the height of the canopy, which is not the case in this study, where U_w presented a variation with depth above the canopy layer.

3.3.3 Differences between rigid and flexible vegetation

Results for the dense (10% SPF) submerged flexible vegetation were significantly different from those found for rigid vegetation. The canopy-base region of the flexible

vegetation was thinner than that found in the rigid vegetation. For the layer occupied by plants, U_c in the gap was close to that found without plants. In this layer, U_c for the lateral vegetation was also close to that for the no-gap experiment, indicating similar development of the current in canopies with gaps and canopies without gaps. Flexible vegetation was found to attenuate the wave velocity to a lower degree than rigid vegetation. Therefore, the flexibility of the stems is a key parameter determining the wave attenuation. The back and forth motion of flexible plants makes possible a deeper penetration of the wave than does rigid vegetation. Koch and Gust (1999) also found a larger energy transfer in flexible vegetation under wave-dominated flows.

In this study, the wave attenuation for rigid canopies was double the wave attenuation measured by Neumeier and Amos (2006) in a *Spartina anglica* canopy, which has a semirigid structure. The difference in wave attenuation was attributed to the difference in the plant rigidity. Using an analysis of wave height within *Zostera noltii*, Paul and Amos (2011) found 20% wave attenuation within a canopy of 4164 shoots m^{-2} and a 10% wave attenuation within a canopy of 600 shoots m^{-2} . Granata et al. (2001) found a 75% reduction in total kinetic energy above and within a *Posidonia oceanica* canopy and a 50% reduction over a nearby bare sediment, accounting for a 25% of total kinetic energy reduction between vegetated and bare soil regions. Our study using flexible vegetation agrees with this prior work.

3.3.4 Sedimentary significance

Our results have demonstrated that the canopy density is one of the key parameters in determining both the mean wave induced current and the wave velocity; for larger canopy densities the wave velocity at the canopy-base layer is more attenuated in the lateral vegetation than in the gap. The height of the plants also had an important effect in both the mean wave induced current and the wave velocity, especially at the surface layer. The decrease in the ratio GW/h_v was found to play an important role in the degree of wave

attenuation in both the gap and the adjacent canopy, with lower wave velocities for taller (emergent) plants for all plant densities and gap widths. Flexibility was crucial in determining the wave penetration within the vegetation. That is, the submerged flexible vegetation behaved significantly differently from the rigid vegetation. Due to the back and forth movement of the blades, the wave penetrated deeper within the canopy and as a result, the canopy-base layer for flexible vegetation was thinner than that for the rigid vegetation.

Several studies (Leonard et al., 1995, Neumeier and Amos, 2006, Bouma et al., 2007) have shown that suspended sediments settle progressively as they travel over a canopy area as turbulence, currents and wave action decreased. Yang et al. (2007) and Uncles and Stephens (2009) correlated the sediment concentration with current and wave action. In the present study, the wave attenuation in intermediate to dense canopies was larger in the rigid vegetation than in the flexible vegetation. This is in accordance with the laboratory results of Ros et al. (2014), who found higher values of the turbulent kinetic energy in rigid canopies than in flexible canopies. Larger turbulent kinetic energies were associated to higher wave attenuation by the canopy. Ros et al. (2014) proved that the crucial parameter in determining the sediment resuspension was the turbulent kinetic energy. They found higher sediment resuspension for rigid canopies, with higher turbulent kinetic energy, than for flexible canopies, with lower turbulent kinetic energy. The presence of a gap within a canopy should increase the rate of erosion (and the sediment resuspension) in the gap area compared to vegetated areas; but the degree of erosion would be lower than in areas of bare sand. This should apply for gap widths no larger than ~ 1.5 the height of the plant.

Chapter 4. Hydrodynamics in boundary of vegetation to oscillatory flows

The response of meadows to natural and man-induced disturbances is complex and not fully understood. Some authors report the response of the meadows to both a decline biomass and canopy density (Terrados and Medina-Pons, 2010) or to a partial modification of the spatial structure, in terms of spatial variations in within bed architectural characteristics (Borg et al., 2005). Meadow-scale morphodynamics modifications result in fragmented seagrass communities defined by the discontinuous presence of patches of plants and gaps. Seagrass discontinuities affect hydraulics and consequently macroscale suspended particulate matter budgets (Fonseca and Fisher, 1986; Folkard, 2005). Some authors divide the seagrass community in three horizontal regions, outside the seagrass, the edge and inside the seagrass (Tanner, 2005). The division is based on the distribution of crustaceans in these regions. Furthermore, Tanner (2005) also showed the gradual increase in the canopy density from the

region outside the canopy towards the region inside the seagrass. Therefore they clearly show that the edge is the region with characteristic properties. Both the hydrodynamics and sedimentary regimes at the edge result in differentiate canopy densities compared with the region situated inside the canopy.

Nezu and Onitsuka (2001) demonstrated the presence of tridimensional structures developing at the edge of a rigid submerged canopy under the effect of unidirectional flow. They found that outside the canopy, the turbulent kinetic energy increased approaching the canopy edge, where it reached a maximum. The turbulent kinetic energy decreased gradually afterwards while going further into the canopy. White and Nepf (2008) measured the Reynolds stress in a partially vegetated flume with rigid plants in order to explain the penetration of momentum between the adjacent high-discharge main channel and the more quiescent vegetated region. In their study they found a two layer structure with a high shear across the vegetation interface and a more gradual boundary layer outside the vegetation.

The present research focuses at understanding the above mentioned issue by reporting detailed flume investigations of oscillatory flows in and around a longitudinal model of rigid and flexible vegetation. The considered architectural canopies are wave exposed longitudinal canopies with different canopy densities. The specific objectives of this study are to identify and quantify the patterns of mean current, wave velocity and turbulence near the edge of the canopy. The effect of the canopy on the nearby bare soil will be accounted with a characteristic length scale. Similarly, the effect of the bare soil within the canopy will be also accounted. The canopy density and the canopy model (flexible or rigid plants) are the parameters under study.

4.1 Experimental set up for the study of the boundary of a canopy

In this sub-chapter I present the detailed methodology corresponding to the experiments for the detailed hydrodynamics at the boundary of a canopy. In this study two types of submerged vegetation models were considered, rigid and flexible. The canopy model was placed 1 m from the paddle-type wave maker until the slope beach situated at the end of the flume. The study was carried out at four canopy densities 320, 640, 960 and 1280 shoots/m² corresponding to solid plant fractions of 2.5, 5, 7.5 and 10%. A complete list of the experiments carried out is listed in Table 4.1, accounting for a total of 8 experiments.

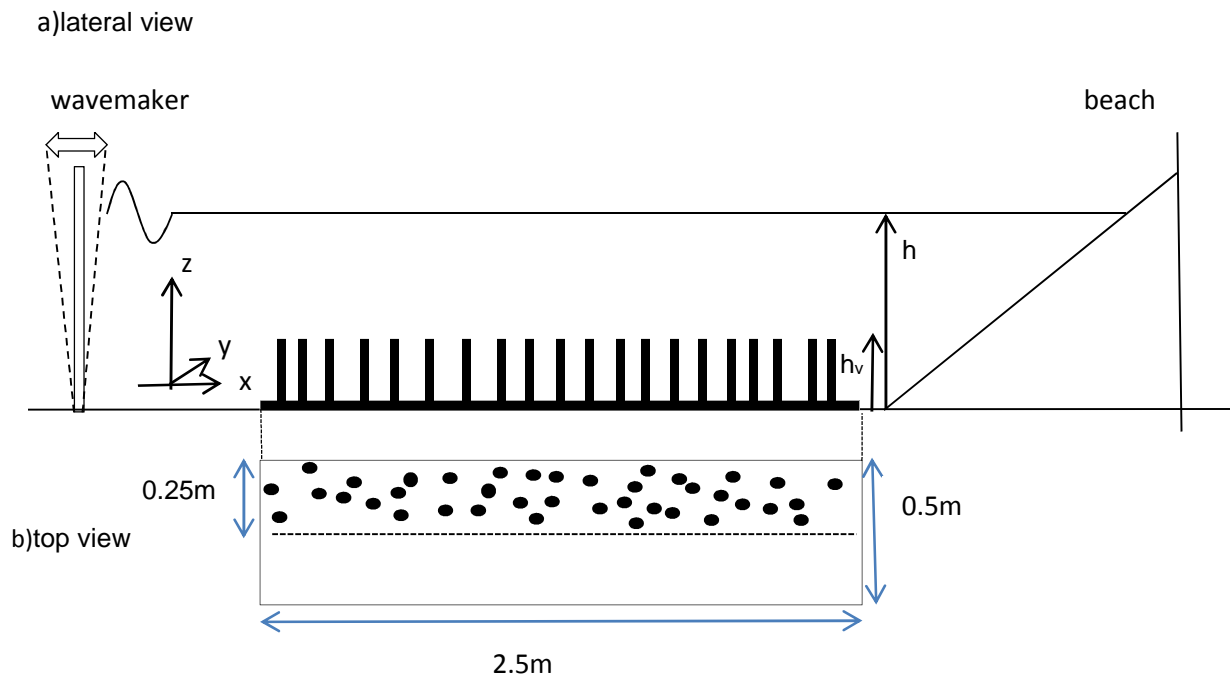


Figure 4.1 Scheme of the experimental set up. a) lateral-view of the flume with the canopy distribution, the wave maker and the beach. b) Top-view of the canopy and boundary.

SPF (%)	n/A(shouts/m ²)	h _v (cm)	Type	GW/b
2.5	320	14	flexible	0.5
2.5	320	14	rigid	0.5
5	640	14	flexible	0.5
5	640	14	rigid	0.5
7.5	960	14	rigid	0.5
10	1280	14	flexible	0.5
10	1280	14	rigid	0.5
0	-	-	-	-

Table 4.1. Summary of the different experimental conditions. A is the horizontal area and b is the width of the flume.

All measurements were taken in the central z–y plane, at x=150 cm. Sixteen vertical velocity profiles were measured at different y positions with a transversal separation of 2 cm from y=-23 cm from the edge of the canopy within the vegetation to y= 7 cm outside the edge of the canopy. The edge of the canopy was situated at y=0 cm, corresponding to the center of the flume width.

The ADV was mounted in a frame that allowed to perform vertical velocity profiles at each y position above mentioned. Vertical profiles were made from z=1 - 20 cm from the bottom of the flume, with a vertical resolution of 2 cm. Measurements with cases of without plants were also carried out at the center of the flume in order to compare with the present results.

4.2 Results

4.2.1 The mean current distribution

Horizontal transects of the mean current velocities at different selected water depths (5, 7, 10 cm) and for both flexible (left panels) and rigid (right panels) vegetation are presented in figure (4.2). The y-axis corresponds to different points along the transversal axis of the flume

where measurements were taken (Figure 4.1). The region situated at $y < 0$ was in all the experiments covered by vegetation, the edge of the vegetation corresponded to $y = 0$ and positive y corresponded to the region without plants (i.e. the bare soil).

For the without plants experiment, U_c was negative (i.e. directed towards the wave maker) and constant along the transect at all depths between 5 and 10 cm above the bottom (Figure 4.2.a-c) with similar values at all depths. For the flexible vegetation and for all the depths studied, U_c was constant along the transect, but lower for the greater canopy densities, showing a decrease in the mean current for greater canopy densities. Higher water depths ($z = 7$ and $z = 10$ cm above the bottom) had greater U_c whereas the deepest layers of the water column well inside the canopy showed smaller U_c . In the transversal y -axis, U_c outside the canopy remained constant for the region studied, up to 7 cm far from the edge of the flexible canopy. For the experiment with rigid vegetation (Figure 4.2.d-f), U_c outside the canopy increased gradually towards the canopy boundary, reaching a maximum at the canopy edge that remained constant hereafter within the vegetated region until the layer of 5 cm of thickness close to the wall of the flume, where U_c decreased again slightly but only for densities below 7.5% SPF and not for the greatest density of 10%. U_c within the rigid vegetated region was positive in all the cases indicating a change in the flow direction compared with the without plants experiment and also compared with the flexible canopy model. The densest the vegetation the greatest the mean positive current inside the vegetation was for all the depths studied (Figure 4.2.d-f). The same pattern described was observed for all the water depths shown, at $z = 10$ cm (Figure 4.2.d), at $z = 7$ cm (Figure 4.2.e) and at $z = 5$ cm (Figure 4.2.f). Outside the vegetation, U_c decreased gradually reaching negative values nearer the canopy edge for the sparser canopies and farther for the densest canopies. However, U_c at 7 cm far from the vegetation edge was still below the U_c for the without plants experiment.

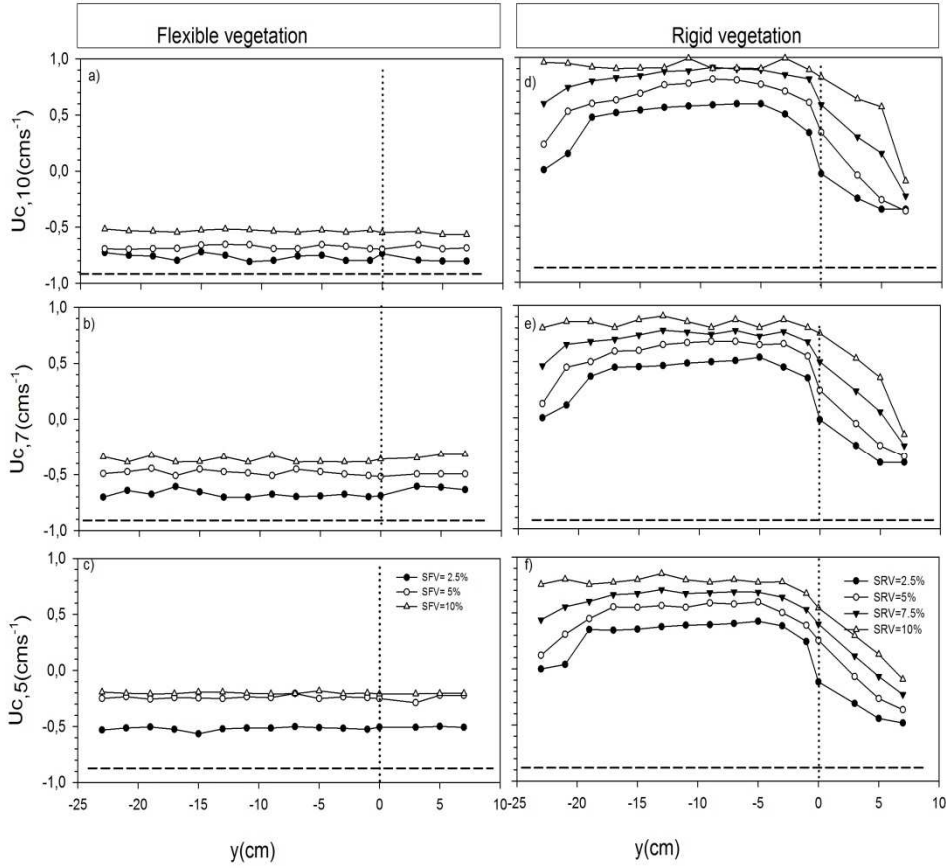


Figure 4.2 Mean current velocity transects at $z=5$ cm (bottom panels, c and d), $z=7$ cm (middle panels, b and e) and $z=10$ cm (top panels, a and d) along the y -axis for the different experiments carried out for the flexible (left panels) and rigid (right panels) vegetations. Vertical dashed line represented the position of boundary. The horizontal dashed line corresponds to the U_c for the without plants experiment. Different plots in each figure represent different SPFs.

4.2.2 The wave velocity field

Wave velocity (U_w) velocity transects at three different depths (5, 7 and 10 cm above the bottom) are presented in Figure 4.3 for both flexible (left panels) and rigid (right panels) vegetation.

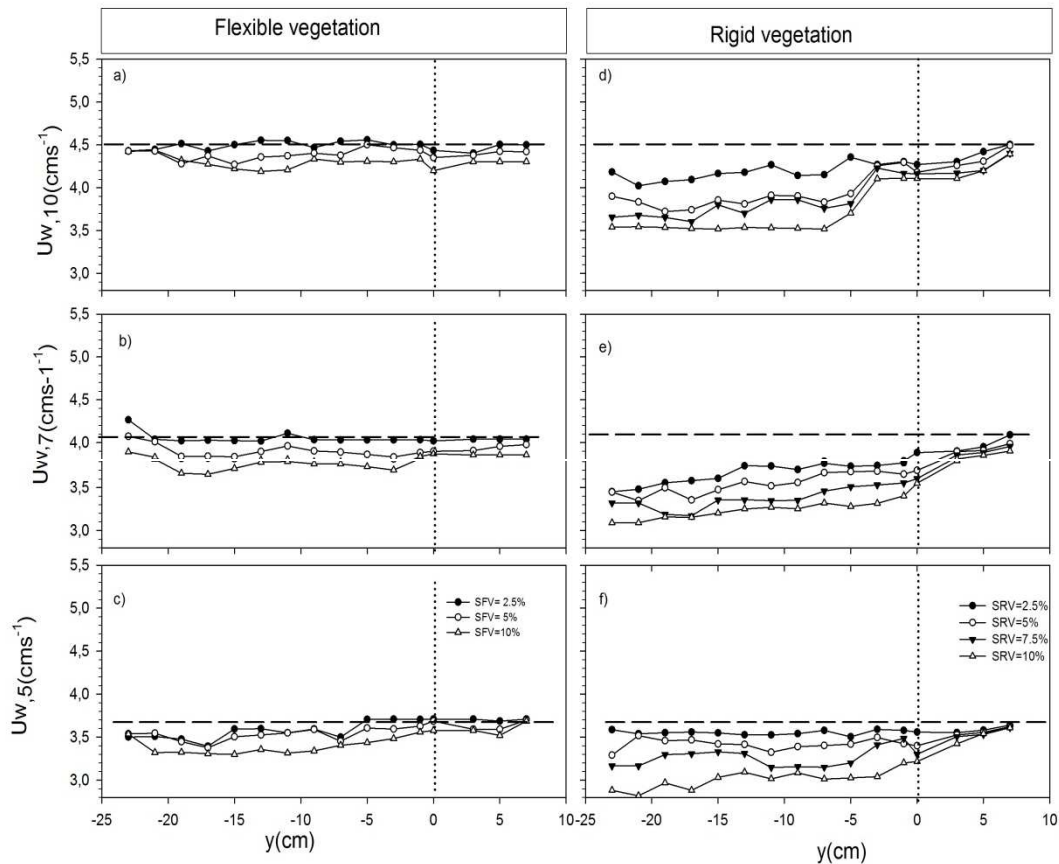


Figure 4.3 Wave velocity transect at $z=5$ cm (bottom panels, c and f), $z=7$ cm (middle panels, b and e) and $z=10$ cm (top panels, a and d) along the y -axis for the different experiments carried out for the flexible (left panels) and rigid (right panels) vegetation. Vertical dashed line represented the position of the canopy boundary. The horizontal dashed lines correspond to the U_w result for the without plants experiment. Different plots in each figure represent different SPFs.

For the without plants experiment, U_w decreased towards the bed from 10 cm to 5 cm above the bottom. For the flexible vegetation, U_w outside the vegetation from 7 cm of distance from the edge to the edge, U_w remained nearly constant (Figure 4.3.a-c) and close to the case without plants, whereas it decreased gradually within the vegetation until the layer of 5 cm of thickness near the wall, where U_w increased slightly. Within the vegetation, U_w for the densest canopy was lower than U_w for the sparser canopy, with U_w close to those for the without plants experiment for the two depths situated well inside the canopy, $z=5$ and $z=7$ cm (Figure 4.3.a-b). However, for the upper layer ($z=10$ cm, Figure 4.3.a) U_w was slightly above U_w for the without plants experiment. Outside the canopy, U_w was close to the without plants case. However, bare soil regions close to denser canopies had smaller U_w than sparser canopies. For rigid canopies, U_w decreased from 7 cm far from the edge of the canopy towards the canopy edge for all the depths studied (Figure 4.3.d-f). When into the canopy, U_w kept decreasing until approximately 5 cm from the edge of the canopy in the inner side, from where it showed only a small decrease until the wall of the flume. The denser the canopy smaller U_w were observed. For a fixed SPF, U_w decreased approaching the bed as can be observed from $z=10$ cm (Figure 4.3.d) to $z=5$ cm (Figure 4.3.f).

4.2.3 The turbulent kinetic energy (TKE)

Figure 4.4 shows the horizontal transects of the turbulent kinetic energy at different water depth (5, 7, 10 cm) and for both flexible (left panels) and rigid (right panels) vegetation.

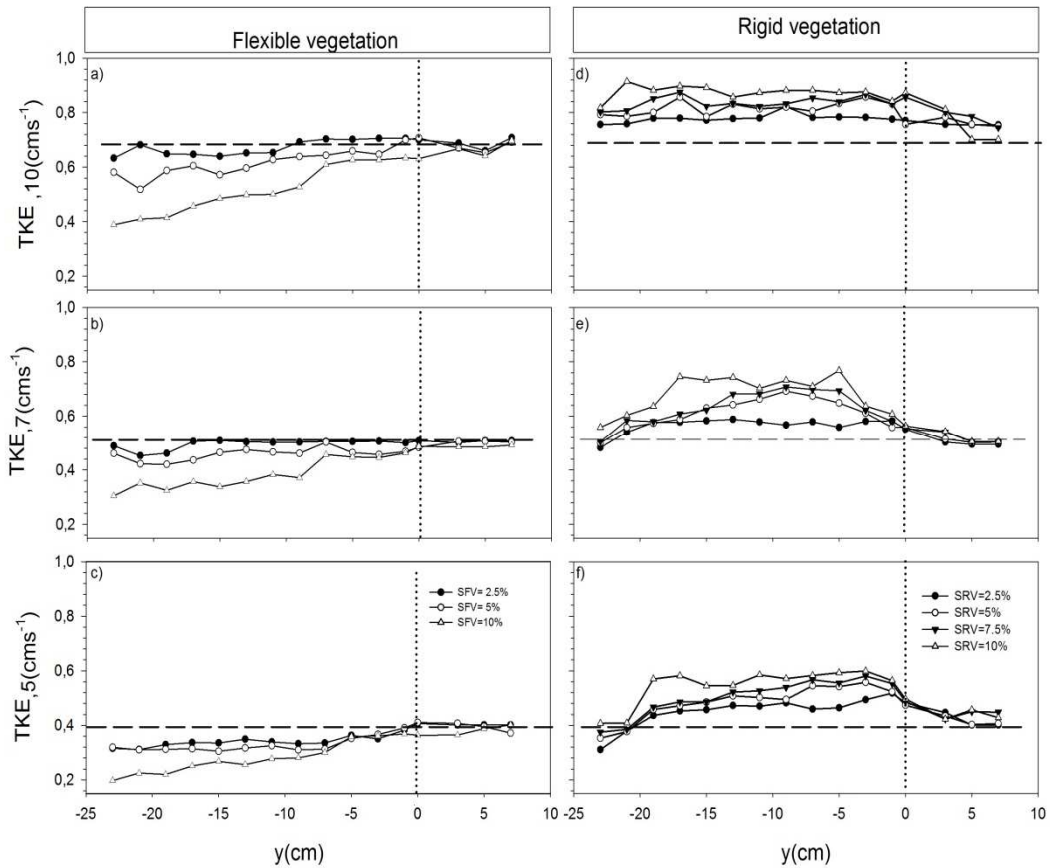


Figure 4.4 Turbulent kinetic energy transect at $z=5$ cm (bottom panels, c and f), $z=7$ cm (middle panels, b and e) and $z=10$ cm (top panels, a and d) along the y -axis for the different experiments carried out for the flexible (left panels) and rigid (right panels) vegetation. Vertical dashed line represented the position of the edge of the canopy. The horizontal dashed lines correspond to the TKE result for the without plants experiment. Different plots in each figure represent different SPFs.

For the without plants experiment, the TKE decreased with depth within the canopy (Figure 4.4.a-c). The TKE outside the flexible vegetation was nearly constant and equal to the TKE for the without plants experiment for all the depths studied within the canopy (Figure 4.4.a-c). Inside the flexible vegetation, the TKE decreased gradually until the wall of the flume with greater TKE for the upper layers (Figure 4.4.a) and decreasing gradually down to the bed (Figure 4.4.c). The densest flexible canopies showed the lowest TKE for all depths (Figure

4.4.a-c). For the rigid canopy model the TKE outside the vegetation at $y=7$ cm far from the edge was close to the without plants experiment. The TKE increased gradually when approaching the edge of the vegetation with a similar trend for all the canopy densities. Inside the vegetation the TKE increased with a smaller rate for the upper layer ($z=10$ cm, Figure 4.4.d) whereas the TKE increased at a greater rate near the bed, for $z=5$ and $z=7$ cm above the bottom (Figure 4.4.e and f). The increase in the TKE within the rigid vegetation was greater for the densest canopies.

4.3 Discussion

Flexible and rigid vegetation modified the hydrodynamics in bare soil regions close to the boundary of the vegetation. The presence of a boundary nearby a canopy modifies the hydrodynamics within the canopy. Hydrodynamics for experiments with flexible plants were different from those with rigid plants.

The mean current within a canopy of flexible plants flowed in the same direction than that for the case without plants but the mean velocity was lower within canopies (Figure 4.5) decreasing for layers situated well inside the canopy. The denser the canopy the lower the mean current was. Therefore, the flexible canopy reduced the mean flow within the canopy without changing its direction. The effect of the plants extended outside the canopy until a distance of 7 cm from the edge of the canopy. Contrary to what was found for flexible plants, rigid plants changed the direction of the flow within the canopy with greater mean currents for denser canopies (Figure 4.5). Outside the canopy the mean current decreased with a tendency to attain the mean current for the without plants experiment, i.e. directed against the wave propagation. However, within the canopy, the flow was in the same direction than the wave propagation. Therefore, rigid canopies generate a flow that allow to divide the y -axis in three regions, the layer within the vegetation, the layer far from the vegetation (i.e. that for the

without plants) and the boundary layer nearby the plants where the presence of a shear across the density interface might strongly determine the fluxes of nutrients and the transport of sediment. A similar description was made by White and Nepf (2008) for a case of unidirectional flow through a partially vegetated channel with rigid plants. Pujol et al. (2013b) also found that rigid plants thicken the boundary layer in the vertical direction, resulting in a positive mean current in the same direction of the wave propagation. The reason for the difference in the hydrodynamics of rigid versus flexible canopies might be in the fact that the back and forth movements of blades for flexible vegetation allows the penetration of the wave and also the current associated to the wave motion. Luhar et al. (2010) highlighted the important role of the mean wave induced current in determining both the health of submerged canopy beds and their ecological contribution to the system. It is well known that the mean current is able to speed up the rate of water renewal within a meadow thus enhancing the nutrient cycling capabilities of the canopy, as well as generating a net transport of sediments, such as seeds and pollen. The presence of a canopy zone also affected the mean current in the shear zone differently depending on whether plants are flexible or not and also depending on the canopy density.

U_w was reduced by the both flexible and rigid submerged vegetation models. However, the flexible vegetation model produced a lower reduction of U_w within the canopy than the rigid vegetation. This result is in accordance with the result found by Pujol et al. (2013b), who attributed the smaller wave attenuation to the fact that flexible structures allow the wave penetrate within the vegetation. For both types of vegetation, the denser the canopy the greater the wave velocity attenuation. Outside the vegetation, the wave velocity increased gradually until it reached the value for the case without vegetation, this effect extended in a wider region for the rigid vegetation than for the flexible vegetation. Lower wave velocities

were found when approaching the bed, due to the wave attenuation with depth by both the bed and the canopy, as also found by Ros et al. (2014).

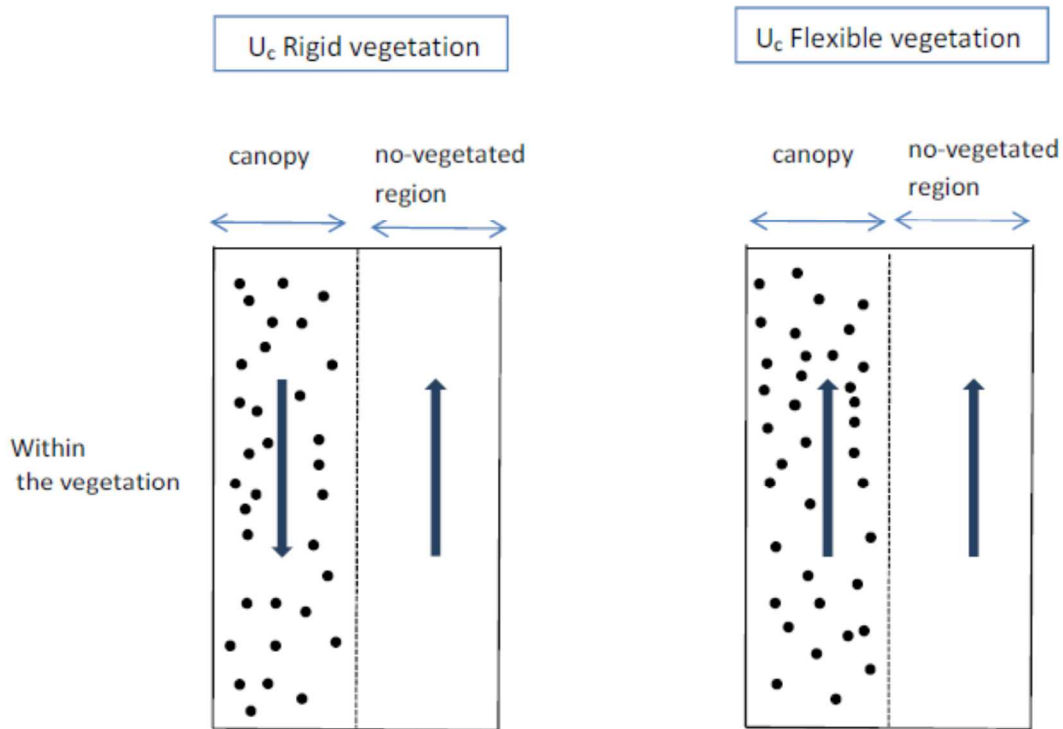


Figure 4.5 Scheme of the direction on the mean current velocity in the region free of plants and in the region covered by the vegetation for the layer $z < 14$ cm above the bottom. The diagram corresponds to a canopy of rigid vegetation (a) and a canopy of flexible vegetation (b).

It is also interesting to notice that U_w at the upper layer of the canopy ($z=10$ cm above the bottom, Figure 4.3.d) was slightly above that found for the without plants case. This result is in accordance to the result found by Pujol et al (2013b) for a full coverage of rigid vegetation. This result may be explained by the fact that rigid plants act as a false floor, reducing the available volume of water and enhancing the wave velocity in both the upper canopy layer and above the canopy region. As also found by Pujol et al. (2013b), this result was not found.

For the case of the rigid vegetation, the extension of the effect of the canopy on the bare soil and vice-versa the extension of the effect of the bare soil within the canopy were determined by means of the boundary layer thickness estimation.

The wave boundary layer thickness (δ_w) and the current boundary layer thickness (δ_c) were calculated from transects of U_w and U_c at $z = 5$ cm above the bottom for case the rigid vegetation model. Straight lines were fitted to the results for U_c and U_w versus y for each SPF (Figure 4.2.d, Figure 4.3.d) inside the canopy and outside the canopy. δ within the canopy for the wave transect ($\delta_{w,in}$) and for the mean current transect ($\delta_{c,in}$) was considered as the y -distance where the straight line fitting curve intersected U_w or U_c found within the canopy region (Figure 4.6 and Figure 4.7). δ outside the canopy for the wave transect ($\delta_{w,out}$) and for the mean current transect ($\delta_{c,out}$) was the y -distance from the boundary where the straight line fitting curve intersected U_w or U_c for the without plants experiment. For a canopy of rigid plants, the presence of the canopy changed the mean current velocity in the region close to the edge of the canopy, the shear layer. $\delta_{c,out}$ increased with SPF, indicating that a dense canopy provides a larger shear layer in the nearby zone outside the canopy (Figure 4.6.b). Conversely, U_c for the region within the vegetation close to the boundary was also affected by the without plants zone. However, the greater the SPF the smaller was the penetration of the current inside the canopy and therefore, the smaller the inner boundary layer thickness was (Figure 4.6.a).

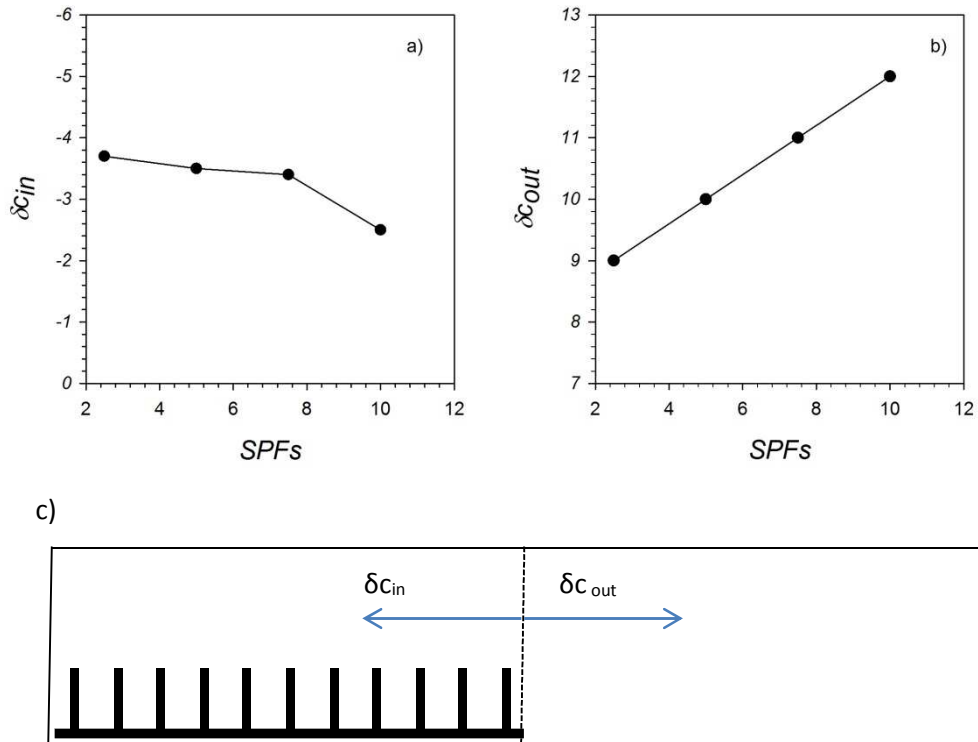


Figure 4.6 Boundary layer thickness based on the mean current transect (δ_c) versus the solid plant fraction (SPF) for the region within the canopy, δ_{cin} (a) and for the region outside the canopy, δ_{cout} (b). c) Diagram of the boundary layers δ_{cout} and δ_{cin} .

In Figure 4.7 δw_{in} and δw_{out} were plotted versus SPF. The boundary layer thickness inside the canopy (δw_{in}) decreased with SPF indicating that the denser the canopy the smaller is the layer inside the canopy where the wave penetrates (Figure 4.7.a). Conversely, for the boundary outside the canopy zone, a dense canopy had an effect that extended further from the edge of the boundary towards the bare soil, producing a greater sheltering in this region compared with the sheltering provided by sparse canopies (Figure 4.7.b). These results are in accordance to those found in chapter 3, for a longitudinal gap within a canopy. In such case, the denser the canopy the greater the protection of the vegetation on the nearby gap and the effect of the protection extended further within the gap for denser canopies.

The reduction of the TKE within a canopy of flexible plants was previously found in laboratory experiments by Luhar et al. (2010), Pujol et al. (2013b) and Ros et al. (2014) for a region full of vegetation and therefore far from any boundary. Granata et al. (2001) also found a reduction in the TKE within a *Posidonia oceanica* canopy. Pujol et al. (2013b) and Ros et al. (2014) attributed the reduction in the TKE within a flexible canopy to the movement of blades that dissipated the wave energy and resulted in a decrease in the TKE within a canopy compared with that over a bare soil. The dissipation of TKE by flexible vegetation produced sheltering and resulted in a reduction of the sediment resuspension (Leonard and Croft, 2006; Kosten et al., 2009, Ros et al., 2014). The reduction in the sediment resuspension improves water clarity, which in turn provides greater light penetration and consequently an increase in productivity, thus creating a positive feedback for seagrass growth (Ward et al., 1984). However, the flexible vegetation did not reduce the TKE outside the canopy near the boundary. According to Ros et al. (2014) the sediment resuspension is not expected to change nearby the flexible vegetated region compared with the case without plants.

In contrast, the TKE increased towards the boundary of rigid plants where it kept constant within the canopy compared to the TKE for the without plants experiment and showed a tendency to decrease well inside the canopy. This decrease can be attributed to two possible reasons, the presence of the wall boundary layer of the flume or to the reduction of the TKE by rigid plants for regions far from a boundary, which would be in agreement with the results found by Nezu and Onitsuka (2001) for a similar experiment but for the case of a unidirectional flow. The increase in the TKE in the boundary layer for a rigid canopy was also found by Nezu and Onitsuka (2001) and White and Nepf (2008) both for canopies under a unidirectional flow.

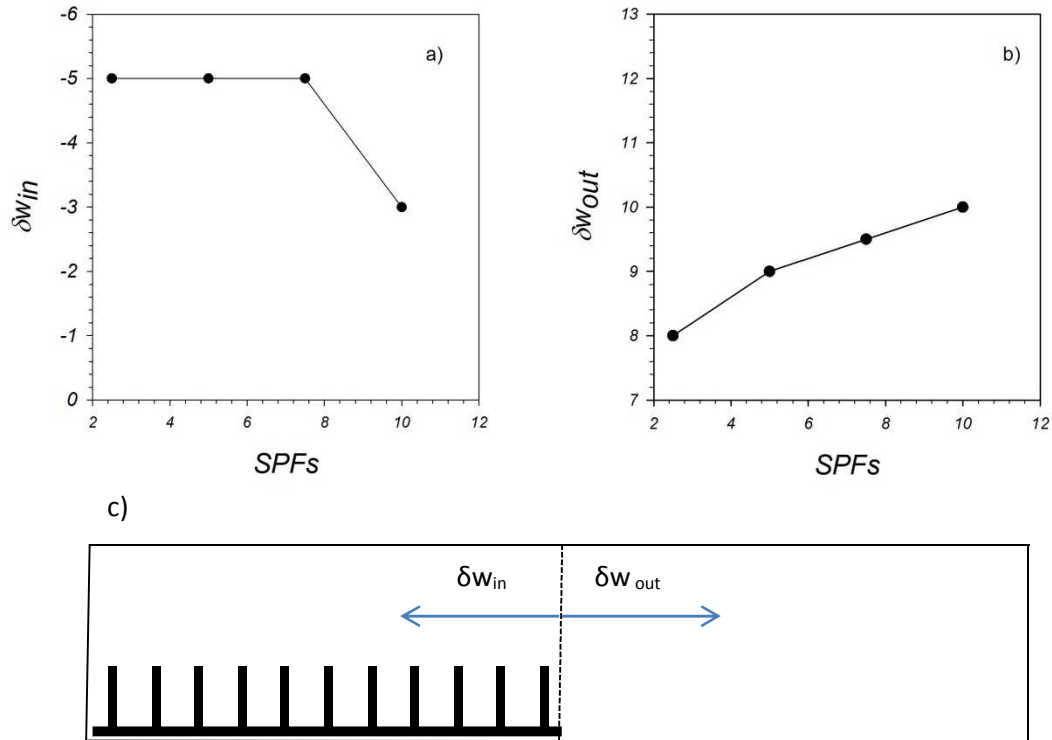


Figure 4.7 Boundary layer thickness based on the wave velocity transect (δw) versus the solid plant fraction (SPF) for, the region within the canopy, δw_{in} (a) and and for the region outside the canopy, δw_{out} (b). c) Diagram of the boundary layers δw_{out} and δw_{in} .

The turbulence found inside the meadow has positive biological consequences, such as improvement in the transfer of CO_2 (in the form of bicarbonate) from the water to the surface layer of leaves. Without turbulence, the only physical mechanism capable of capturing CO_2 would be by means of molecular diffusion from the boundary layer, which is an extremely inefficient transport mechanism (Denny, 1988). In the case of the rigid canopy boundary, the TKE outside the vegetation near the canopy decreased gradually extending through a region. Therefore, bare soil regions near canopies of rigid vegetation experience a sheltering with both lower wave velocities and lower TKE than bare soil regions close to canopies of flexible plants.

Chapter 5. Hydrodynamics canopies with transversal gaps exposed to oscillatory flows

Posidonia oceanica has been found to be present in coastal regions with its lower depth not only related to light limitation (Montefalcone, 2009) but also to the depth where waves interact with the bottom (Vacchi et al., 2012). Therefore, the lower depth of *Posidonia oceanica* might change in future climate change scenarios, increasing the vulnerability of these seagrasses. Koch and Gust (1999) found that plants play different roles depending on the environmental hydrodynamics, thus waves are able to penetrate more within the canopy due to the back and forth movement of the blades compared to the case of unidirectional flow. The increase in the vulnerability has been found to lead to a decrease in the canopy density or in the fragmentation of the meadow. While the effect of a decrease in the canopy density on the hydrodynamics has been previously addressed by some authors (Pujol et al., 2013b), the

effect of the orientation of the gaps within the canopy on the hydrodynamics has not been previously analysed. In Chapter 3, gaps within seagrasses oriented perpendicular to the coast (i.e. with the same direction than the on-shore waves, what they called longitudinal gaps) had important effects on the flow within the nearby vegetation. Furthermore, longitudinal gaps were sheltered by the nearby lateral vegetation. While longitudinal gaps might be more exposed to the hydrodynamics, transversal gaps, i.e. gaps oriented parallel to the coast (i.e. perpendicular to the on-shore waves) may remain sheltered by the nearby vegetation.

Therefore this study investigates the effect of transversal gaps (with the main axis of the gap in the direction perpendicular to the wave propagation) within a canopy. Furthermore, I am interested to check whether and in what conditions the nearby vegetation shelters the gap. Attention is paid to the modification of ambient hydrodynamics as a function of the gap width and the canopy density.

5.1 Experimental set up for the study of canopies with transversal gaps

In this sub-chapter I present the detailed methodology corresponding to the experiments for the detailed hydrodynamics in canopies with the presence of transversal gaps. In this study, a transversal gap is a gap within a canopy with its main axis oriented perpendicular to the wave flow propagation. In this case the direction of the wave propagation is aligned to the main axis of the flume. Therefore, the gap is perpendicular to the main axis of the flume.

In this study a model of submerged flexible vegetation, with height $h_v=14$ cm was considered with two canopy densities of 320 and 1280 shoots/m², corresponding to solid plant fractions of 2.5 and 10%, respectively. These densities were considered in order to be able to compare between the effect of a gap performed in a well-established dense canopy with a gap performed in a sparse canopy.

The canopy model was placed 1 m from the paddle-type wave maker until the slope beach situated at the end of the flume (Figure 5.1). Three different gap widths (GW) were considered and scaled with the height of the plants (h_v), $GW=h_v/2$, h_v and $2h_v$ (see Figure 5.1.b). Also, experiments with a full canopy coverage (no-gap experiments) and experiments without plants (no-vegetation) were carried out to compare with the experiments of canopies with gaps, see Table 5.1. The x position $x=0$ cm was considered at 200 cm from the wave maker. All the gaps were generated from $x=0$ cm, to $x= h_v/2$, h_c and $2h_v$, depending on the size of the gap performed, as shown in Figure 5.1.b.

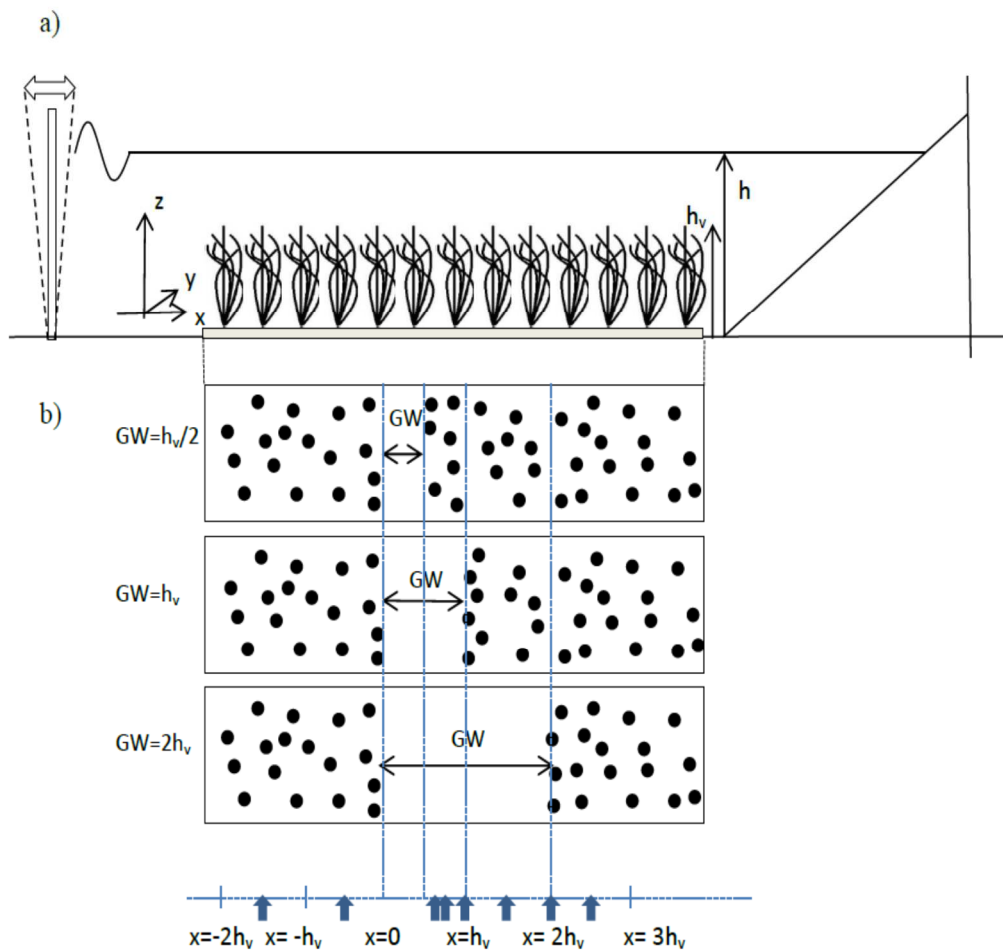


Figure 5.1 Scheme of the experimental set up. a) Side-view of the flume with the canopy distribution, the wave maker and the beach. b) Top-view of the three different gaps studied.

SPF (%)	$n/A(\text{shouts}/\text{m}^2)$	GW(cm)	$h_v(\text{cm})$	Type
2.5	320	$h_v/2=7$	14	flexible
2.5	320	$h_v=14$	14	flexible
2.5	320	$2h_v=28$	14	flexible
2.5	320	0	14	flexible
10	1280	$h_v/2=7$	14	flexible
10	1280	$h_v=14$	14	flexible
10	1280	$2h_v=28$	14	flexible
10	1280	0	14	flexible
0	-	-	-	-

Table 5.1. Summary of the different experimental conditions. A is the horizontal area.

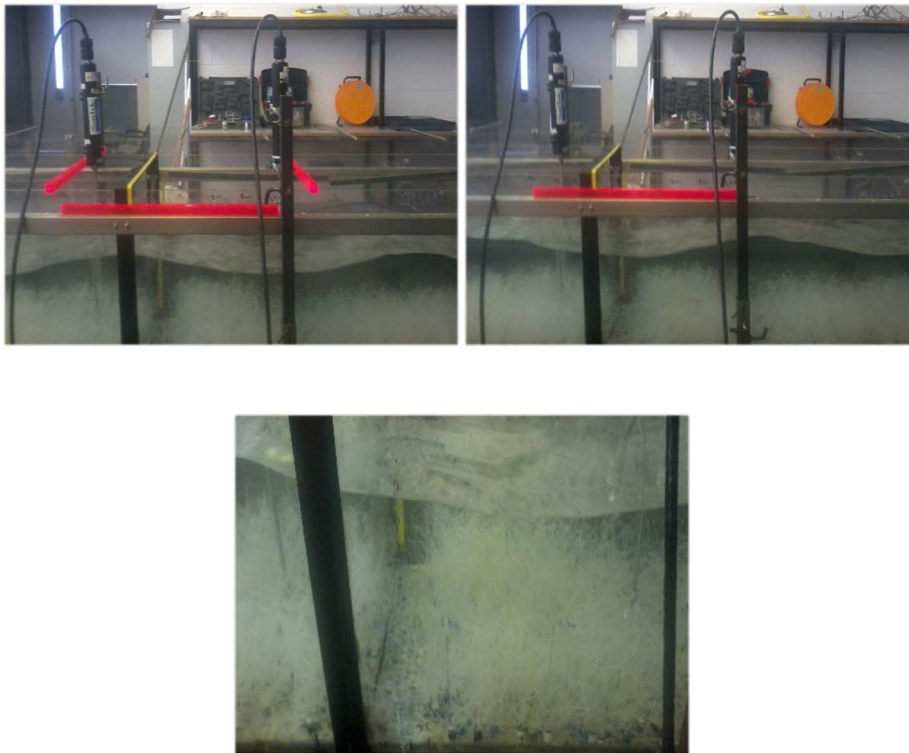


Figure 5.2 Photographs of canopies with transversal gaps.

The ADV was mounted in a frame that allowed to perform velocity profiles from $z=1 - 20$ cm from the bottom of the flume, with a vertical resolution of 2 cm. Eight velocity profiles were carried out for each case at different positions along the main axis of the flume at $x=-3h_v/2, -h_v, h_v/2, h_v/4, h_v/2, h_v, 3h_v/2, 2h_v$ and $5h_v/2$, considering the origin of x at 200 cm from the wave.

5.2 Results

From the wave velocity profiles the water column can be divided in three layers, the above canopy layer, the canopy top layer and the within canopy layer. Within the canopy, the wave velocity for the no-gap experiments was lower than in the without plants experiments for both canopy densities of 2.5% (Figure 5.1.a) and 10% (Figure 5.1.b).

In the canopy top layer, wave velocities for gapped canopies were close to those found for the without plants experiment for the canopy density of 2.5% (Figure 5.3.a). However, for the canopy density of 10% (Figure 5.3.b), wave velocities in this layer for both gapped and no gapped canopies were slightly lower than those for the without plants experiment. Above the canopy, wave velocities for the no-gap experiments were similar to those for the without plants experiment and also to those found within the gap for the gapped canopies. From the wave velocity profile obtained for experiments with the largest gap studied ($GW=2h_v$) it can be observed that wave velocities in the center of the gap were larger than those obtained for the no-gap for both canopy densities, the 2.5% (Figure 5.3.a) and the 10% (Figure 5.3.b). In fact, wave velocities within the gap of gapped canopies are closer to those found for the experiment without plants.

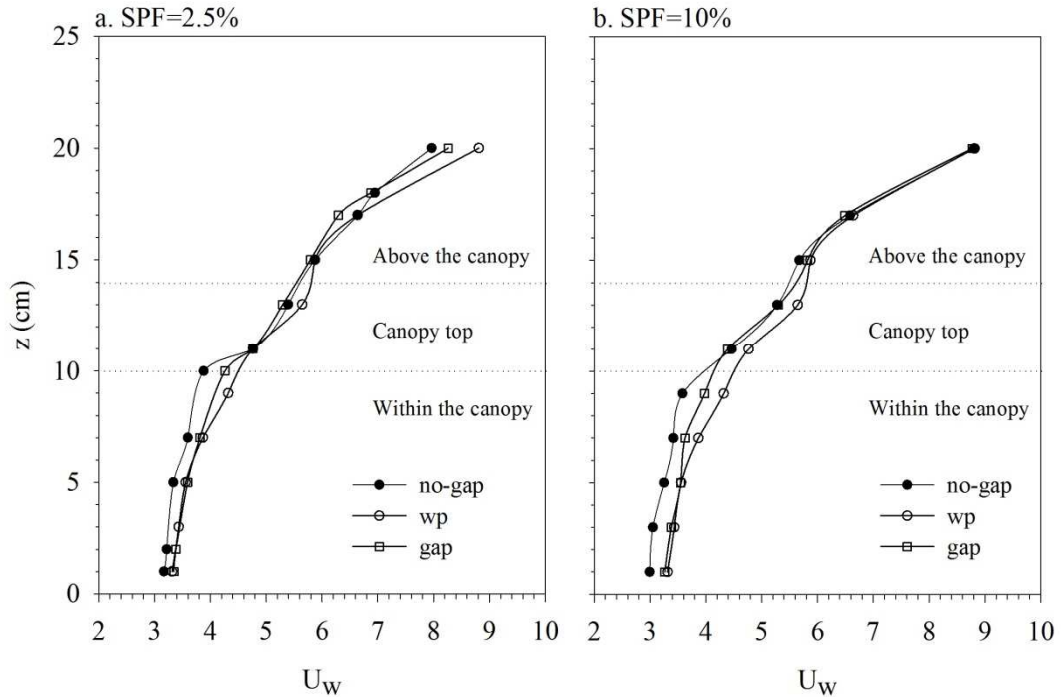


Figure 5.3 Vertical profiles of the wave velocity for the no-canopy, no-gap and the gapped canopy of $GW=2h_v$ for a) 2.5% SPF and b) 10% SPF. The center of the gap was the point selected in x for the wave velocity profile within the gap. Horizontal dashed lines represent the vertical extension of the three layers, the above canopy layer, the canopy top layer and the within canopy layer.

The turbulent kinetic energy (TKE) profile can be observed in Figure 5.4 for the two SPFs of 2.5% (Figure 5.4.a) and 10% (Figure 5.4.b). Within the canopy layer, the TKE was reduced for the no-gap experiments compared to the TKE obtained in this layer for the experiment without plants. From the TKE profile obtained for experiments with the largest gap ($GW=2h_v$) it can be observed that TKE at the center of the gap was larger than that obtained for the no-gap but it remained below the TKE obtained for the without plants experiment. At the canopy top layer for the canopy density of 2.5%, the TKE for both gapped and no-gapped canopies remained close to those without plants (Figure 5.4.a). However, at the canopy top for the canopy density of 10% (Figure 5.4.b), the TKE for the no-gapped canopy was below the TKE for either gapped and without plants experiments. Above the canopy layer,

the TKE for both gapped and no gapped canopies was close to the TKE for the without plants experiment for both canopy densities of 2.5% and 10%.

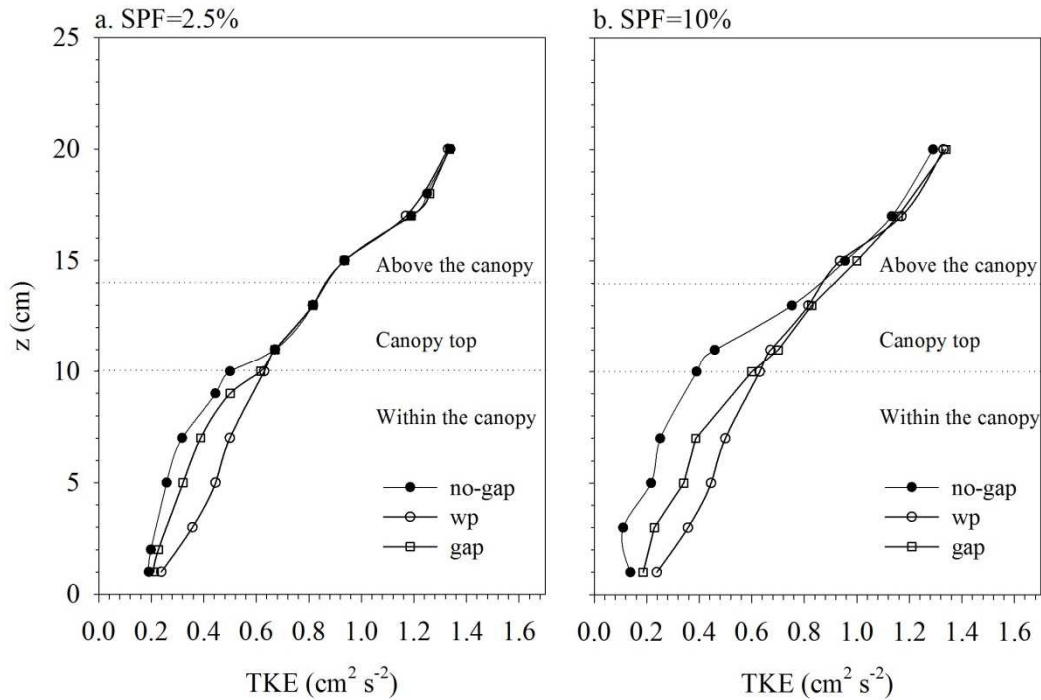


Figure 5.4 Vertical profiles of the turbulent kinetic energy for the no-canopy, no-gap and the gapped canopy of $GW=2h_v$ for a) 2.5% SPF and b) 10% SPF. The center of the gap was the point selected in x for the wave velocity profile within the gap. Horizontal dashed lines represent the vertical extension of the three layers, the above canopy layer, the canopy top layer and the within canopy layer.

In order to account for the horizontal distribution of the wave velocities along the gap and within the canopy, the wave velocity at $z=5$ cm was considered under study. The wave velocity at $z=5$ cm ($U_{w,5}$) for SPF=2.5% and SPF=10% was represented for the different gaps, the no-gap and the without plants experiments. The x -axis corresponds to different points within the canopy and along the gap where measurements were taken (Figure 5.1). The region situated at $x < 0$ was in all the experiments covered by vegetation. Wave velocities measured at $-3/2h_v$ for the gaps $h_v/2$ and h_v were close to the wave velocities for the no-gapped canopy. In

contrast, for the canopy with the largest gap of $2h_v$, the wave velocity at this point was larger than that for the no-gapped canopy for both canopy densities of 2.5% (Figure 5.5.a) and 10% (Figure 5.5.b). Within the gap wave velocities increased gradually to the center of the gap from where it decreased again with x , approaching the next boundary of the canopy. Once again within the canopy, wave velocities were close to those for the no-gap canopies. The largest the gap the largest was the maximum wave velocity reached within the gap. For example, for the experiment of SPF=2.5% (Figure 5.5.a), and for $GW = h_v/2$, U_w was 3.5 cm/s (i.e., a 4.8% larger than for the no gapped canopy); for $GW = h_v$, U_w was 3.52 cm/s (i.e., a 5.4% larger than for the no gapped canopy); and for the experiment of $GW = 2h_v$, U_w was 3.56 cm/s (i.e., 6.6% larger than for the no gapped canopy). For the largest gap and for both canopy densities (Figure 5.3.a and b), wave velocities within the gap reached values close to those found for the no-canopy experiments. For SPF=10% (Figure 5.5.b) and for $GW = h_v/2$, U_w was 3.5 cm/s (i.e., a 7% higher than that for the no gapped canopy); for $GW = h_v$, U_w was 3.52 cm/s (i.e., a 7.6% higher than that for the no gapped canopy); and for $GW = 2h_v$, U_w was 3.54 cm/s (i.e., a 8.3% higher than that for the no gapped canopy). It must be also noticed that U_w was 3.34 cm/s for the no gapped canopy of 2.5% of density (Figure 5.5.a), which was a 2.1% higher than U_w for the no gapped canopy of 10% of density (Figure 5.5.b).

The TKE at $z=5$ cm (TKE_5) presented a similar pattern than the wave velocity. Within the canopy and at $x=-3/2h_v$ and for the two canopy densities studied, TKE_5 was close to the no-gapped canopy (Figure 5.6).

Within the gap, the TKE_5 increased gradually reaching a maximum at the center of the gap, from where it decreased again approaching the next canopy boundary. The maximum TKE_5 attained within the gap for both the 2.5% (Figure 5.6.a) and the 10% (Figure 5.6.b) canopy densities was lower ($0.34 \text{ cm}^2/\text{s}^2$ and $0.41 \text{ cm}^2/\text{s}^2$, respectively) than the TKE_5 for the without plants experiment (of $0.45 \text{ cm}^2/\text{s}^2$).

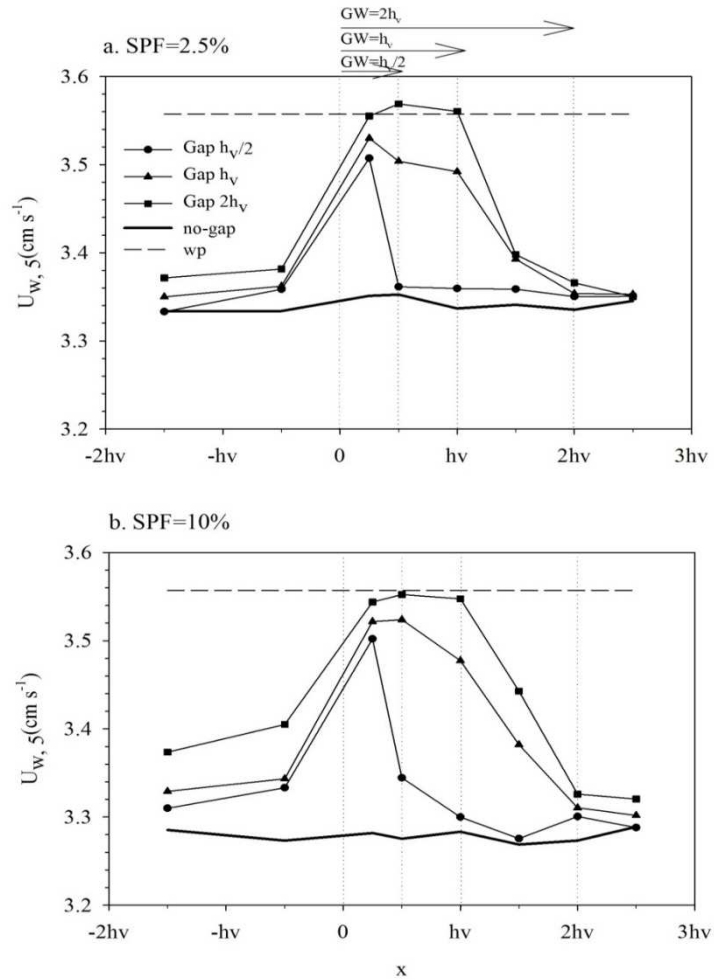


Figure 5.5 Wave velocity transect at $z=5$ cm along the x -axis for the different experiments carried out for a) 2.5% SPF and b) 10% SPF. Vertical dashed lines represent the positions of the boundary for the three different gap widths considered. Horizontal arrows at the top of the figure represent the lengths of the gap widths considered.

However, it must be noticed that the maximum TKE_5 attained within the gap for the canopy density of 2.5% (Figure 5.6.a) is larger ($0.41 \text{ cm}^2 \text{ s}^{-2}$) than that (of $0.34 \text{ cm}^2 \text{ s}^{-2}$) attained within the gap for the canopy density of 10% (Figure 5.6.b). It must be noticed that TKE_5 for the no gap canopy of 2.5% was $0.25 \text{ cm}^2 \text{ s}^{-2}$, which is a 25% larger than TKE_5 for the 10% canopy density (Figure 5.6.b), with a $TKE_5=0.20 \text{ cm}^2 \text{ s}^{-2}$.

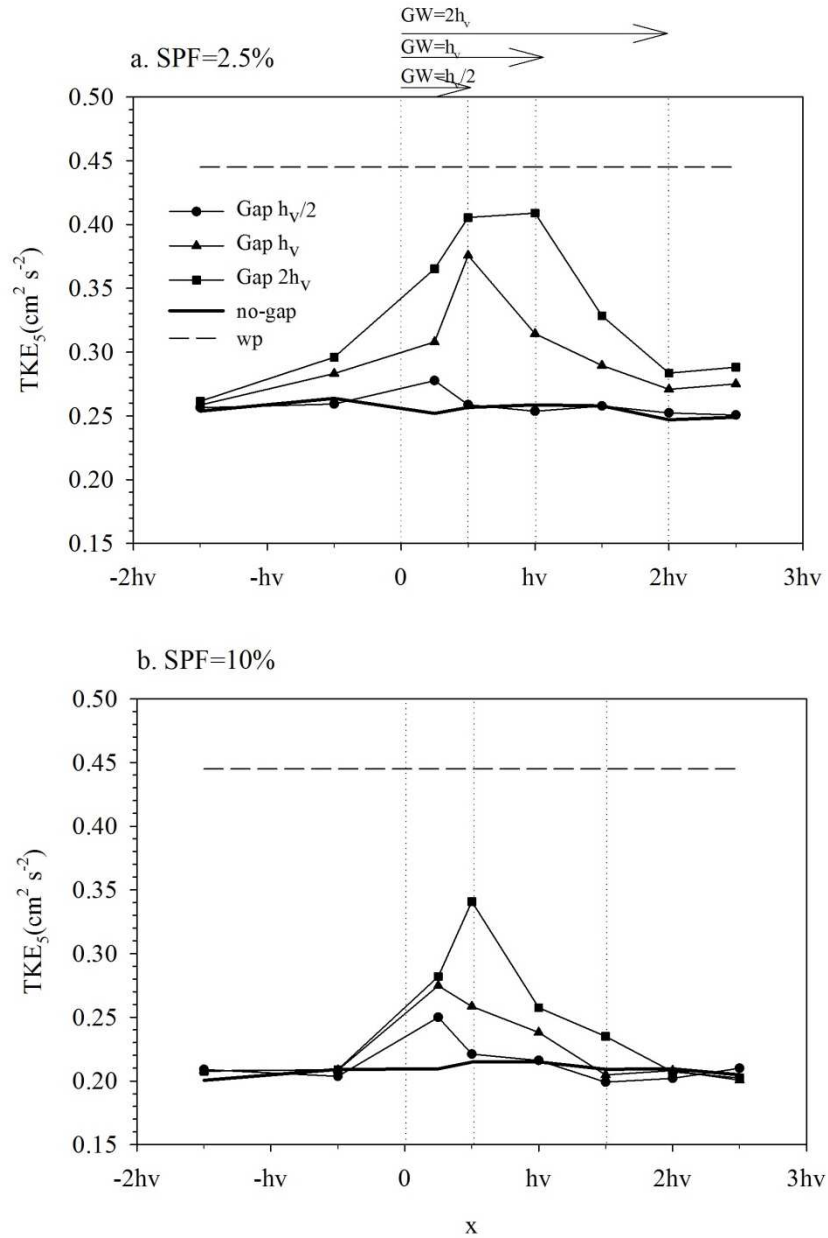


Figure 5.6 Turbulent kinetic energy transect at $z=5$ cm along the x -axis for the different experiments carried out for a) 2.5% SPF and b) 10% SPF. Vertical dashed lines represent the positions of the boundary for the three different gap widths considered. Horizontal arrows at the top of the figure represent the lengths of the gap widths considered.

The TKE_5 at the center of the gap decreased gradually with the gap width. For the canopy density of 2.5% (Figure 5.6.a), a reduction of 58.9% in the TKE_5 was found from the gap width of $2h_v$ to the gap width of $h_v/2$. For the canopy density of 10% (Figure 5.6.b) a reduction of 34% in TKE_5 was found from the gap width of $2h_v$ to the gap width of $h_v/2$.

The TKE at $z=10$ cm (TKE_{10}) was considered representative for the TKE at the canopy top layer. The TKE_{10} for both canopy densities of 2.5% and 10% was represented versus the longitudinal axis x (Figure 5.7). For all the experiments (gapped and no gapped canopies), the TKE_{10} was larger for the canopy density of 2.5% (Figure 5.7.a) than for the canopy density of 10% (Figure 5.7.b). For all the gapped canopies, the TKE_{10} increased within the gap reaching a maximum at the center of the gap, which was larger for larger gap widths. Within the lateral vegetation and for the two canopy densities studied, TKE_{10} was larger than the TKE_{10} for the no gap canopy. Furthermore, TKE_{10} increased with the gap width in all the measured points, either within the gap or within the lateral vegetation, but always remaining below the without plants experiment, unless for the measurements within the gap for the gap width of $2h_v$ and the canopy density of 2.5%. In addition, the TKE_{10} ($=0.35$ cm²/s²) for the no gapped canopy of 2.5% density was a 14.3 % larger than the TKE_{10} ($=0.40$ cm²/s²) for the no gapped canopy of 10% density (Figures 5.7.a and 5.7.b, respectively).

5.3 Discussion

In a transversal gap with its main axis perpendicular to the wave direction the vertical distribution of both the wave velocity and the turbulent kinetic energy within the gap depended on both the architecture of the gap and the canopy density. In the vertical direction, gapped canopies can be divided in three layers, the above canopy layer, the canopy-top layer and the within canopy layer. The U_w and TKE in the above canopy layer was similar to those for no gap canopies and for experiments without plants. Both U_w and TKE in the canopy top layer and within canopy layer for gapped canopies differed from that found in the no gap canopies but also differed from the without plants experiment.

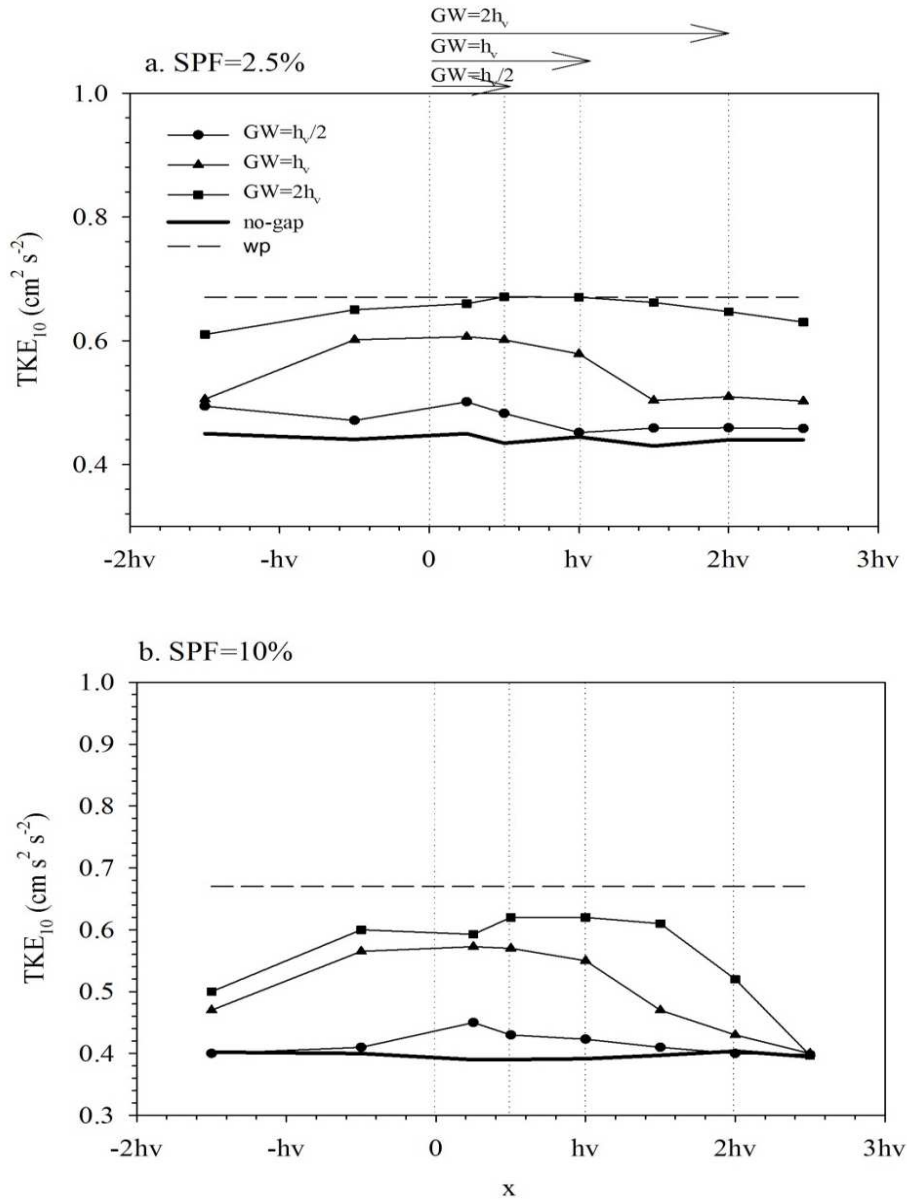


Figure 5.7 Turbulent kinetic energy transect at $z=10$ cm along the x -axis for the different experiments carried out for a) 2.5% SPF and b) 10% SPF. Vertical dashed lines represent the positions of the boundary for the three different gap widths considered. Horizontal arrows at the top of the figure represent the lengths of the gap widths considered.

The presence of the nearby canopy sheltered the gap reducing the wave velocity within it for the gaps of widths $GW < 2h_v$. For the gap width of $GW = 2h_v$, the gap was exposed to

wave velocities close to those for the without plants experiment for the two canopy densities of 2.5% and 10%. In contrast, the nearby canopy reduced the TKE_5 within the gap for all the GW studied. Moreover, the canopy density was an important parameter that determined the sheltering degree of the gap by the nearby vegetation. For example, for the case of $GW=2h_v$, the maximum value of the TKE_5 within the gap was $0.41 \text{ cm}^2/\text{s}^2$ for the canopy density of 2.5% while it was $0.34 \text{ cm}^2/\text{s}^2$ for the canopy density of 10%, indicating a reduction in the TKE_5 within the gap of 16.67% and 29.17%, respectively. That is, the denser the nearby canopy, the lower was the TKE_5 (Figures 5.6.a and b) within the gap, as a result of the sheltering effect of the nearby vegetation on the gap. In contrast, the wave velocity $U_{w,5}$ (Figure 5.5.a and 5.5.b) within the gap was less reduced than the TKE_5 (Figures 5.6.a and 5.6.b) when compared with the no vegetation experiments. That is, for the largest gap width, the maximum wave velocity attained was close to the without plants experiment for the two canopy densities of 2.5% and 10%, but the TKE_5 was reduced in a 8.9% for the canopy density of 2.5% (Figure 5.6.a) and in a 24% for the canopy density of 10% (Figure 5.6.b). Moreover, both the TKE_5 and the wave velocity within the gapped canopy in the region close to the boundary were larger than for no-gapped canopies, showing the effect of the wave penetration within the canopy due to the presence of the adjacent gap. The reduction of the total kinetic energy within a submerged canopy was also observed by (Granata et al., 2001). Granata et al. (2001) found a reduction in the total kinetic energy in the range of 75%-90% in the vertical direction comparing the energy above and within the canopy. The reduction in regions without plants was only of a 50%. These results account for a reduction of total kinetic energy in the range of 25%-40% by the vegetation compared to regions without plants. In their work, the canopy density ranged between 200 and 400 shoots/ m^2 that could be compared to the canopy density of 2.5% used in this study. In the present study, the TKE_5 for the no gapped canopy density of 2.5% was reduced in a 44% comparing with the without plants experiments and the reduction for the U_w accounted for a 5.9% giving a reduction in the total kinetic energy of a 50.3% that is close to

the reduction in the total kinetic energy found by Granata et al. (2001). In their work they also found that the total kinetic energy in regions without plants but close to the canopy was larger than that on bare soils far from the boundary, showing the effect of the canopy in sheltering the adjacent bare soil.

Since the TKE_5 within the gap was found a function of the architecture of the system such as the gap width or the canopy density, a scaling law of the TKE_5 with the characteristic parameters governing the turbulence evolution in the system was investigated. The parameters considered were the gap width (GW), the plant-to-plant distance (S), the orbital excursion length ($A_w=U_w/2\pi f$) and the distance (x) from the nearest vegetation to the point within the gap where the TKE_5 was measured.

In order to obtain a non-dimensional model for the TKE within the vegetation the Buckingham pi-theorem was used, which is based on the assumption that physical laws should be independent of the units used to express the variables (Evans, 1972). This theorem sets the relation among the number of dependent variables (n) with the number of physical dimensions (m). The TKE at $z=5\text{cm}$ was considered a proxy to characterize the TKE within the vegetation. In accordance with this scheme, we have 5 dependent variables (A_w should be a variable but since the frequency was not varied it turns to be only a function of U_w , which is already counted in the list of dependent variables) and 2 dimensions (length and time), therefore $n-m=3$ will be the number of non-dimensional parameters for this model (TKE/U_w^2 , x/S , A_w/GW). Therefore, the relationship between the governing variables used to quantify the turbulence within the gap will scale as follows:

$$\left(\frac{TKE_5}{U_{w,5}^2}\right) = K \left(\frac{x}{S}\right)^\alpha \left(\frac{A_w}{GW}\right)^\beta \quad (5.1)$$

where K is a non-dimensional constant and α and β are exponents.

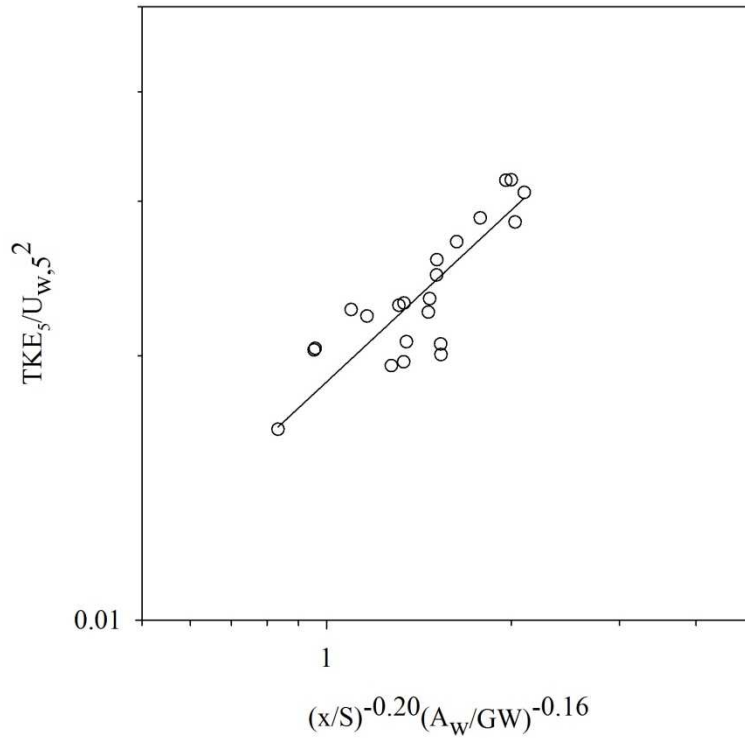


Figure 5.8 Relationship between the non-dimensional number $(TKE_5/U_{w,5}^2)$ and the parameter $(x/S)^{-0.20}(A_w/GW)^{-0.16}$. The distance x is the closest distance to the nearest canopy boundary.

Considering this equation, we plotted $TKE_5/U_{w,5}$ versus x/S (plot not shown) for constant values of A_w/GW and an exponent of $\alpha=-0.20$ was found. The same was done for the plot between $TKE_5/U_{w,5}^2$ versus A_w/GW for constant values of x/S , with an exponent $\beta=-0.16$ (plot not shown). As such, the relationship between the $TKE_5/U_{w,5}$ and $(x/S)^\alpha(A_w/GW)^\beta$ presented a linear trend as can be observed in Figure 5.6. From the parameterization found in equation 5.1 we can observe that the ratio $(TKE_5/U_{w,5}^2)$ increases with both S/x and GW/A_w . Therefore, for a constant x/S , an increase in the gap width produces an increase in the ratio (TKE_5/U_w^2) , that is, a larger increase in the TKE_5 than the $U_{w,5}$ at $z=5\text{cm}$ for gapped canopies when compared to a no-gapped canopy. Furthermore, from equation 5.1 it holds that at the center of the gap, and given that S decreases with increasing the canopy density, the TKE_5 in

the gap is larger for sparser adjacent canopies, indicating a lower sheltering capability of sparser gapped canopies.

Within a no gapped canopy, the TKE_{10} was also smaller than the TKE_{10} for the without plants experiments. Compared to the without plants experiment, the TKE_{10} for the sparser no gapped canopy of 2.5% was reduced in a 32.8%, smaller than the reduction in the TKE_{10} for the denser no gapped canopy of 10 % of density that was of a 34.3%. However, the TKE_{10} within the gapped canopy was larger than that for the no gapped canopy unless for the smaller gap of $h_v/2$ of the denser canopy of 10% (Figure 5.7.b). In this case, the denser nearby canopy was still able to provide shelter to the small gap at this depth. As was also found for the TKE_5 , the TKE_{10} within the gapped canopy of 2.5% (Figure 5.7.a) was larger than the TKE_{10} within the canopy of 10% of density (Figure 5.7.b), showing the strong sheltering effect of denser canopies. In a gapped canopy, the TKE_{10} within the gap was smaller than the TKE_{10} for the without plants experiment for all the gap widths (Figure 5.7.b). In contrast, for the gapped canopy of 2.5% density, the TKE_{10} in the center of the gap attains the TKE_{10} for the without plants experiment for the largest gap widths of $2h_v$. In this situation, the nearby sparse vegetation was not able to provide any shelter to the gap when this gap had a width of $2h_v$.

The mean of the TKE_{10} ($\langle TKE_{10} \rangle$) for the whole canopy including the gap was calculated as the mean between both the mean TKE at $z=10$ cm of the measurements taken within the gap and the mean TKE at $z=10$ cm for the measurements taken within the vegetation (Figure 5.9). For completeness, results for the no gapped canopy were also included considering in this case $GW/h_v=0$. From Figure 5.9, and for a constant h_v , the larger the gap width the larger the TKE_{10} , thus producing a reduction in the sheltering effect of the canopy when a gap is opened and when the gap increases in size. The increase of TKE_{10} with the non-dimensional gap width GW/h_v followed a linear trend (Figure 5.9). The lowest mean TKE_{10} was $0.42 \text{ cm}^2/\text{s}^2$, for the

gapped canopy of 10% with $GW/h_v=0.5$, which is 5% higher than that for the no gapped canopy of the same density.

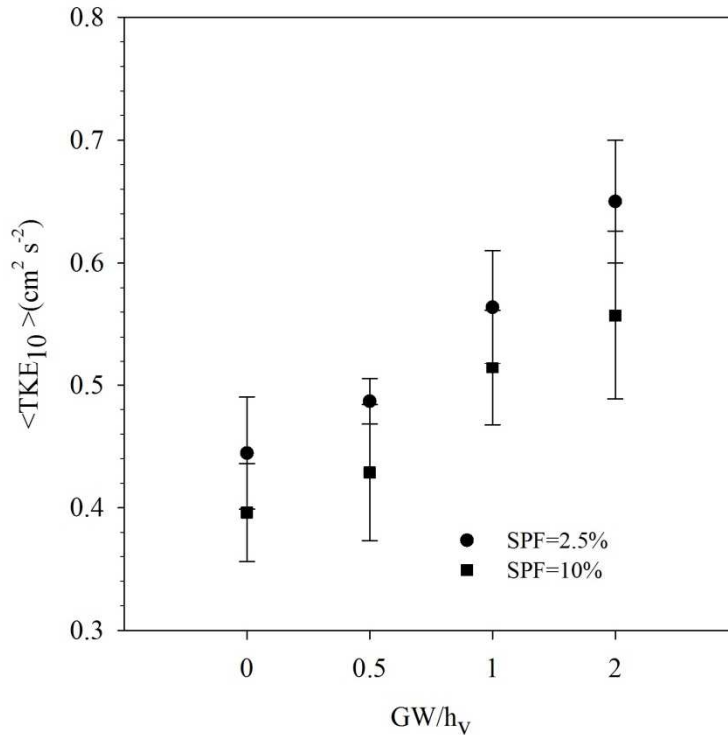


Figure 5.9 Relationship between the mean TKE at the top of the canopy ($z=10$ cm, $\langle TKE_{10} \rangle$) and the ratio GW/h_v for the two canopy densities of $SPF=2.5\%$ and $SPF=10\%$.

For the same canopy, the largest TKE_{10} was 0.55 cm^2/s^2 , which is a 17.9% of the TKE_{10} for experiments without plants (with $TKE_{10}=0.67$ cm^2/s^2 , Figure 5.7). For all the gap widths studied, the TKE_{10} for the gapped canopies of density 2.5% was larger than that for the canopy of 10% of density, consistent with the fact that denser canopies produce a larger sheltering. Especially, for $GW/h_v=0$, the TKE_{10} for the no gapped canopy density of 10% was smaller than that for the no gapped canopy density of 2.5%. These results are in accordance with those found by Pujol et al. (2013b) for the TKE at the top of a flexible canopy in oscillating flows.

Chapter 6. General Discussion

This Ph. D. thesis has focused to study the hydrodynamics in fragmented canopies exposed to oscillatory flows. Each Chapter includes its own results and discussion section. Therefore, this Chapter aims to produce a more general discussion comparing our results with those from others and also setting all the results together with the idea of providing an overview of the findings of this thesis.

Chapters 3 and 4 in the present thesis dealt with the effect of a longitudinal gap within a meadow, i.e. a gap perpendicular to the direction of the wave propagation. This experiment studied both emergent and submerged vegetation cases. However, the other two following experiments were focused on submerged vegetations.

6.1 The effect of the gap orientation

The results in both experiments (Chapter 3 and 5) with longitudinal and transversal gap show that the wave velocity increased inside the gap compared with wave velocities within the vegetation. In the gap, wave velocities approached those for the without plant experiments. The maximum wave velocities within the gap were found to depend on the nearby vegetation density, with low wave velocities for dense nearby canopy densities, and also depended on the gap width. Furthermore, regions close to the vegetation had lower wave velocities than regions far from the vegetation, i.e. the sheltering effect of the nearby canopy increased when approaching the canopy. Results also showed that the presence of the gap also produced an effect within the vegetation. Wave velocities inside the canopy in regions close to the gap were larger than wave velocities in canopies without gaps.

Results also demonstrated that densest canopies were less disturbed than sparsest canopies. These results found in controlled experiments in the laboratory gave results close to those found in the field by Granata et al. (2001). Granata et al. (2001) found that the total kinetic energy in a gap within a meadow was lower than the total kinetic energy for regions far from the meadow. Furthermore, they also found a gradual increase in the total kinetic energy from regions within the meadow towards the gap, showing that the overall sheltering capacity of the canopy was diminished in canopies with the presence of a gap.

Results from Chapter 5 show that a transversal distribution of plants (with the edge perpendicular to the wave direction) also modifies the hydrodynamics in the nearby region without plants. Furthermore, the wave velocity decreases from the region outside the canopy towards the edge of the canopy like it was found in the longitudinal gap experiment.

Results show also that a gap within flexible vegetation and aligned with the direction of the wave propagation is not sheltered by the nearby vegetation, showing neither a

reduction in the wave velocity nor in the turbulent kinetic energy. However, transversal gaps within flexible meadows showed a greater sheltering by the nearby vegetation, showing a reduction of both the wave velocity and the turbulent kinetic energy. These results might provide information for future restoration projects, where the gap orientation needs to be considered. Furthermore, gap orientation might also compromise the future of seagrasses under changes in the wave direction caused by manmade activities.

6.2 The effect of the plant flexibility

Flexible plants have been found to attenuate less the wave velocity than rigid plants, coinciding with the results from Pujol et al. (2013b). Furthermore, due to the back and forth movement of flexible blades, waves were able to penetrate more within the canopy than in rigid plant canopies. The turbulent kinetic energy within both rigid and flexible canopies was reduced compared with the case without plants, which is in accordance with the results found by (Granata et al., 2001; Luhar et al., 2010 and Pujol et al., 2013b). For flexible canopies with the presence of gaps, the turbulent kinetic energy decreased approaching the edge of the canopy, with a larger effect in transversal gaps than in longitudinal gaps. However, for rigid canopies, the turbulent kinetic energy increased approaching the edge of the canopy. Inside the rigid canopy, the turbulent kinetic energy for regions close to the gap remained higher than for the no plants case. Well inside the canopy (for regions far from the gap) the turbulent kinetic energy had a tendency to decrease again, providing sheltering. These results are also in accordance with the results found by Nezu and Onitsuka (2001) for a case of a submerged rigid vegetation under an unidirectional flow.

6.3 Ecological implications

The presence of gaps (horizontal and transversal) within canopies have been found to modify the kinetic energy within the canopy. This might result in different levels of sediment

resuspension that will ultimately depend on the canopy density. Canopies with a great level of fragmentation will present more wave penetration, resulting in a greater sediment resuspension (Lawson et al., 2007; Ricart et al., 2015) that will decrease the water clarity. Due to the large effect that light availability has on seagrass occurrence; the effect of a decrease of the light conditions can be a negative feedback for the canopy resilience (Boer, 2005).

In addition, the fact that the edge of the canopy present different characteristics from the region outside and the region inside the canopy explains why some authors divide the seagrass and nearby zone in three regions: inside the canopy, the edge and outside the canopy. This division might explain the different distribution of species in each region. Tanner (2005) pointed that ecological processes associated with edges may differ from those in interior habitats. Those species requiring interior habitat may respond negatively to edges, and can be greatly endangered by increased levels of habitat fragmentation. Tanner (2005) also found that seagrass biomass tended to vary smoothly with distance from the no vegetated region towards the region inside the canopy, rather than abruptly increase from zero to a maximum density. This pattern might be the result of a negative feedback of the increase in turbulence in the edge, which results in an increase in turbidity and a decrease in light availability. Tanner (2005) and Bologna and Heck (1999) found an increase in some crustans at the edges of the meadow. This process occurs because relative larval settlement rates are increased near the edge of these meadows due to passive depositional forces. Inside the meadow the abundance decreases afterwards due to the larval depletion. In contrast, adult scallops might present different patterns of distribution different from their initial larval settlement patterns due to their swimming abilities to travel long distances. However, Bologna and Heck (1999) still found greater scallops densities at edges than inside the meadows. Their explanation was that edges provide greater food fluxes relative to interior regions of the meadow. Therefore, such organisms might reflect trade off between the risk of predation and their foraging success rates (Bologna and Heck, 1999).

All in all, these relationships will impact the fluxes of biological particles, nutrients and sediments between the canopy and the adjacent zones, and therefore the canopy ecological function. Canopies may optimize their structural characteristics, particularly plant density, to moderate the impacts of fragmentation and optimize ecological function, however this thesis shows that plant density interacts with gap width and degree of fragmentation to facilitate sheltering in a manner not previously predicted.

Chapter 7. Conclusions

This doctoral thesis has focused to study the hydrodynamics in fragmented canopies exposed to oscillatory flows.

1. This study has analyzed detailed experimental data to increase our understanding of how the hydrodynamics in canopies with longitudinal gaps are altered by plant flexibility, canopy density and gap width. Chapter 3 has highlighted the modification in vertical and horizontal distributions of the mean wave induced current and wave velocities in fragmented canopies with longitudinal gaps. The penetration of wave velocities in vegetated areas adjacent to gaps indicates that in a canopy affected by gaps, the inherent faculty of producing sheltering is notably reduced, with all the implications for the modification of the inner canopy habitat. How such gaps affect the development of a canopy is of primary interest given increasing pressures on coastal seagrass meadows and salt marshes. Furthermore, this study demonstrated the role of the vegetation in sheltering the adjacent gap. Denser canopies are

able to produce a greater sheltering on a nearby gap than sparser canopies. Our results (Chapter 3) demonstrated that the canopy architecture is crucial in determining both the mean wave induced current and the wave velocity. That is, the canopy density, the plant height (emergent or submerged vegetation), the gap width and the plant flexibility are the main parameters describing the flow within a canopy affected by a gap. Also, this study demonstrated that gaps with widths of 1.5 times the plant height the sheltering of the vegetation on the nearby gap is nearly unnoticeable and therefore the wave field approaches that of the case without plants.

2. In Chapter 4, the hydrodynamics in a boundary of vegetation aligned with the direction of the wave propagation was studied. The study explored the hydrodynamics for two different types of plants, flexible and rigid. The results indicated that the submerged rigid vegetation produced a stronger shear layer of the wave associated mean current in the canopy boundary zone outside the vegetation, compared with flexible vegetation. This effect might have important consequences at understanding the dynamics of the transport of both seeds and nutrients, which, in turn, has important implications for the canopy development and the whole ecosystem functioning. Furthermore, it was demonstrated that a canopy of rigid plants has a greater wave attenuation than a canopy of flexible plants. The greater attenuation of wave velocities observed for rigid canopy canopies can be associated with a production of TKE by the rigid stems in the boundary layer. In contrast, flexible vegetation did not produce TKE at the boundary; instead the TKE within the flexible vegetation was reduced through dissipation. Therefore, these results points out the importance of choosing the appropriate vegetation model when trying to mimic real field situations. The flexibility of plants is a crucial parameter to determine the role of the canopy in sheltering the environment, especially in the edges of the meadow, where hydrodynamics have been found to present noticeable differences in terms of the mean current, the wave velocity and the turbulent kinetic energy.

3. In Chapter 5 the modification of hydrodynamics with transversal gaps was studied. Gapped canopies with a small gap width were sheltered by the nearby vegetation. However, large gap widths present within a canopy are exposed to wave velocities close to those found in non-vegetated regions. Furthermore, the presence of a gap within the canopy was found to increase the mixing rate between the water parcels within the canopy with those situated above the canopy. Therefore, a large gap produced an increase in the turbulent kinetic energy and therefore a reduction in the sheltering generated by the vegetation. Large gap widths determined the mixing ratio between the layers above and below the canopy independently on the canopy density. However, for small gap widths both the canopy density and the gap width determined the mixing ratio between the layer within the canopy and the layer above the canopy. Small gaps are more sheltered by the nearby vegetation, with a smaller increase in both the wave velocity and the turbulent kinetic energy than large gaps, which presented the same wave velocities than in the no-canopy cases but with smaller turbulent kinetic energies. Furthermore, the canopy density plays an important role in sheltering the nearby gap in terms of the turbulent kinetic energy attenuation. Therefore, a gap within a sparse canopy might not be sheltered depending on the size of this gap, where both wave velocities and turbulent kinetic energies might be close to those found in bare soils. The presence of the gap might therefore produce an impact in the transport of nutrients and sediments altering the fluxes between the canopy and the adjacent zones.

All in all, the present Thesis demonstrated the heterogeneity in the hydrodynamics on fragmented canopies. The gap architecture, gap orientation and width, was demonstrated to be crucial in determining such heterogeneity and also the level of mixing of the overall canopy. Other parameters such as the plant flexibility, the canopy density and the plant height determined the level of energy and the wave field within the meadow and on the nearby gap.

The presence of gaps of vegetation (longitudinal or transversal) within a canopy results in the canopy fragmentation. From the results obtained in this doctoral Thesis, fragmented canopies are expected to present greater wave velocities and greater turbulent kinetic energies, especially in regions within the canopy close to the edges of the vegetation. This increase in the total energy in the canopy might compromise the role of seagrasses as ecosystem engineers. The increase in fragmentation is expected to also increase the area of edges versus the within canopy area, resulting in a shift in habitats and favouring edge specialized species in front of within canopy specialized species.

This Thesis also opens a future line of research on the hydrodynamics within fragmented canopies and their role in the modification of the fluxes of materials in seagrasses. Fragmented canopies are expected to favor more the settling of allochthonous materials than continuous seagrasses, therefore enhancing the sedimentation rates. However, gaps expose sediments and detritus from the canopies, allowing their resuspension under high energy events, therefore scouring the bottom. More knowledge on this area is needed to finally address which one of these processes will dominate, and also what fragmentation limit might threaten the canopy itself through a modification in the sedimentation patterns.

Chapter 8. References

Adams, J.B. and Bate, G.C., 1994. The effect of salinity and inundation on the estuarine macrophyte *Sarcocornia perennis*. *Aquatic Botany*. 47: 347-348.

Airoldi, L. and Beck, M.W., 2007. Loss, status and trends for coastal marine habitats of Europe. *Marine Biology Annual Review*. 345–405.

Bianchi, C.N. and Buia, M.C., 2008. Seagrass ecosystems. In: *Seagrass meadows. Flowering plants in the Mediterranean Sea*. Ministero dell’Ambiente e della Tutela del Territorio e del Mare (Roma). Museo Friulano di Storia Naturale (Udine). *Quaderni Habitat* (19): 23-41. ISBN 88 88192 395.

Boer, W.F., 2005. Seagrass-sediment interactions, positive feedbacks and critical thresholds for occurrence: a review. *Hydrobiologia*. 591: 5-24.

Bologna, P. and Heck, K., 1999. Differential predation and growth rates of bay scallops within seagrass habitat. *Journal of Experimental Marine Biology and Ecology*. 239: 299-314.

Borg, J.A., Attrill, M., Rowden, A.A. and Jones, M.B., 2005. Architectural characteristics of two bed types of the seagrass *Posidonia oceanica* over different spatial scales. *Estuarine, Coastal and Shelf Science*. 62(4): 667-678.

Boudouresque, C.F., Bernard, G., Pergent, G., Shili, A. and Verlaque, M., 2009. Regression of Mediterranean seagrasses caused by natural processes and anthropogenic disturbances and stress: a critical review. *Botanica Marina*. 52: 395-418.

Boudouresque, C.F., Bernard, G., Bonhomme, P., Diviacco, G., Meinesz, A., Pergent, G., Pergent-Martini, C., Ruitton, S. and Tunessi, L., 2012. Protection and conservation of *Posidonia oceanica* meadows. *Tunis*, 1-202.

Bouma, T.J., van Duren, L.A., Temmerman, S., Claverie, T., Blanco-Garcia, A., Ysebaert, T. and Herman, P.M.J., 2007. Spatial flow and sedimentation patterns within patches of epibenthic structures: Combining field, flume and modeling experiments. *Continental Shelf Research*. 27: 1020–1045.

Bradley, K. and Houser, C., 2009. Relative velocity of seagrass blades: Implications for wave attenuation in low-energy environments. *Journal of Geophysical Research Earth Surface*. 114: 1-13.

Britter, R. and Hanna, S., 2003. Flow and dispersion in urban areas. *Annual Review of Fluid Mechanics*. 35: 469-496.

Capehart, A.A. and Hackney, C.T., 1989. The potential role of roots and rhizomes in structuring salt-marsh benthic communities. *Estuaries*. 12:119-122.

Charpy-Roubaud, C., and A. Sournia., 1990. The comparative estimation of phytoplanktonic and microphytobenthic production in the oceans. *Marine Microbial Food Webs*. 4: 31–57.

Coates, M.J. and Folkard, A.M., 2009. The effects of littoral zone vegetation on turbulent mixing in lakes. *Ecological Modelling*. 220: 2714-2726.

Coulombier, T., Neumeier, U. and Bernatchez, P., 2012. Sediment transport in a cold climate salt marsh (St. Lawrence Estuary, Canada), the importance of vegetation and waves. *Estuarine, Coastal and Shelf Science*. 101: 64-75.

Dean, R.G. and Dalrymple, R.A., 2002. *Coastal processes in engineering applications*. First ed. Cambridge University Press, Cambridge.

Denny, M.W., 1988. *Biology and the mechanics of the wave-swept environment*, Princeton University Press.

Duarte, C.M., 1991. Allometric scaling of seagrass form and productivity. *Marine Ecology Progress Series*. 77: 192-206.

Duarte, C.M., 2002. The future of seagrass meadows. *Environmental Conservation*. 29: 192-206.

EEC1992. The habitats directive-environment-european commission. <http://eur-lex.europa.eu/legal-content/EN/TXT/?uri=CELEX:31992L0043>.

Evans, J.H., 1972. Dimensional Analysis and the Buckingham Pi Theorem. *American Journal of Physics*. 40: 1815-1822.

Ewel, K.C., Zheng, S., Pinzón, Z.S. and Bourgeois, J.A., 1998. Environmental Effects of Canopy Gap Formation in High-Rainfall Mangrove Forests. *Biotropica* 30: 510-518.

Feller, I.C. and McKee, K.L., 1999. Small Gap Creation in Belizean Mangrove Forests by a Wood Boring Insect. *Biotropica*. 31: 607-617.

Folkard, A.M., 2005. Hydrodynamics of model *Posidonia oceanica* patches in shallow water. *Limnology and Oceanography*. 50: 1592-1600.

Folkard, A.M., 2011. Flow regimes in gaps within stands of flexible vegetation: laboratory flume simulations. *Environmental Fluid Mechanics*. 11: 289–306.

Fonseca, M.S. and Fisher, J.S., 1986. A comparison of canopy friction and sediment movement between four species of seagrass with reference to their ecology and restoration. *Marine Ecology Progress Series*. 29: 15-22.

Fonseca, M.S. and Cahalan, J.A., 1992. A preliminary evaluation of wave attenuation by four species of seagrass. *Estuarine, Coastal and Shelf Science*. 35: 565-576.

Fredriksen, S., De Backer, A., Bostrom, C. and Christie, H., 2010. Infauna from *Zostera marina* L. meadows in Norway. Differences in vegetated and unvegetated areas. *Marine Biology Research*. 6: 189-200.

Gacia, E. and Duarte, C.M., 2001. Sediment retention by a Mediterranean *Posidonia oceanica* meadow: The balance between deposition and resuspension. *Estuarine, Coastal and Shelf Science*. 52: 505-514.

Ghisalberti, M. and Nepf, H.M., 2002. Mixing layers and coherent structures in vegetated flows. *Journal of Geophysical Research. Oceans*. 107, C2.

Granata, T.C., Serra, T., Colomer, J., Casamitjana, X., Duarte, C.M. and Gacia, E., 2001. Flow and particle distributions in a nearshore seagrass meadow before and after a storm. *Marine Ecology Progress Series*. 218: 95-106.

Gruber, R.K. and Kemp, W.M., 2010. Feedback effects in a coastal canopy-forming submersed plant bed. *Limnology and Oceanography*. 55: 2285-2298.

Hansen, J.C.R. and Reidenbach, M.A., 2012. Wave and tidally driven flows in eelgrass beds and their effects on sediment suspension. *Marine Ecology Progress Series*. 448: 271-287.

Hemminga, M. and Duarte, C.M., 2000. *Seagrass Ecology*. Cambridge (United Kingdom): Cambridge University Press.

Hendriks, I.E., Sintes, T., Bouma, T.J. and Duarte, C.M., 2008. Experimental assessment and modeling evaluation of the effects of the seagrass *Posidonia oceanica* on flow and particle trapping. *Marine Ecology Progress Series*. 356: 163-173.

Hendriks, I.E., Cabanelles-Reboredo, M., Bouma, T.J., Deudero, S. and Duarte, C.M., 2011. Seagrass meadows modify drag forces on the shell of the fan mussel *Pinna nobilis*. *Estuaries and Coasts*. 34: 60-67.

Hopkins, G.W. 2002. Identifying rarity in insects: the importance of host plant range. *Biology Conservation*. 105: 293-297.

Koch, E. and Gust, G., 1999. Water flow in tide- and wave-dominated beds of seagrass *Thalassia testudinum*. *Marine Ecology Progress Series*. 184: 63-72.

Koch, E., Ackerman, J.D., Verduin, J. and van Keulen, M., 2006. Fluid dynamics in seagrass ecology-from molecules to ecosystems. In: Larkum, A.W.D., Orth, R.J. eds.

Kosten S., Lacerot G., Jeppesen D. E., Marques D., van E.H. Mazzeo N., Scheffer M., 2009., Effects of submerged vegetation on water clarity across climates. *Ecosystems*. 12: 1117-1129.

Lasagna, R., Montefalcone, M., Albertelli, G., Corradi, N., Ferrari, M., Morri, C. and Bianchi, C.N., 2011. Much damage for little advantage: Field studies and morphodynamic modelling highlight the environmental impact of an apparently minor coastal mismanagement. *Estuarine, Coastal and Shelf Science*. 94: 255–262.

Lawson, S.E., Wiberg, P.L., McGlathery, K.J. and Fugate, D.C., 2007. Wind-driven sediment suspension controls light availability in a shallow coastal lagoon. *Estuaries and Coasts*. 30(1): 102-112.

Leonard L.A. and Croft, A.L., 2006. The effect of standing biomass on flow velocity and turbulence in *Spartina alterniflora* canopies. *Estuarine, Coastal and Shelf Science*. 69: 325–336.

Leonard, L.A., Hine, A.C. and Luther, M.E., 1995. Surficial sediment transport and deposition processes in *Juncus Romerianusmarsh*, West-Central Florida. *Journal of Coastal Research*. 11: 322-326.

Lowe, R., Kossef, J. and Monismith, S., 2005. Oscillatory flow through submerged canopies: 1. Velocity structure. *Journal of Geophysical Research. Oceans*. 110, C10016.

Luhar, M., Coutu, S., Infantes, E., Fox, S. and Nepf, H.M., 2010. Wave-induced velocities inside a model seagrass bed. *Journal of Geophysical Research. Oceans*. 115, C12005.

Manca, E., Cáceres, I., Alsina, J.I., Stratigaki, V., Townend, I. and Amos, C.L., 2012. Wave energy and wave-induced flow reduction by full-scale model *Posidonia oceanica* seagrass. *Continental Shelf Research*. 50-51: 100-116.

- Marbà, N., Cebrian, J., Enriquez, S. and Duarte, C.M., 1996. Growth patterns of Western Mediterranean seagrasses: species-specific responses to seasonal forcing. *Marine Ecology Progress Series*. 133: 203-215.
- Montefalcone, M., 2009. Ecosystem health assessment using the Mediterranean seagrass *Posidonia oceanica*: A review. *Ecological Indicators*. 9: 595–604.
- Moore, K.A., Wilcox, D.L. and Orth, R.J., 2000. Analysis of abundance of submersed aquatic vegetation communities in Chesapeake Bay. *Estuaries*. 23: 115-127.
- Nepf H, Ghisalberti M, 2008. Flow and transport in channels with submerged vegetation. *Acta Geophysica*. 56, 753-777.
- Neumeier, U. and Amos, C.L., 2006. Turbulence reduction by the canopy of coastal *Spartina* salt-marshes. *Journal of Coastal Research*. 39: 433–439.
- Neumeier, U. and Ciavola, P., 2004. Flow resistance and associated sedimentary processes in a *Spartina maritime* salt-marsh. *Journal of Coastal Research*. 39: 433–439.
- Nezu I. and Onitsuka K., 2001. Turbulent structures in partly vegetated open-channel flows with LDA and PIV measurements. *Journal of Hydraulic Research*. 39(6): 1-13.
- Orth, R.J., Marion Garnger, S.R. and Traber, M., 2009. Evaluation of a mechanical seed planter for transplanting *Zoostera marina* (eelgrass) seeds. *Aquatic Botany*. 90: 204–208.
- Paul, M. and Amos, C.L., 2011. Spatial and seasonal variation in wave attenuation over *Zostera noltii*. *Journal of Geophysical Research* 116(C8), C08019.

Pujol, D., Colomer, J., Serra, T. and Casamitjana, X., 2010. Effect of submerged aquatic vegetation on turbulence induced by an oscillating grid. *Continental Shelf Research*. 30: 1019-1029.

Pujol, D., Casamitjana, X., Serra, T. and Colomer, J., 2013a. Canopy-scale turbulence under oscillatory flow. *Continental Shelf Research*. 66: 9-18.

Pujol, D., Serra, T., Colomer, J. and Casamitjana, X., 2013b. Flow structure in canopy models dominated by progressive waves. *Journal of Hydrology*. 486: 281-292.

Ricart, A.M., Dalmau, A, Pérez, M. and Romero, J., 2015. Effects of landscape configuration on the exchange of materials in seagrass ecosystems. *Marine Ecology Progress Series*. 532: 89-100

Robinson, G.R., Holt, R.D., Gaines, M.S., Hamburg, S.P., Johnson, M.L., Fitch, H.S. and Martinko, E.A., 1992. Diverse and contrasting effects of habitat fragmentation. *Science*. 257: 524-526.

Ros, À., Colomer, J., Serra, T., Pujol, D., Soler, M. and Casamitjana, X., 2014. Experimental observations on sediment resuspension within submerged model canopies under oscillatory flow. *Continental Shelf Research*. 91: 220-231.

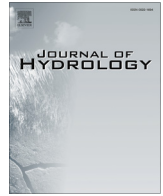
Saintilian, N., 2009. *Australian Saltmarsh Ecology*. CSIRO Publishing.

Sontek YSi, Acoustic Doppler Velocimeter Technical Instrumentation. ftp://ftp.mumm.ac.be/oostende/tripode_WZ_boei/SonTek_Software/ViewHydra2.93/ADVFieldManual_v790.pdf.

Tanner, J.E., 2003. Patch shape and orientation influences on seagrass epifauna are mediated by dispersal abilities. *Oikos*. 100: 517–524.

- Tanner, J.E., 2005. Edge effects in fauna in fragmented seagrass meadows. *Austral Ecology*. 30: 210-218.
- Terrados, J. and Medina-Pons, F., 2010. Inter-annual variation of shoot density and biomass, nitrogen and phosphorus content of the leaves, and epiphyte load of the seagrass *Posidonia oceanica* (L.) Delile off Mallorca, western Mediterranean. *Scientia Marina*. 75(1): 61-70.
- Tscharntke, T., Steffan-Dewenter, I., Kruess, A. and Thies, C., 2002. Characteristics of insect populations on habitat fragments: A mini review. *Ecological Research*. 17(2): 229-239.
- Uncles, R.J. and Stephens, J.A., 2009. Turbidity and sediment transport in a muddy subestuary. *Estuarine, Coastal and Shelf Science*. 87: 213-224.
- Vacchi, M., Montefalcone, M., Bianchi, C.N., Morri, C. and Ferrari, M., 2012. Hydrodynamic constraints to the seaward development of *Posidonia oceanica* meadows. *Estuarine, Coastal and Shelf Science*. 97: 58–65.
- Ward, L.G., Kemp, W.M. and Boynton, W.R., 1984. The influence of waves and seagrass communities on suspended particulates in an estuarine embayment. *Marine Geology*. 59: 85–103.
- White, B. L., and H. M. Nepf., 2008. A vortex-based model of velocity and shear stress in a partially vegetated shallow channel. *Water Resources Research*. 44, W01412.
- Yang, S.L., Li, P., Gao, A., Zhang, W.X. and Li, M., 2007. Cyclical variability of suspended sediment concentration over low-energy tidal flat in Jiaoshou Bay China: effect of shoaling on wave impact. *Geo-Marine Letters*. 27: 345-353.

Annex



Modified hydrodynamics in canopies with longitudinal gaps exposed to oscillatory flows



Nazha El Allaoui^a, Teresa Serra^{a,*}, Marianna Soler^a, Jordi Colomer^a, Dolors Pujol^a, Carolyn Oldham^b

^a Department of Physics, University of Girona, 17071 Girona, Spain

^b School of Environmental Systems Engineering, The University of Western Australia, Crawley, WA 6009, Australia

ARTICLE INFO

Article history:

Received 22 April 2015

Received in revised form 9 October 2015

Accepted 14 October 2015

Available online 23 October 2015

This manuscript was handled by Corrado Corradini, Editor-in-Chief, with the assistance of Masaki Hayashi, Associate Editor

Keywords:

Gap

Submerged and emergent rigid vegetation

Flexible vegetation

SUMMARY

Longitudinal gaps are commonly found in aquatic canopies. While the ecological significance of gaps may be large, we know little about their impact on the hydrodynamics within the canopy. We used laboratory experiments to investigate the effect of longitudinal gaps within canopies exposed to a wave field. In rigid submerged and emergent vegetation, wave velocities were reduced compared to the case without vegetation. Flexible canopies also attenuated waves, but this attenuation was lower than for rigid canopies. The presence of the gap modified the mean current associated with the waves in both the gap and the lateral vegetation. A gap within a canopy of 5% solid plant fraction did not show differences in the wave attenuation between the gap and the lateral vegetation. In contrast, gaps within canopies of 10% solid plant fraction resulted in large differences between the gap and the lateral vegetation. In all the experiments, the effect of a gap within a canopy reduced the wave attenuation within the lateral vegetation adjacent to the gap when compared with a canopy without a gap. In canopies with rigid plants, the lateral vegetation modified the wave attenuation in the nearby gap. In contrast, the lateral flexible vegetation did not produce any effect on the wave attenuation of the adjacent gap. Canopy density, plant height and plant flexibility were critical for determining the hydrodynamics throughout the canopy and in the gap.

© 2015 Elsevier B.V. All rights reserved.

1. Introduction

Salt marshes, seagrass meadows and mangroves forests are characteristic of shallow coastal and littoral zones and support a large variety of infauna relative to bare substrate areas (Feller and McKee, 1999; Fredriksen et al., 2010; Hendriks et al., 2011; Coulombier et al., 2012). These vegetated systems cover less than 0.5% of the seabed but account for up to 70% of the carbon storage in ocean sediments. Submerged and emergent aquatic plants also influence the spatial distribution of key water quality parameters. Therefore, aquatic plants are recognized as water quality indicators and their restoration and protection is a priority given that their regrowth is slow and variable (Moore et al., 2000; Orth et al., 2009). Submerged coastal canopies reduce ambient flows and turbulence (Koch et al., 2006; Pujol et al., 2010, 2013a, 2013b) and attenuate waves (Granata et al., 2001; Lowe et al., 2005; Luhar et al., 2010; Pujol et al., 2013a), resulting in a reduction in sediment resuspension (Gacia and Duarte, 2001; Bouma et al., 2007; Hendriks et al., 2008; Coulombier et al., 2012). Emergent vegetation reduces

turbulence depending on wind stress, solar irradiative forcing and macrophyte mechanical forcing (Coates and Folkard, 2009). Aquatic vegetation ranges in flexibility, from rigid emergent mangroves to highly flexible canopies such as submerged seagrasses. Coral reefs can also be considered to be a rigid structure. Pujol et al. (2010, 2013a) found that flexibility and canopy density play a major role in the effectiveness of the canopy to attenuate waves and turbulence.

Salt marshes, seagrasses and mangroves are vulnerable to environmental changes. Sagittal channels in meadows run perpendicular to the coast and are formed by return currents transporting wind- and/or wave-mixed surface waters to depth. Erosive intermattes appear like oval potholes in seagrass mattes and are probably formed by whirling currents carrying rocks and stones to depth, locally destroying the mattes (Bianchi and Buia, 2008). The formation of gaps within meadows may also be triggered by human activities such as anchoring, trawling, fish farming, laying cables and pipes (Boudouresque et al., 2012). Once formed the gap changes the local environmental conditions and Ewel et al. (1998) found that water temperature, salinity and light in mangrove forest gaps were all higher than those within the canopy. Similarly Folkard (2011) found different flow regimes in

* Corresponding author.

E-mail address: teresa.serra@udg.edu (T. Serra).

unidirectional flows through transversal gaps of submerged vegetation and showed that Reynolds number (based on canopy over-flow speed and the gap depth) and the gap aspect ratio were the most important parameters in determining the modification of bed shear stress.

Despite their variety, little research has been done to elucidate the effects of gaps on adjacent vegetation, especially in wave-dominated domains. Therefore this study investigates the effect of a longitudinal gap within a canopy (with the main axis of the gap in the same direction as the wave propagation) on the hydrodynamics within the canopy and in the gap. Attention is paid to the modification of ambient hydrodynamics as a function of the ratio of gap width to plant height. Laboratory experiments were conducted on a longitudinal gap using a model canopy exposed to waves, mimicking structural disturbances of canopies in benthic salt marshes and seagrasses that are dominated by waves in shallow conditions. Two vegetation models (rigid and flexible), two gap sizes (0.25 and 0.375 of the flume width), two vegetation densities (solid plant fraction, SPF, of 5 and 10%), one wave frequency ($F = 1.2$ Hz) and two plant heights (submerged and emergent) were considered, along with a case without plants, totalling 15 experiments (Table 1). The specific objectives of our study were firstly to identify and quantify patterns of mean flow and turbulence found in the interior of simulated longitudinal gaps, and secondly to determine how these gaps affected the hydrodynamic environment within the adjacent vegetation patches. Special attention was paid to the effects of both the gap width to plant height ratios and the canopy density on the hydrodynamics within the gaps.

2. Methods

2.1. Laboratory setup

The experiments were performed in a flume (6 m × 0.5 m × 0.5 m), with a mean water height of 0.3 m. A schematic view of the experimental setup is shown in Fig. 1a. The flume was equipped with a vertical paddle-type wave maker that was placed at the beginning of the flume. The vertical paddle was driven by a variable-speed motor that operated at a frequency of 1.2 Hz. This frequency was chosen in accordance to the frequencies used by other authors (Bradley and Houser, 2009; Hansen and Reidenbach, 2012; Pujol et al., 2013a). Furthermore, with this frequency, waves had a wavelength of 1.03 m, which corresponds to transitional water waves, typical for regions dominated by the presence of aquatic vegetation. Following Pujol et al. (2013b), a plywood beach of slope 1:3 was situated at the end of the flume. It was covered in foam to better attenuate incoming waves. For

details of the experimental set up see Pujol et al. (2013a). We define the longitudinal direction as x , and $x = 0$ at the wavemaker; y is the lateral direction and $y = 0$ at the centreline of the tank, and z is the vertical direction, with $z = 0$ at the flume bed.

The model canopies were 2.5 m long and they were situated at the centre of the flume. A rigid canopy model was considered with two heights: submerged (plant height $h_v = 14$ cm) and emergent (plant height $h_v = 29$ cm). Following Pujol et al. (2013a, 20013b), emergent canopies were defined as vegetation whose height was emergent for nearly half of the wave cycle. Rigid plants consisted of PVC cylinders, 1 cm in diameter. Two canopy densities of 640 and 1280 shoots m^{-2} were considered and a model of flexible vegetation was studied for the 1280 shoots m^{-2} submerged canopy to compare the results with the rigid canopy model. A summary of the different experimental conditions is presented in Table 1. Typical vegetation densities in salt marshes vary from 296 stems m^{-2} to 505 stems m^{-2} (Capehart and Hackney, 1989). Paul and Amos (2011) found that a seagrass population of *Zostera noltii* had strong seasonal variability, from 4600 shoots m^{-2} in summer to 600 shoots m^{-2} in winter. Fonseca and Cahalan (1992) found densities of 1900–2870 shoots m^{-2} for *Halodule wrightii*, 230–1350 shoots m^{-2} for *Syringodium filiforme*, 850–1500 shoots m^{-2} for *Thalassia testudinum* and 750–1000 shoots m^{-2} for *Zostera marina*. Neumeier and Amos (2006) reported densities of 1140 and 1450 shoots m^{-1} for a salt marsh canopy of *Spartina anglica*. Therefore, the plant densities used in the present study would represent intermediate to high canopy densities. The SPF is defined as the fractional plant area at the bottom occupied by stems i.e. SPF (%) = $n_{stems}A_{stem}/A_{total} \times 100$, where n_{stems} is the number of stems, A_{stem} is the horizontal cross sectional area of each stem ($A_{stem} = \pi d^2/4$), d is the plant diameter and A_{total} is the total horizontal area. Therefore, the solid plant fractions for the two canopy densities considered (640 and 1280 shoots m^{-2}) corresponded to SPF of 5% and 10%, respectively.

A region free of plants (hereafter called the gap) was situated at the centre of the flume in the y -direction and extended longitudinally the full length of the canopy (Fig. 1). Two different gap widths (GW), were considered (0.25 and 0.375 of the flume width; Fig. 1), therefore the ratios GW/h_v were ~ 0.9 and 1.3 for the submerged canopies and ~ 0.4 and 0.6 for the emergent vegetation.

Experiments with flexible vegetation were also carried out for 10% SPF and 0.25 gap width. The flexible canopy model was constructed following Pujol et al. (2013a), i.e., six individuals of high-density polyethylene blades of 0.14 m length and 0.004 m width were attached with a plastic band to a PVC dowel (2-cm long × 1-cm diameter). The thickness of the plastic blades was ~ 0.075 mm. As stated by Pujol et al. (2013a), the model plants were dynamically and geometrically similar to typical seagrasses.

Velocity measurements were made with an Acoustic Doppler Velocimeter (16 MHz-ADV, Sontek Inc.) that recorded the three instantaneous velocity components at a single depth situated 5 cm from the tip of the probe with a sampling volume of 0.09 cm^3 . The ADV was placed in the flume in a downward-looking configuration and connected to a PC with data acquisition software.

The ADV was configured to transmit 50 signals per second over a sampling window of 10 min (30,000 records per sample). The ADV was mounted in a frame and velocity profiles measured from 1 to 23 cm from the bottom of the flume, with a vertical resolution of 1 cm. Five independent velocity measurements were completed for each case at four selected depths, in order to estimate measurement error. Velocity measurements near the surface were limited by both wave shape and the 5-cm sampling volume of the ADV. To avoid spikes, beam correlations lower than 80% were removed. At two vertical positions ($z = 8$ cm and $z = 20$ cm above the bottom) low correlation was obtained. These “weak spots” occur when the

Table 1
Summary of the different experimental conditions. A is the horizontal area and b is the width of the flume.

SPF (%)	n/A (shoots/ m^2)	GW/ b	h_v (cm)	Type
5	640	0.25	14	Rigid
5	640	0.375	14	Rigid
5	640	0	14	Rigid
10	1280	0.25	14	Rigid
10	1280	0.375	14	Rigid
10	1280	0	14	Rigid
5	640	0.25	29	Rigid
5	640	0.375	29	Rigid
5	640	0	29	Rigid
10	1280	0.25	29	Rigid
10	1280	0.375	29	Rigid
10	1280	0	29	Rigid
10	1280	0	14	Flexible
10	1280	0.25	14	Flexible
0	0	–	–	–

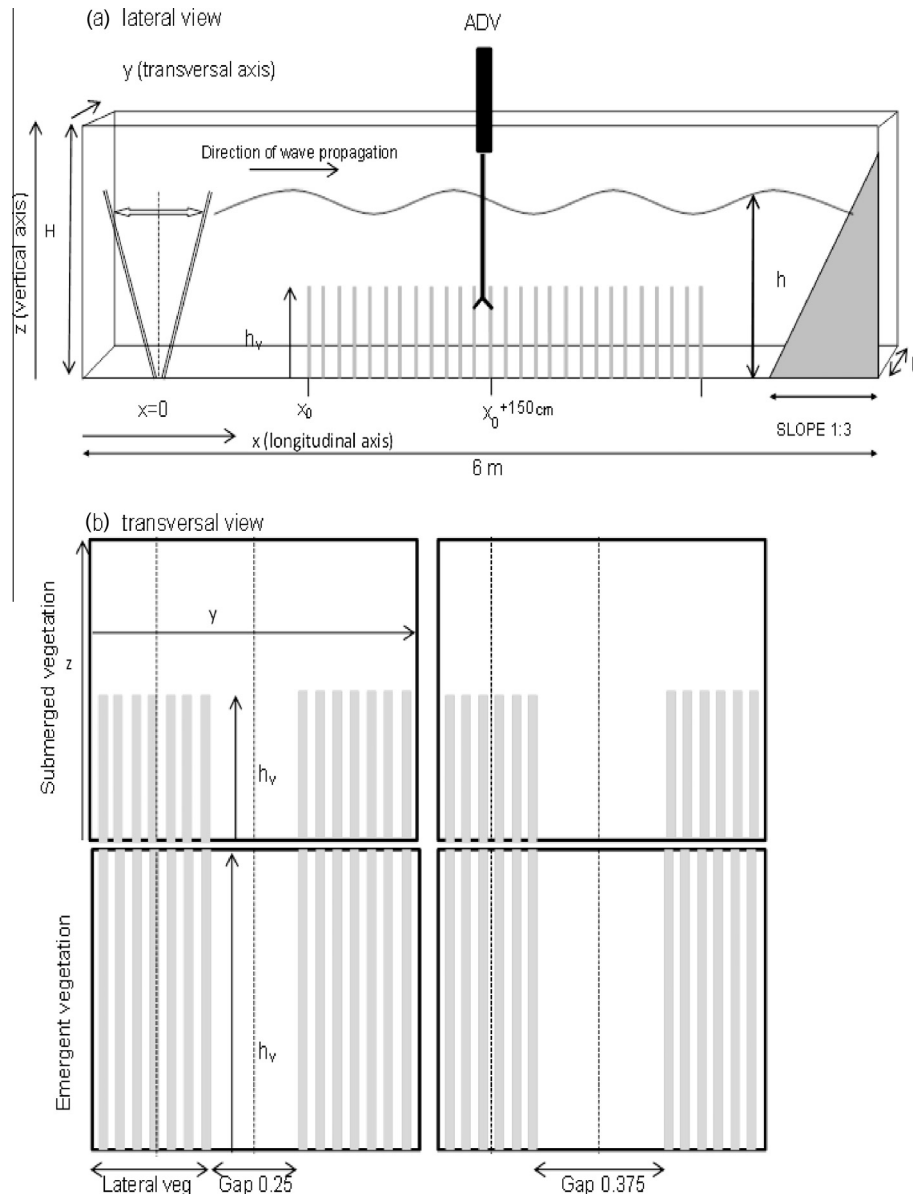


Fig. 1. (a) Schematic diagram of the experimental flume. (b) Transversal section with the gap and the vegetation zones. Vertical dashed lines represent the y -positions where vertical velocity profiles were measured.

first pulse emitted from the ADV is reflected at the bottom of the flume and meets in time and space the second pulse at the sampling volume (Pujol et al., 2013a). As the time lag between pulses depends on the velocity range, the ADV operational range was changed for these points (Sontek YSI, Acoustic Doppler Velocimeter Technical Instrumentation). To determine the effect of the ADV operational range on S wave velocity determination, measurements were done 10 cm above the bed of the flume in two ranges: up to 30 cm s^{-1} and up to 100 cm s^{-1} ; wave velocities only differed by 0.7%.

In order to obtain valid data acquisition within the canopy, a few stems were removed to ensure the ADV beam was not blocked and the acoustic receivers and transmitter performed properly (Neumeier and Ciavola, 2004; Neumeier and Amos, 2006). To test the effect of the ‘hole’ on the ambient hydrodynamics, velocities were measured half a centimetre above the top of the canopy, both with and without the hole. A 3% difference in velocities between ‘hole’ and ‘no hole’ canopies was observed at the highest SPF; only 1% difference was observed at the lowest SPF. We therefore

concluded that the ‘hole’ made minimal modification to the ambient hydrodynamics.

In oscillatory flows the instantaneous velocity u can be decomposed into mean wave induced current (U_c), orbital velocity (U_w) and turbulent velocity (u') components as

$$u = U_c + U_w + u'. \quad (1)$$

The above decomposition was made by using a phase-averaging technique (Luhar et al., 2010; Pujol et al., 2013a). The Hilbert transform was used to average oscillatory flow velocities with a common phase (ϕ). The velocity readings were binned into different phases following the procedure described by Pujol et al. (2013a). The instantaneous velocity measurements for each phase bin $u(\phi)$ were then time-averaged for the entire record to yield the phase-averaged velocity values, U_c .

$$U_c = \frac{1}{2\pi} \int_0^{2\pi} u(\phi) d\phi \quad (2)$$

The root mean square of $u(\varphi)$ was then defined as the orbital velocity U_w^{rms} as:

$$U_w^{\text{rms}} = \sqrt{\frac{1}{2\pi} \int_0^{2\pi} (u(\varphi) - U_c)^2 d\varphi} \quad (3)$$

U_w^{rms} will be named hereafter as U_w .

Vertical profiles of U_c were measured for experiments using submerged rigid vegetation with two gap widths and two solid plant fractions (SPF). In addition, six control experiments were conducted, one without plants (denoted as “no-veg”) and another with a fully vegetated canopy i.e. without a gap (denoted as “no-gap”), one for each SPF studied for rigid emergent and submerged vegetation and one for the experiment with submerged flexible vegetation. Velocities were measured at the centre of the gap and at the middle of the lateral vegetation, and were compared to velocities measured within similar canopies with no gaps and experiments with no vegetation (Fig. 1). Preliminary profiles of wave velocities were completed to characterise the different boundary layers, and to ensure measurements were taken at locations outside the flume wall boundary layer and also outside the boundary layers generated by the gap and the vegetation. Transsects of U_w along the transversal section of the flume at $z = 5$ cm above the bottom were used to characterise the different boundary layers at SPF = 10% for both submerged (Fig. 2a and b) and

emergent (Fig. 2c and d) plants. For experiments with a 0.25 gap, U_w was almost constant from -13 cm to -19 cm within the lateral vegetation for both the submerged (Fig. 2a) and emergent (Fig. 2c) plants. Within the lateral vegetation of the 0.375 gap condition, U_w may be partially affected by the gap boundary layer (Fig. 2b and d). The vegetation boundary layer within the gap, may affect those experiments using the 0.25 gap (Fig. 2a and c). In contrast, U_w within the 0.375 gap was almost constant from -9 cm and 5 cm for the submerged vegetation (Fig. 2b) and from -5 cm to 5 cm for the emergent vegetation (Fig. 2d) suggesting that the measurements were not affected by the vegetation boundary layer. A wall boundary layer formed in the region from -20 cm to -25 cm for the emergent vegetation (Fig. 2c and d). From these measurements, values of current velocity U_c and wave velocity U_w were calculated following the calculations presented in the analysis section. For experiments without plants, profiles of U_c in the centre of the flume were not significantly different to profiles closer to the flume side-wall, indicating that the mean current was not biased in the transversal section of the channel.

The specific geometry of the canopy stems is known to determine the flow structure within a canopy. Several studies (Bitter and Hanna, 2003; Lowe et al., 2005; Luhar et al., 2010) use the lambda parameters λ_p and λ_f to determine the flow structure within the canopy, where,

$$\lambda_f = \frac{h_v d}{(S + d)^2} \quad \text{and} \quad \lambda_p = \frac{\pi d^2}{4(S + d)^2}$$

where d is the stem diameter and S is the plant-to-plant distance.

Lowe et al. (2005) defined different canopy flow regimes depending on the ratio $A_{\infty}^{\text{rms}}/S$, where $A_{\infty}^{\text{rms}} = U_{\infty,w}^{\text{rms}}/\omega$ ($\omega = 2\pi f$ and $U_{\infty,w}^{\text{rms}}$ is the wave velocity above the canopy layer). A_{∞}^{rms} is the rms wave orbital excursion length of the free-stream potential flow. Lowe et al. (2005) classified the flow into three possible regimes: the canopy independent flow, the inertia flow dominated regime and the unidirectional limit. As we will see further in this study, the experiments considered in this study corresponded to the inertia dominated regime. From Lowe et al. (2005), in the inertia flow dominated regime, the wave attenuation can be calculated from the lambda parameters as,

$$\alpha_w = \frac{1 - \lambda_p}{1 + (C_M - 1)\lambda_p}$$

Here, C_M was considered equal to 2 for potential flow around circular cylinders (Dean and Dalrymple, 2002).

3. Results

3.1. Mean wave induced currents – submerged rigid vegetation

Canopy density, SPF, impacted on U_c (Fig. 3) in the above-canopy layer ($z > 15$ cm above the bottom up to the water surface), in the canopy-top layer ($z = 7-15$ cm) and in the canopy base layer ($z = 0-7$ cm). In the canopy-base layer, the presence of the vegetation reduced the negative values of U_c obtained for the no-veg experiments to nearly 0 cm s^{-1} (Fig. 3a and b) and for the densest canopies, U_c in this layer was positive. The greatest U_c was within the lateral vegetation. In the canopy-top layer, U_c within the gap was in general negative, but lower than that found for the no-veg experiments. In this layer, U_c for the lateral vegetation and the no-gap experiments was in general positive except for the case of the lateral vegetation corresponding to the sparser canopy of 5% and the larger gap width of 0.375 (Fig. 3b).

Increasing the gap width from 0.25 to 0.375 created small differences in U_c for the sparser canopy (Fig. 3a and b). However, it had a greater effect for the denser canopy of 10% SPF

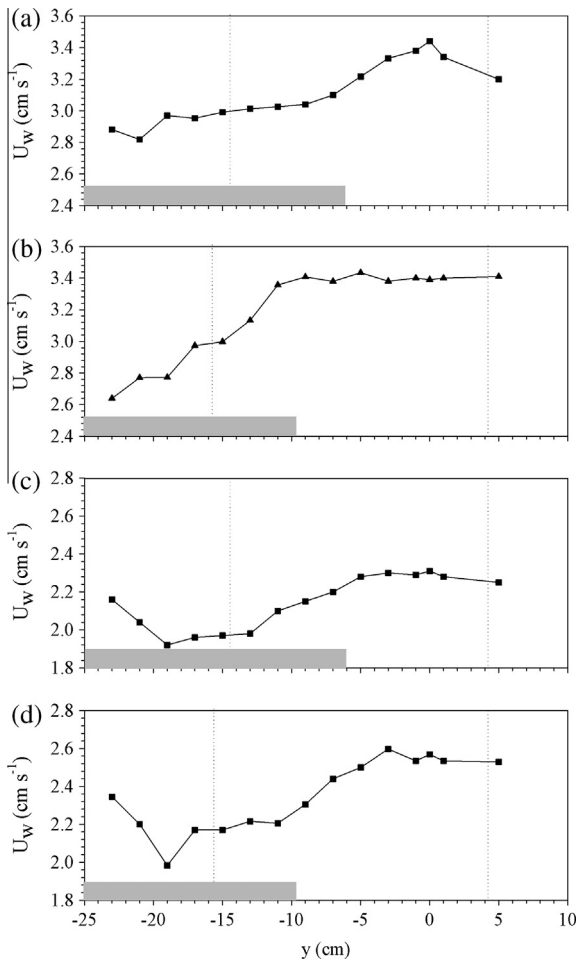


Fig. 2. Wave velocity transects along the y -axis at $z = 5$ cm for (a) submerged vegetation with a 0.25 gap, (b) submerged vegetation with a 0.375 gap, (c) emergent vegetation with a 0.25 gap and (d) emergent vegetation with a 0.375 gap. Vertical dashed lines show the y -positions where vertical velocity profiles were measured. Grey boxes represent the zone covered by the vegetation.

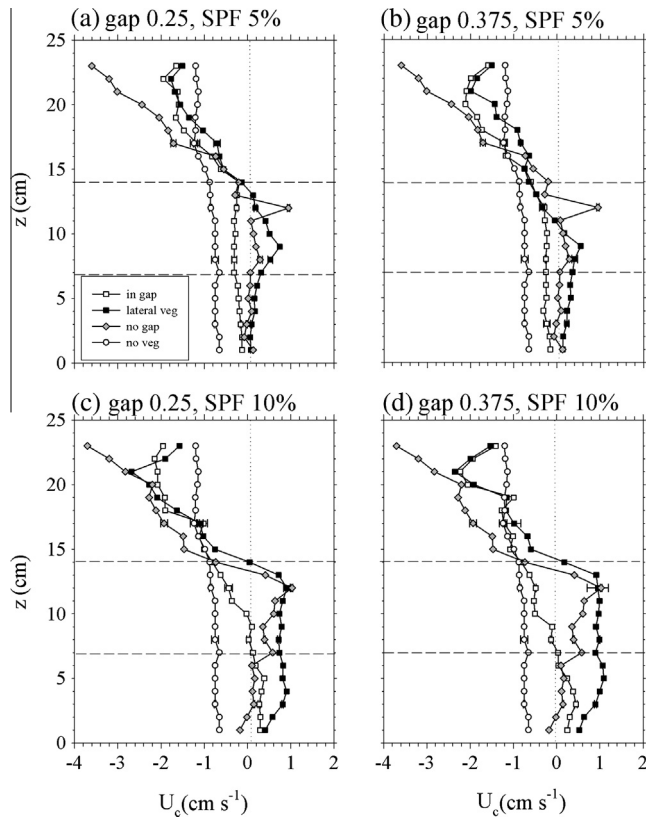


Fig. 3. Mean current (U_c) for the submerged rigid vegetation experiments. (a) 0.25 gap and 5% SPF; (b) 0.375 gap and 5% SPF; (c) 0.25 gap and 10% SPF; (d) 0.375 gap and 10% SPF. Horizontal dashed lines show the limits of the above-canopy region (>14 cm above the bottom), the canopy-top region (7–14 cm) and the canopy-base region (<7 cm). Horizontal error bars represent the standard deviation over different replicates.

(Fig. 3c and d) and mainly at the canopy-top layer in the gap. For this case, U_c was closer to the no-veg experiments for the larger gap width (Fig. 3d) than for the smaller gap width (Fig. 3c).

3.2. Mean wave induced currents – emergent rigid vegetation

In the experiments using emergent rigid vegetation the SPF had a large effect on U_c within the lateral vegetation, but SPF did not have an effect on U_c within the gap (in contrast to the submerged vegetation experiments). We note that the most significant difference between the submerged and the emergent vegetation was observed in the top 10 cm of the surface waters. Two distinct regions within the U_c profiles can be observed: an in-canopy region ($z < 17$ cm), and a surface boundary layer region ($z > 17$ cm). For 5% SPF and 0.25 gap width U_c at the in-canopy region within the lateral vegetation was negative (Fig. 4a). The largest U_c was measured within the gap and U_c for the no-gap control experiments was larger than measured within the lateral vegetation. The no-veg control experiments resulted in the smallest mean velocity observed at the in-canopy region. U_c became constant and negative throughout most of the surface boundary layer within the gap and for the no-veg control experiments, however above 20 cm within the gap and in the lateral vegetation U_c had a tendency to reverse, becoming positive at 21 cm above the bottom. The increase to 0.375 gap width did not produce appreciable changes in the U_c profiles (Fig. 4b). The increase in the canopy density to 10% SPF with 0.25 gap width increased U_c within the gap, within the lateral vegetation and also for the no-gap experiment (Fig. 4c). As was found

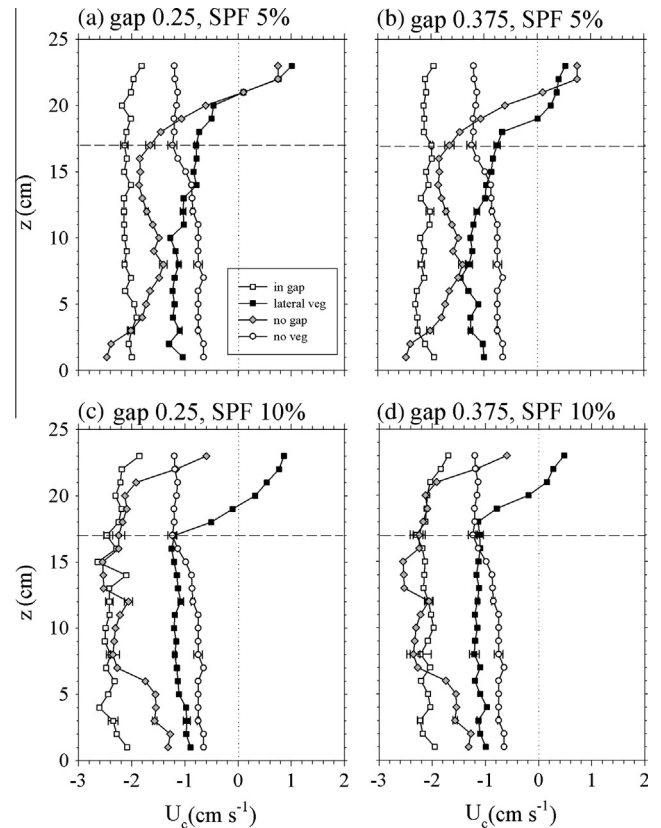


Fig. 4. Mean current (U_c) for the emergent rigid vegetation experiments. (a) 0.25 gap and 5% SPF; (b) 0.375 gap and 5% SPF; (c) 0.25 gap and 10% SPF; (d) 0.375 gap and 10% SPF. The dashed horizontal line represents the limit of the in-canopy region (<17 cm above the bottom) and the surface boundary layer (>17 cm). Horizontal error bars represent the standard deviation over different replicates.

for 5% SPF, the increase to 0.375 gap width did not result in changes in U_c (Fig. 4d).

3.3. Wave velocities – submerged rigid vegetation

The wave velocity ratio $\alpha_w = U_w/U_{w,\text{no-veg}}$ (called hereafter wave attenuation) was calculated to quantify differences in wave velocities between cases with plants and the no-veg cases. Since this ratio can vary with height within the canopy, a vertically-averaged ratio, $\langle \alpha_w \rangle$, over the canopy layer will be considered representative of the local wave attenuation induced by the canopy. The wave velocity ratio $\beta_w = U_w/U_{w,\text{no-gap}}$ was calculated to quantify differences between wave velocities in canopies with gaps and in no-gap canopies. Also, a vertically-averaged value of β_w within the canopy was calculated and denoted as $\langle \beta_w \rangle$.

For all experiments, U_w was calculated at different depths. U_w profiles for the case of the submerged vegetation of 5% SPF and 0.25 gap is presented in Fig. 5. U_w above the canopy in either the lateral vegetation, in the gap or in the no-gap canopy was close to U_w in the no-veg experiment. However, in the layer occupied by the canopy U_w was reduced compared to the no-veg experiment. The no-gap canopy experiment showed minimum U_w , i.e. the maximum wave reduction, compared to the no-veg experiment.

Vertical profiles of orbital velocity (U_w) were normalized by the $U_{w,\text{no-veg}}$ profile to obtain wave attenuation α_w (see Section 2) for all experiments across different SPF and gap widths (Fig. 6a–d). The wave velocity was, in general, reduced at the canopy-base region in the gap and lateral vegetation compared to the no-veg

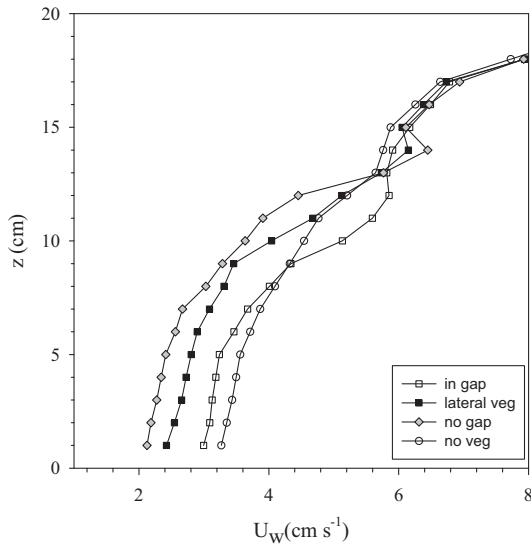


Fig. 5. Wave velocity (U_w) profiles for all experiments carried out with submerged vegetation at 10% SPF and 0.25 gap. The horizontal scale has been reduced to highlight U_w at both the canopy-top and the canopy-base regions.

experiment, although it was greater than compared to the no-gap experiment. In all experiments, and above the canopy region, α_w in the gap and in the lateral vegetation (including the no-gap experiment) was slightly above 1 (Fig. 6a–d). In the canopy-top region,

for both gaps studied (Fig. 6a and b), α_w for both within the gap and the lateral vegetation, increased to a maximum at $z/h_v = 0.7$ (mid-depth of the canopy-top region). At the canopy-base region, for 5% SPF, α_w within the gap was close to that measured within the lateral vegetation (Fig. 6a and b) but still with $\alpha_w < 1$, indicating an equal wave attenuation in both the gap and the lateral vegetation. However, this value was above that observed in the no-gap control experiment, where it peaked in the upper part of the canopy-top region.

In contrast, for the densest canopy of 10%, α_w was lower in the lateral vegetation than in the gap, for both gap widths studied (Fig. 6c and d).

3.4. Wave velocities – emergent rigid vegetation

In the experiments using emergent rigid vegetation, SPF had a significant effect on wave velocity attenuation, similar to the experiments with submerged vegetation. In all cases, vertical profiles of α_w within the lateral vegetation and the gap were greater than measured in the no-gap experiments. For 5% SPF, there were minimal differences between α_w within the lateral vegetation and the gap (Fig. 7a), remaining constant with depth but slightly above α_w in the no-gap experiment (Fig. 7a). An increase to 0.375 gap width did not change the α_w vertical profile within the gap nor within the lateral vegetation (Fig. 7b). However an increase to 10% SPF caused a decrease in α_w within the lateral vegetation (Fig. 7c and d). For experiments using 10% SPF, an increase in the gap width resulted in an increase in α_w , in both the lateral vegetation and the gap (Fig. 7d).

The vertical profile of the orbital velocity (U_w) was normalized by the vertical profile measured in the no-gap control experiment,

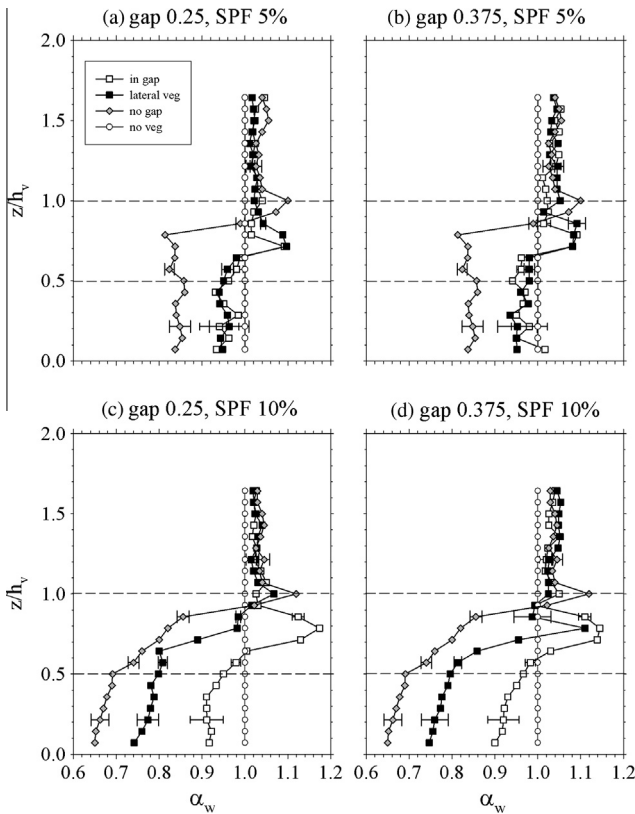


Fig. 6. Wave velocity attenuation (α_w) for the submerged rigid vegetation experiments for (a) 0.25 gap, SPF = 5%; (b) 0.375 gap, SPF = 5%; (c) 0.25 gap, SPF = 10%; (d) 0.375 gap, SPF = 10%. Horizontal dashed lines show the limits of the above-canopy region (>14 cm), the canopy-top region (7–14 cm) and the canopy-base region (<7 cm). Horizontal error bars represent the standard deviation over different replicates.

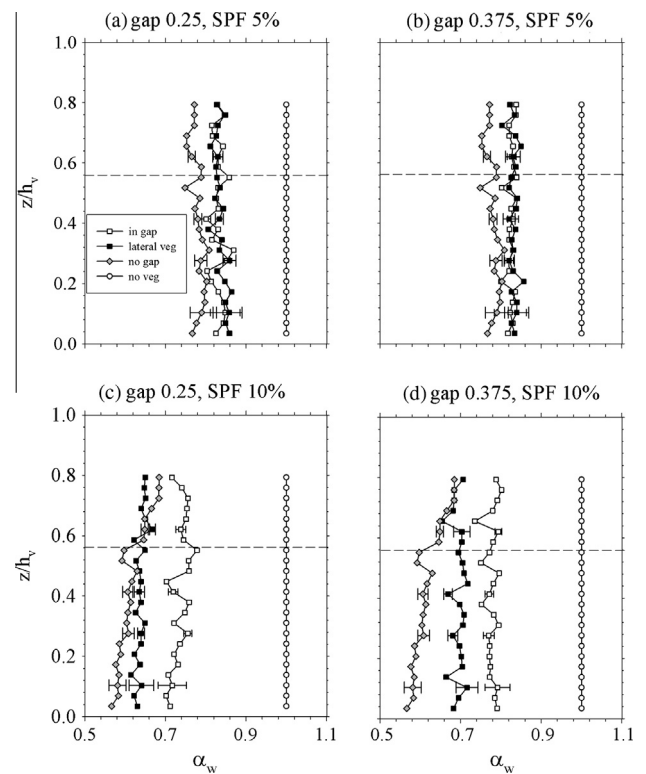


Fig. 7. Wave velocity attenuation (α_w) for the emergent rigid vegetation experiments for (a) 0.25 gap, SPF = 5%; (b) 0.375 gap, SPF = 5%; (c) 0.25 gap, SPF = 10%; (d) 0.375 gap, SPF = 10%. The dashed horizontal line represents limits of the in-canopy region (<17 cm above the bottom) and the surface boundary layer (>17 cm). Horizontal error bars represent the standard deviation over different replicates.

$U_{w,\text{no-gap}}$, in order to obtain β_w (see Section 2). The mean vertical value of the orbital velocity ratios ($\langle\alpha_w\rangle$ and $\langle\beta_{wp}\rangle$) in the canopy-base region were calculated and plotted versus the non-dimensional gap width (GW/h_v , where GW is the gap width and h_v is the plant height). In Fig. 8a and b, no-gap experiments were also included for completeness. In these experiments, the plant-to-plant distance (S) was considered a proxy for gap width. The ratio between the gap width (GW) and the plant height was found to have a large effect on wave attenuation in the canopy layer. The larger the GW/h_v , the lower the wave attenuation compared with the no-veg experiment, within both the lateral vegetation and the gap. For these cases, the higher the canopy density the larger the wave attenuation when compared with the no-veg experiment. $\langle\alpha_w\rangle$ increased with the ratio GW/h_v within both the gap (Fig. 8a) and the lateral vegetation (Fig. 8b), for both 5% and 10% SPF. $\langle\alpha_w\rangle$ was smallest for the highest canopy density. The change in SPF had a larger effect in $\langle\alpha_w\rangle$ at the lateral vegetation (Fig. 8b) than at the gap (Fig. 8a). $\langle\beta_w\rangle$ also increased with GW/h_v within the gap and the lateral vegetation (Fig. 8c and d, respectively). $\langle\beta_w\rangle$ within the gap and the lateral vegetation was smaller for the higher SPF. The change in SPF impacted velocities within the gap (Fig. 8c) more than within the lateral vegetation (Fig. 8d).

3.5. Submerged flexible vegetation

For experiments using submerged flexible vegetation with 10% SPF, the flexibility of the plant reduced the thickness of the canopy-base layer, allowing the wave and the mean current to penetrate deeper inside the vegetation. The vertical profiles of U_c measured in the lateral vegetation and in the no-gap control experiment were similar, with positive values at the canopy-base (Fig. 9a). In this case, the canopy-base region was defined as $z = 0$ –4 cm above the bottom. The canopy-top region was defined as the layer $z = 4$ –14 cm, and the above-canopy region was defined as $z > 14$ cm. U_c at the canopy-top region increased upwards, within the lateral vegetation and the no-gap experiment. U_c in the gap was similar to that measured within the lateral vegetation for the canopy top layer, while at the canopy-base it was more similar to that found for the no-veg experiment (Fig. 9a).

At the above-canopy region, α_w was slightly above 1 as was measured in the experiments with submerged rigid vegetation. However, in the upper part of the canopy-top region, α_w was slightly above 1 and decreased gradually below 1 in the lower part of the region (Fig. 9b). Below 7 cm, α_w remained close to 1 within the gap. However for the lateral vegetation, α_w decreased to 0.85 (Fig. 9b), which was greater than measured in the no-gap experiment, with a value of 0.8 at the bottom (Fig. 9b).

4. Discussion

The presence of a longitudinal gap within a rigid canopy was found to alter the mean wave-induced current in the lateral vegetation. This occurred whether the vegetation was submerged or emergent. At the same time, the lateral vegetation determined hydrodynamics within the gap.

4.1. Interaction between plant density and flows through gaps

The canopy density was found to be a key parameter in determining not only sheltering within the vegetation but also the hydrodynamics in the nearby gap. The increase in the canopy density to 10% SPF produced considerable differences in the hydrodynamics within the gap and in the lateral vegetation. The reduction in wave velocities inside both intermediate and high density canopies agrees with the results of Manca et al. (2012) and Pujol et al.

(2013a), i.e. the higher the canopy density, the larger the reduction in the wave velocity inside the canopy. Furthermore, the wave attenuation inside the canopy with a nearby gap was smaller than for the no-gap experiment. In their study on the hydrodynamics around and within canopy patches under uni-directional flow, Bouma et al. (2007) highlighted the variability across a canopy. They found a larger erosion rate at the front of a canopy patch than well inside the patch, showing the heterogeneous spatial distribution of energy. Furthermore, they found that denser patches produced larger sedimentation rates when compared with sparser patches. These results are in accordance with the findings of the present study, where there is a larger reduction in the wave velocities within denser canopies.

4.2. Vertical flow structure within a rigid canopy

In general, the submerged vegetation induced a positive mean flow (i.e. in the direction of the wave propagation) within the canopy with greater positive values for the densest canopies, and a stronger return current above the canopy relative to the no-veg case. This result is in accordance with the results of Luhar et al. (2010) and Pujol et al. (2013). For the emergent vegetation, U_c was always negative in the canopy. This result might have important implications for the flushing of solids and nutrients in areas dominated by vegetation. At the canopy-base layer, opening a gap within a submerged canopy also increased the mean flow through the vegetation that was greater for larger gap widths. This mean current at the canopy-base was greater for denser canopies.

In emergent vegetation, the presence of a gap affected wave velocities in the lateral vegetation and in the gap, and facilitated sheltering inside the canopy; this effect was augmented at high canopy densities. This effect has been documented in salt marshes where emergent vegetation attenuates the flow at the edge of the vegetation differently to that within the vegetation patch (Bouma et al., 2007; Coates and Folkard, 2009).

Our results suggested that large values of GW/h_v could be associated with lower sheltering of the adjacent vegetation, and small GW/h_v could be associated to a large sheltering of the adjacent vegetation. Furthermore, increasing canopy density had a larger effect in the lateral vegetation than in the gap, with a larger wave velocity attenuation in the lateral vegetation than in the gap. Results also show that the wave attenuation in a gap adjacent to nearby vegetation becomes larger for low GW/h_v . Denser canopies provided greater wave attenuations within the gap. Furthermore, in the gap and independently of the canopy density, it can be estimated that for $GW > 1.5h_v$, the wave does not attenuate (Fig. 8a). In contrast, the wave velocity in the canopy layer was greater than the wave velocity for the no-gap experiment. This result showed that the greater GW/h_v , i.e. lower sheltering, the larger the wave velocity at both the gap and at the lateral vegetation. Furthermore, the presence of a gap played a greater effect at the gap than at the lateral vegetation, with greater $\langle\beta_w\rangle$ in the gap than in the lateral vegetation. Within the lateral vegetation, for $GW < 0.4h_v$, β_w approached 1, that is, U_w was closer to that for the no-gap canopy.

Considering now only the experiments of rigid submerged vegetation, and for canopies of 5% SPF and 10% SPF without a gap, $\langle\alpha_w\rangle$ was 0.84 and 0.68, respectively. The theoretical value of α_w can be calculated if the inertial flow dominated regime held for the cases studied here. An inertial flow dominated regime occurs when $A_{\infty}^{\text{rms}}/S < 1$. In the present study $A_{\infty}^{\text{rms}}/S = 0.24$ for 5% SPF and 0.39 for 10% SPF. The lambda parameters in the present study are $\lambda_p = 0.05$ (for 5% SPF) and $\lambda_p = 0.10$ (for 10% SPF), giving $\alpha_w = 0.9$ and 0.82, respectively. The experimental values obtained in this study were below those predicted by the theory. The reason for this discrepancy might be that the model presented by Lowe et al. (2005) holds for cases where the wave velocity varies

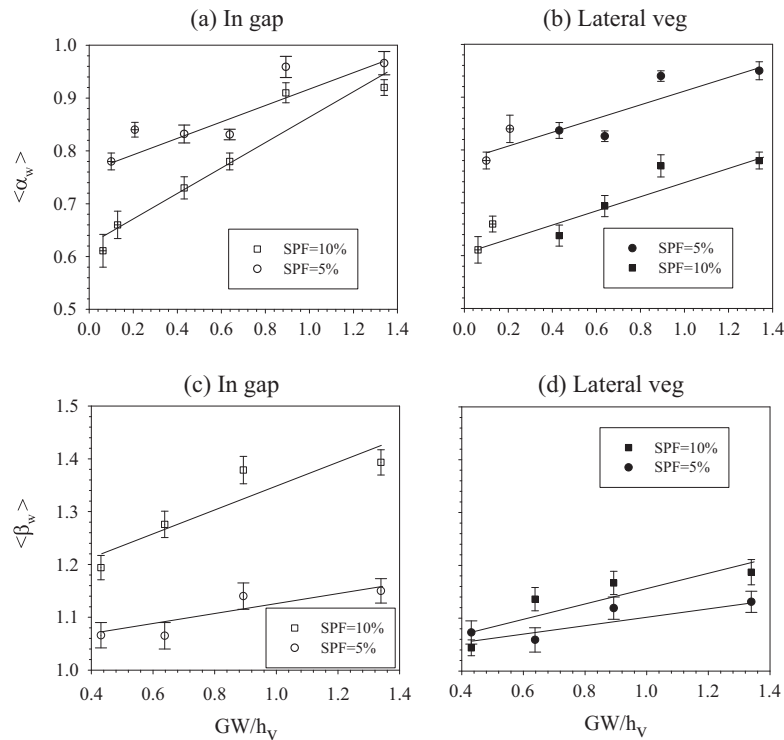


Fig. 8. $\langle \alpha_w \rangle$ in the (a) gap and (b) lateral vegetation. $\langle \beta_w \rangle$ in the (c) gap and (d) lateral vegetation, plotted against GW/h_v . Different vegetation density (SPF) treatments are plotted and regression equations were (a) $y = 0.15x + 0.78$ (SPF = 5%, $R^2 = 0.813$) and $y = 0.25x + 0.62$ (SPF = 10%, $R^2 = 0.922$), (b) $y = 0.13x + 0.78$ (SPF = 5%, $R^2 = 0.805$) and $y = 0.13x + 0.61$ (SPF = 10%, $R^2 = 0.851$), (c) $y = 0.10x + 1.02$ (SPF = 5%, $R^2 = 0.788$) and $y = 0.22x + 1.13$ (SPF = 10%, $R^2 = 0.823$) and (d) $y = 0.08x + 1.03$ (SPF = 5%, $R^2 = 0.752$) and $y = 0.13x + 1.027$ (SPF = 10%, $R^2 = 0.730$), all 95% probability level. Crosses in figures (a) and (b) correspond to no-gap experiments using the plant-to-plant distance as the 'gap width'. Error bars represent the standard deviation of $\langle \alpha_w \rangle$ and $\langle \beta_w \rangle$ through the canopy base layer.

minimally over the height of the canopy, which is not the case in this study, where U_w presented a variation with depth above the canopy layer.

4.3. Differences between rigid and flexible vegetation

Results for the dense (10% SPF) submerged flexible vegetation were significantly different from those found for rigid vegetation. The canopy-base region of the flexible vegetation was thinner than that found in the rigid vegetation. For the layer occupied by plants, U_c in the gap was close to that found without plants. In this layer, U_c for the lateral vegetation was also close to that for the no-gap experiment, indicating similar development of the current in canopies with gaps and the no-gap canopies. Flexible vegetation was found to attenuate the wave velocity to a lower degree than rigid vegetation. Therefore, the flexibility of the stems is a key parameter determining wave attenuation. The back and forth motion of flexible plants makes possible a deeper penetration of the wave than does rigid vegetation. Koch and Gust (1999) also found a larger energy transfer in flexible vegetation under wave-dominated flows.

In this study, wave attenuation for rigid canopies was double that measured by Neumeier and Amos (2006) in a *Spartina anglica* canopy, which has a semi-rigid structure. The difference in wave attenuation can be attributed to the difference in the plant rigidity. Using an analysis of wave height within *Zostera noltii*, Paul and Amos (2011) found 20% wave attenuation within a canopy of 4164 shoots m^{-2} and a 10% wave attenuation within a canopy of 600 shoots m^{-2} . Earlier, Granata et al. (2001) found a 75% reduction in total kinetic energy above and within a *Posidonia oceanica* canopy, and a 50% reduction over a nearby bare sediment, accounting for a 25% total kinetic energy reduction between vegetated and

bare sediment regions. Our study using flexible vegetation agrees with this prior work.

4.4. Sedimentary significance

Our results have demonstrated that canopy density is one of the key parameters in determining both the mean wave-induced current and the wave velocity; for larger canopy densities the wave velocity at the canopy-base layer is more attenuated in the lateral vegetation than in the gap. Several studies (Leonard et al., 1995; Neumeier and Amos, 2006; Bouma et al., 2007) have shown that suspended sediments settle progressively as they travel over a canopy area as turbulence, currents and wave action decreased. Yang et al. (2007) and Uncles and Stephens (2009) correlated the sediment concentration with current and wave action. In the present study, the wave attenuation in intermediate to dense canopies was larger in the rigid vegetation than in the flexible vegetation. This is in accordance with the laboratory results of Ros et al. (2014), who found higher values of the turbulent kinetic energy in rigid canopies than in flexible canopies. Larger turbulent kinetic energies were associated to higher wave attenuation by the canopy. Ros et al. (2014) proved that the crucial parameter in determining the sediment resuspension was the turbulent kinetic energy. They found higher sediment resuspension for rigid canopies, with higher turbulent kinetic energy, than for flexible canopies, with lower turbulent kinetic energy. The presence of a gap within a canopy should increase the rate of erosion (and the sediment resuspension) in the gap area compared to vegetated areas; but the degree of erosion would be lower than in areas of bare sand. This should apply for gap widths no larger than ~ 1.5 the height of the plant.

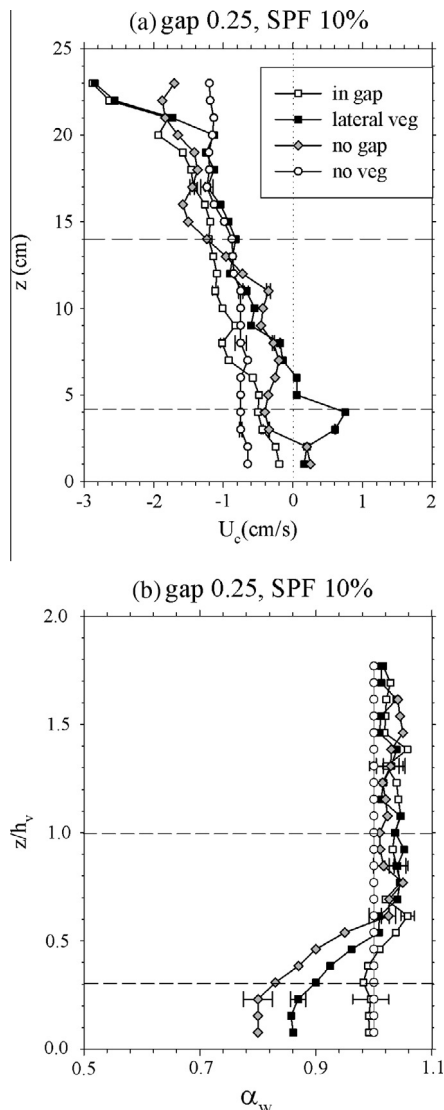


Fig. 9. (a) Mean current (U_c) and (b) wave velocity attenuation (α_w) for experiments with submerged flexible vegetation with a 0.25 gap and 10% SPF. Horizontal dashed lines show the limits of the above-canopy region (>14 cm above the bottom), the canopy-top region (4–14 cm) and the canopy-base region (<4 cm). Horizontal error bars represent the standard deviation over different replicates.

5. Conclusions

Our results demonstrate that the canopy architecture is crucial in determining both the mean wave induced current and the wave velocity. That is, the canopy density, plant height (emergent or submerged vegetation), gap width and plant flexibility are the main parameters describing the flow within a canopy affected by a gap. An increase in spatial hydrodynamic heterogeneity was observed in canopies with longitudinal gaps. The penetration of wave velocities in vegetated areas adjacent to gaps indicates that in a canopy affected by gaps, the inherent faculty of producing sheltering is notably reduced, with implications for the modification of the inner canopy habitat. How such gaps affect the development of a canopy is of primary interest given increasing pressures on coastal seagrass meadows and salt marshes. Detailed investigations into the turbulent dynamics close to the gap-canopy boundary are still required, along with investigation of hydrodynamics around low-density canopies more typical of meadows in coastal regions under stress.

Acknowledgements

This work was supported by Ministerio de Ciencia e Innovación of the Spanish Government through grant CGL2010-17289. Oldham was supported by a Study Leave Grant from The University of Western Australia. All data necessary to understand or replicate the reported research can be downloaded from the following site http://webfísica.udg.edu/tserra/data_files.zip.

References

- Bianchi, C.N., Buia, M.C., 2008. Seagrass Ecosystems. In: Minelli (Ed.), Seagrass Meadows. Flowering Plants in the Mediterranean Sea.
- Boudouresque, C.F., Bernard, G., Bonhomme, P., Diviacco, G., Meinesz, A., Pergent, G., Pergent-Martini, C., Ruitton, S., Tunessi, L., 2012. Protection and Conservation of *Posidonia oceanica* meadows, Tunis, pp. 1–202.
- Bouma, T.J., van Duren, L.A., Temmerman, S., Claverie, T., Blanco-Garcia, A., Ysebaert, T., Herman, P.M.J., 2007. Spatial flow and sedimentation patterns within patches of epibenthic structures: combining field, flume and modeling experiments. *Cont. Shelf Res.* 27, 1020–1045.
- Bradley, K., Houser, C., 2009. Relative velocity of seagrass blades: implications for wave attenuation in low-energy environments. *J. Geophys. Res. Earth Surface* 114, 1–13.
- Britter, R., Hanna, S., 2003. Flow and dispersion in urban areas. *Annu. Rev. Fluid Mech.* 35, 469–496.
- Capehart, A.A., Hackney, C.T., 1989. The potential role of roots and rhizomes in structuring salt-marsh benthic communities. *Estuaries*, 119–122.
- Coates, M.J., Folkard, A.M., 2009. The effects of littoral zone vegetation on turbulent mixing in lakes. *Ecol. Model.* 220, 2726.
- Coulombier, T., Neumeier, U., Bernatchez, P., 2012. Sediment transport in a cold climate salt marsh (St. Lawrence Estuary, Canada), the importance of vegetation and waves. *Estuar. Coast. Shelf Sci.* 101, 64–75.
- Dean, R.G., Dalrymple, R.A., 2002. Coastal Processes in Engineering Applications, first ed. Cambridge University Press, Cambridge.
- Ewel, K.C., Zheng, S., Pinzón, Z.S., Bourgeois, J.A., 1998. Environmental effects of canopy gap formation in high-rainfall mangrove forests. *Biotropica* 30, 510–518.
- Feller, I.C., McKee, K.L., 1999. Small gap creation in Belizean Mangrove Forests by a wood boring insect. *Biotropica* 31, 607–617.
- Folkard, A.M., 2011. Flow regimes in gaps within stands of flexible vegetation: laboratory flume simulations. *Environ. Fluid Mech.* 11, 289–306.
- Fonseca, M.S., Cahalan, J.A., 1992. A preliminary evaluation of wave attenuation by four species of seagrass. *Estuar. Coast. Shelf Sci.* 35, 565–576.
- Fredriksen, S., De Backer, A., Bostrom, C., Christie, H., 2010. Infauna from *Zostera marina* L. meadows in Norway. Differences in vegetated and unvegetated areas. *Mar. Biol.* 158, 189–200.
- Gacia, E., Duarte, C.M., 2001. Sediment retention by a Mediterranean *Posidonia oceanica* meadow: the balance between deposition and resuspension. *Estuar. Coast. Shelf Sci.* 52, 505–514.
- Granata, T.C., Serra, T., Colomer, J., Casamitjana, X., Duarte, C.M., Gacia, E., 2001. Flow and particle distributions in a nearshore seagrass meadow before and after a storm. *Mar. Ecol. Prog. Ser.* 218, 95–106.
- Hansen, J.C.R., Reidenbach, M.A., 2012. Wave and tidally driven flows in eelgrass beds and their effects on sediment suspension. *Mar. Ecol. Prog. Ser.* 448, 271–287.
- Hendriks, I.E., Cabanelles-Reboredo, M., Bouma, T.J., Deudero, S., Duarte, C.M., 2011. Seagrass meadows modify drag forces on the shell of the fan mussel *Pinna nobilis*. *Estuaries Coasts* 34, 60–67.
- Hendriks, I.E., Sintes, T., Bouma, T.J., Duarte, C.M., 2008. Experimental assessment and modeling evaluation of the effects of the seagrass *Posidonia oceanica* on flow and particle trapping. *Mar. Ecol. Prog. Ser.* 356, 163–173.
- Koch, E., Gust, G., 1999. Water flow in tide- and wave-dominated beds of seagrass *Thalassia testudinum*. *Mar. Ecol. Prog. Ser.* 184, 63–72.
- Koch, E., Ackerman, J.D., Verduin, J., van Keulen, M., 2006. Fluid dynamics in seagrass ecology—from molecules to ecosystems. In: Larkum, A.W.D., Orth, R.J., Duarte, C.M. (Eds.), Seagrasses: Biology, Ecology and Conservation. Springer, Dordrecht, pp. 199–225.
- Leonard, L.A., Hine, A.C., Luther, M.E., 1995. Surficial sediment transport and deposition processes in *Juncus Romerianus* marsh, West-Central Florida. *J. Coastal Res.* 11, 322–326.
- Lowe, R., Kossef, J., Monismith, S., 2005. Oscillatory flow through submerged canopies: 1. Velocity structure. *J. Geophys. Res. Oceans* 110, C10016.
- Luhar, M., Coutu, S., Infantes, E., Fox, S., Nepf, H.M., 2010. Wave-induced velocities inside a model seagrass bed. *J. Geophys. Res. Oceans* 115, C12005.
- Manca, E., Cáceres, I., Alsina, J.L., Stratigaki, V., Townend, I., Amos, C.L., 2012. Wave energy and wave-induced flow reduction by full-scale model *Posidonia oceanica* seagrass. *Cont. Shelf Res.* 50–51, 100–116.
- Moore, K.A., Wilcox, D.L., Orth, R.J., 2000. Analysis of abundance of submerged aquatic vegetation communities in Chesapeake Bay. *Estuaries* 23, 115–127.
- Neumeier, U., Amos, C.L., 2006. Turbulence reduction by the canopy of coastal *Spartina* salt-marshes. *J. Coastal Res.* 39, 433–439.
- Neumeier, U., Ciavola, P., 2004. Flow resistance and associated sedimentary processes in a *Spartina* maritime salt-marsh. *J. Coastal Res.* 39, 433–439.

- Orth, R.J., Marion, S.R., Garnger, S., Traber, M., 2009. Evaluation of a mechanical seed planter for transplanting *Zostera marina* (eelgrass) seeds. *Aquat. Bot.* 90, 204–208.
- Paul, M., Amos, C.L., 2011. Spatial and seasonal variation in wave attenuation over *Zostera noltii*. *J. Geophys. Res.* 116 (C8), C08019.
- Pujol, D., Colomer, J., Serra, T., Casamitjana, X., 2010. Effect of submerged aquatic vegetation on turbulence induced by an oscillating grid. *Cont. Shelf Res.* 30, 1019–1029.
- Pujol, D., Casamitjana, X., Serra, T., Colomer, J., 2013a. Canopy-scale turbulence under oscillatory flow. *Cont. Shelf Res.* 66, 9–18.
- Pujol, D., Serra, T., Colomer, J., Casamitjana, X., 2013b. Flow structure in canopy models dominated by progressive waves. *J. Hydrol.* 486, 281–292.
- Ros, À., Colomer, J., Serra, T., Pujol, D., Soler, M., Casamitjana, X., 2014. Experimental observations on sediment resuspension within submerged model canopies under oscillatory flow. *Cont. Shelf Res.* 91, 220–231.
- Sontek YSI, Acoustic Doppler Velocimeter Technical Instrumentation. <ftp://ftp.mummm.ac.be/oostende/tripode_WZ_boei/SonTek_Software/ViewHydra2.93/ADVFieldManual_v790.pdf>.
- Uncles, R.J., Stephens, J.A., 2009. Turbidity and sediment transport in a muddy subestuary. *Estuar. Coast. Shelf Sci.* 87, 213–224.
- Yang, S.L., Li, P., Gao, A., Zhang, W.X., Li, M., 2007. Cyclical variability of suspended sediment concentration over low-energy tidal flat in Jiaoshou Bay China: effect of shoaling on wave impact. *Geo-Mar. Lett.* 27, 345–353.